Methods for Estimating Capacities and Rates of Gaussian Quantum Channels

Oleg V. Pilyavets, Cosmo Lupo, and Stefano Mancini

***Abstract*—Optimization methods aimed at estimating the capacities of a general Gaussian channel are developed. Specifically evaluation of classical capacity as maximum of the Holevo information is pursued over all possible Gaussian encodings for the lossy bosonic channel, but extension to other capacities and other Gaussian channels seems feasible. Solutions for both memoryless and memory channels are presented. It is first dealt with single-use (single-mode) channel where the capacity dependence on channel's parameters is analyzed providing the full classification of possible cases. Then, it is dealt with multiple uses (multimode) channel where the capacity dependence on the (multimode) environment state is analyzed when both total environment energy and environment purity are fixed. This allows a fair comparison among different environments, thus understanding the role of memory (intermode correlations) and phenomenon like superadditivity of the capacity. The developed methods are also used for deriving transmission rates with heterodyne and homodyne measurements at the channel output. Classical capacity and transmission rates are presented within a unique framework where the rates can be treated as logarithmic approximations of the capacity.**

***Index Terms*—Classical capacity of quantum channels, classical transmission rates of quantum channels, Gaussian quantum channels, quantum information.**

I. Introduction

QUANTUM channels are every means that convey quantum systems on whose states information is encoded. Formally, they are quantum maps from input to output states [1]. The maximum rate at which information can be reliably transmitted through a quantum channel defines its capacity. Actually, one can define several capacities depending on the kind of information transmitted (classical or quantum) and on the additional resources used in the transmission [2].

Evaluation of quantum channel capacities is one of the most important and difficult problems of quantum information theory. Gaussian channels, which maps input Gaussian states into output Gaussian states, are among the simplest models allowing capacities investigation [3]. They are also relevant for experimental implementations in quantum optics [4] and for security analysis in continuous variables quantum key distribution [5], [41].

A paradigmatic example of Gaussian quantum channel is the lossy bosonic channel [3], [6], [45] where states lose energy "en route" from the sender to the receiver. The term bosonic arises because each input (respectively, output) is represented by an optical bosonic field mode. In turn, the effect of losses is usually modeled by letting each input mode interact with an environment mode through a rotation (beam splitter) transform whose angle (transmissivity) determines the loss rate [4].

The classical capacity and the classical assisted capacity for such a channel were evaluated in [7] and [8] by assuming each environment mode in the vacuum state. Subsequently, also the quantum capacity has been derived [9]. However, when more general states of the environment are taken into account, e.g., nonseparable ones giving rise to memory effect [10], the evaluation of capacities becomes much more demanding. Attempts have been carried out in [11] and [12] by resorting to specific parameters' ranges and numerics.

There are different ways to introduce memory effects in such channels (see, e.g., [11] and [13]). Here, we shall refer to the method first presented in [10]. Moreover, we will solely consider classical capacity and classical information transmission rates.

Finding classical capacity results in the constrained maximization of Holevo information [14]–[16] over input states, where constraints appear due to the restriction on input energy. We shall confine our attention to Gaussian inputs which, in practice, are the most important set of states and are also conjectured to be optimal [17], [42]–[44]. However, this gives rise to a maximization problem which in general might be not spectral; therefore, we shall consider only that class of memory models which result in a spectral problem. The latter will allow us to split the maximization for memory channel in two steps: the maximization inside each channel's mode (use) respecting its own energy restriction [it gives the capacity for the single channel use (single-mode)], and a further optimization of the distribution of total input energy over different channel modes (uses). This essential simplification is possible thanks to the obtained proof of concavity for one shot capacity over input energy. Such a proof will also allow us to make an important step towards the additivity property for the capacity of memoryless channel (see also [18]).

As far as the first maximization step involves the optimization inside each channel mode separately, we shall first discuss the single channel use (single-mode). It can be shown that its environment is characterized by two parameters: the amount of squeezing and the average amount of thermal photons. To completely specify the channel usage we also have to consider the transmissivity value and the input energy restriction. Thus, the classical capacity is found to be a monotonic function of all these parameters except of the environment squeezing. This makes the

Manuscript received July 08, 2009; revised August 02, 2011; accepted December 20, 2011. Date of publication March 20, 2012; date of current version August 14, 2012. This work was supported by the European Commission's seventh Framework Programme (FP7/2007-2013) under Grant 213681 and by the ULB funding "Bourses Post-doctorales IN – Ouvertures internationales".

O. V. Pilyavets was with the School of Science and Technology, Physics Division, University of Camerino, I-62032 Camerino, Italy, and also with the P. N. Lebedev Physical Institute, 119991 Moscow, Russia. He is now with the Université Libre de Bruxelles, 1050 Ixelles, Belgium (e-mail: pilyavets@gmail.com).

C. Lupo and S. Mancini are with the School of Science and Technology, Physics Division, University of Camerino, 62032 Camerino, Italy (e-mail: cosmo.lupo@unicam.it; stefano.mancini@unicam.it).

Communicated by P. Hayden, Associate Editor for Quantum Information Theory.

Digital Object Identifier 10.1109/TIT.2012.2191475

latter a specific parameter indicating different channel's regimes. In particular, it turns out that the capacity does not depend on any parameters except the input energy if the environment squeezing tends to infinity (see also [11] and [12]). Then, we shall deeply study this behavior putting forward the existence of *critical parameters* that characterize the general behavior of the channel. We will also find out *supercritical parameters*, which in turn characterize the behavior of the critical parameters, and can be somehow regarded as fundamental constants.

We shall then move to the multimode channel setting to address the second maximization step. This will be done by resorting to convex separable programming techniques [19], [20] and will allow us to draw conclusions about the memory channel. This has became a palatable subject because of the possibility of enhancing the memoryless capacity [21]. This fact gives evidence of the superadditive phenomenon for quantum memory channels. However, in order to establish the superadditivity of the memory channel, one has to fairly compare different environments, by, e.g., using the same energy constraints and purity. We shall investigate this problem showing optimality of nonhomogenuous distribution of energy over modes for some channel's parameters, which happens due to nonmonotonic dependence of the one-shot capacity from the environment squeezing discussed previously. That can be interpreted as violation of mode symmetry, because the optimization problem is completely symmetric over channel modes. In turn, this mode symmetry violation can be related to the quadrature symmetry violation occurring in the single-mode channel. Then, we can conclude that capacity is superadditive if mode symmetry is violated and additive otherwise.

It worth noticing that also the recent study [22] about the effect of noise correlation on the capacity of additive Gaussian noise channel can be brought back to the previously sketched approach.

Finally, we will make use of the developed methods for deriving transmission rates which are even more relevant than capacity for practical purposes. Specifically, we will account for the most common continuous variable measurements at the channel output, namely heterodyne and homodyne measurements [23]. Preliminary studies on such rates for lossy memory channel have been performed in [24] (see also [45]). Here, throughout this paper, capacity and transmission rates are presented in the same framework showing an unexpected parallelism between these quantities. Actually, within this framework, the rates result as logarithmic approximations to the capacity. Similarly to the capacity, in general, they are also subjected to violation of quadrature and mode symmetry, which will allow us to pose the optimal memory problem and calculate the critical parameters for the rates as well.

This paper is organized as follows. In Section II, Gaussian channels are introduced. In Section III, the classical capacity together with the information transmission rates is defined. In Section IV, classical capacity and transmission rates for single-mode lossy bosonic channel are evaluated. In Section V, the role of single-mode channel parameters is discussed by evaluating critical and supercritical parameters for capacity and rates. In Section VI, the capacity and rates for the multimode channel are evaluated and a particular memory model is studied. Section VII draws conclusions.

II. Gaussian Quantum Channels

Quantum mechanics in continuous variables can be introduced independently from Dirac approach as Weyl star-product (also known as Weyl calculus [25]) which operates with Weyl symbols defined on system's phase space $(\mathbf{q}, \mathbf{p})$. Quadratures $\mathbf{q}$ and $\mathbf{p}$ for the system with n degrees of freedom are n-dimensional vectors of canonical variables. In the following, it will be useful to consider a vector

$$\mathbf{x} := (\mathbf{q}, \mathbf{p}) = (q_1, \ldots, q_n, p_1, \ldots, p_n). \tag{1}$$

Any quantum state, usually represented as a density operator $\hat{\rho}$ in the Hilbert space $\mathcal{H} \equiv \otimes^n L_2(\mathbb{R})$, can be specified in the aforementioned framework by its *Wigner function* $W(\mathbf{q}, \mathbf{p})$, which is a Weyl symbol of $\hat{\rho}$. Its relation with the density matrix in the $\mathbf{q}$ representation reads[1]

$$W(\mathbf{q}, \mathbf{p}) = \int \rho\left(\mathbf{q} + \frac{\mathbf{u}}{2}, \mathbf{q} - \frac{\mathbf{u}}{2}\right) e^{-i\mathbf{p}\mathbf{u}} d\mathbf{u}$$

$$\rho(\mathbf{q}, \mathbf{q}') = \frac{1}{(2\pi)^n} \int W\left(\mathbf{p}, \frac{\mathbf{q} + \mathbf{q}'}{2}\right) e^{i\mathbf{p}(\mathbf{q} - \mathbf{q}')} d\mathbf{p}.$$

In this study, we apply Weyl calculus to the system of n 1-D harmonic oscillators; therefore, we will call these degrees of freedom as *modes*. Furthermore, we restrict all possible quantum states of these oscillators by *Gaussian* ones, which are defined as follows. The quantum state $\hat{\rho}$ is called Gaussian if its Wigner function is Gaussian, i.e., such state can be completely specified by quadratures covariance matrix V and vector $\mathbf{a}$ which are parameters (the second and first moments) of its Wigner function[2]:

$$\hat{\rho} \leftrightarrow \{\mathbf{a}, V\} \leftrightarrow W(\mathbf{x}) = \frac{1}{\sqrt{\det V}} e^{-\frac{1}{2}\left(\mathbf{x} - \mathbf{a}, V^{-1}(\mathbf{x} - \mathbf{a})\right)} \tag{2}$$

where $(,)$ stands for the real scalar product. The quantities to be studied do not depend on the displacement $\mathbf{a}$; therefore, each quantum state and each classical[3] Gaussian distribution will be solely labeled by their quadratures covariance matrices, e.g., $\hat{\rho} \leftrightarrow V$.

Notice that any Gaussian distribution of the form (2) is the Wigner function of some quantum state if its covariance matrix V satisfies the Heisenberg uncertainty condition [25], [26]

$$V + \frac{i\Sigma}{2} \geqslant 0 \tag{3}$$

where

$$\Sigma = \begin{pmatrix} \mathbb{O}_n & \mathbb{I}_n \\ -\mathbb{I}_n & \mathbb{O}_n \end{pmatrix} \tag{4}$$

[1]Throughout this paper, it is assumed commutation relations between canonical operators $\hat{q}_h, \hat{p}_l$ belonging to $\mathcal{H}$ to be $[\hat{q}_h, \hat{p}_l] = i\delta_{hl}$ (with δ the Kronecker symbol and $\hbar = 1$), and normalization of a n-mode Wigner function to be $\int W(\mathbf{x})\, d\mathbf{x} = (2\pi)^n$.

[2]Notice that (2) completely specifies the ordering of covariances in matrix V as corresponding to the vector (1).

[3]We will use convention accepted in quantum information theory, where random variables and probability densities of standard (classical) information theory are called *classical* to distinguish them from *quasi-probability* distributions (and variables associated with them) appearing in quantum setting.

is the symplectic form with $\mathbb{O}_n$ and $\mathbb{I}_n$ the $n \times n$ null and identity matrices, respectively. The eigenvalues of ΣV are $2n$ purely imaginary numbers $\{\pm i\nu_k\},\ k = 1, \ldots, n$, where $\{\nu_k\}$ are called *symplectic eigenvalues* of V. Condition (3) can be equivalently written as inequalities $\nu_k \geqslant 1/2$, which are saturated by pure Gaussian states [4], [25].

A *Gaussian quantum channel* acting on n modes is by definition a *completely positive* and *trace preserving* map defined on the set of quantum states, which maps any n-mode Gaussian state into a n-mode Gaussian state. As a consequence, it is any map Φ_n of moments [6]

$$\{\mathbf{a}, V\} \mapsto \left\{X_n^\top \mathbf{a} + \mathbf{d}_n, X_n^\top V X_n + Y_n\right\} \tag{5}$$

characterized by the triad $(\mathbf{d}_n, X_n, Y_n)$, where X_n and Y_n are two real $2n \times 2n$ matrices obeying the inequality

$$Y_n + \frac{i}{2}\left(\Sigma - X_n^\top \Sigma X_n\right) \geqslant 0$$

with $Y_n \geqslant 0$ and symmetric and $\mathbf{d}_n \in \mathbb{R}^{2n}$ a displacement vector.

A very special case is that of the *memoryless channel*, for which $\Phi_n = \Phi_1^{\otimes n}$ is the direct product of n identical maps, i.e., a single-mode Gaussian channel used n times. It is, hence, characterized by a triad

$$\left(\bigoplus^n \mathbf{d}_1, \bigoplus^n X_1, \bigoplus^n Y_1\right)$$

where we have denoted

$$\begin{aligned} \mathbf{d}_1 &:= (d_q, d_p)^\top \\ \bigoplus^n \mathbf{d}_1 &:= (d_q, \ldots, d_q, d_p, \ldots, d_p)^\top \in \mathbb{R}^{2n}. \end{aligned}$$

Notice that X_1 and Y_1 are 2×2 matrices, whose entries are scalars, and the direct sums $\bigoplus^n X_1$ and $\bigoplus^n Y_1$ are 2×2 matrices, whose entries are $n \times n$ diagonal matrices.[4] Loosely speaking, the memoryless channel acts equally and independently on each of its use.

More generally, we can consider the case of a *quantum channel with memory* (or simply a *memory channel*). It is any channel which is *not* memoryless. Making no assumption on additional structures that might be present (e.g., causality, invariance under time translations), we can only say that $\Phi_n \neq \Phi_1^{\otimes n}$ or

$$(\mathbf{d}_n, X_n, Y_n) \neq \left(\bigoplus^n \mathbf{d}_1, \bigoplus^n X_1, \bigoplus^n Y_1\right).$$

The memory channel can be interpreted as a framework to describe correlations between channel actions corresponding to different channel uses.

III. Classical Capacity

The Gaussian quantum channel can be used to transmit classical information by *encoding* a classical stochastic continuous variable $\alpha \in \mathbb{R}^{2n}$, distributed according to a probability density P_α, into a set of quantum states (Wigner functions) W_α. The maximum rate at which classical information can be reliably sent through the channel defines its *classical capacity*. In the case of a memoryless quantum channel, its classical capacity is given by [15], [16]

$$C = \lim_{n \to \infty} \frac{\chi\left(\Phi_n\right)}{n} \tag{6}$$

where the *Holevo function* χ evaluated on n channel uses is defined as[5]

$$\chi\left(\Phi_n\right) = \max_{\{W_\alpha, P_\alpha\}} \left\{ S\left[\int \Phi_n\left(W_\alpha\right) P_\alpha d\alpha\right] - \int S\left[\Phi_n\left(W_\alpha\right)\right] P_\alpha d\alpha \right\} \tag{7}$$

with $\Phi_n = \Phi_1^{\otimes n}$ and S is the von Neumann entropy. Thus, the computation of the memoryless capacity[6] is based on the optimization over all input ensembles W_α, including those made of states which are entangled among different channel uses.

If the input states are restricted to an ensemble of product states, it is reasonable to consider the so-called *one-shot capacity*

$$C_1 = \chi\left(\Phi_1\right)$$

obtained from (6) and (7) by assuming $n = 1$. Clearly, the one-shot capacity is a lower bound on the memoryless capacity. If these two quantities coincide, the Holevo function is said to be additive. In turn, additivity of the Holevo function dramatically simplifies the problem of evaluating the memoryless capacity. Even though the Holevo function has been shown to be additive for several relevant channels, this property does not always hold [27].

Moving to the general case, one could be tempted to generalize the formulas (6) and (7) to the case of memory channels by applying them for $\Phi_n \neq \Phi_1^{\otimes n}$. Quite generally, we can say that relation (6) only provides an upper bound for the capacity of the memory channel [28]. Indeed, it has been proven [29] that it coincides with the memory channel capacity for the class of so-called *forgetful* channels.

Thus, on the one hand, we can define the upper bound

$$\bar{C} := \lim_{n \to \infty} \bar{C}_n, \quad \bar{C}_n := \frac{\chi(\Phi_n)}{n}.$$

On the other hand, for any n, one can look at n uses of the channel described by Φ_n as a single n-mode memoryless channel. Its one-shot capacity found as maximum over the set of Gaussian states provides a lower bound on the capacity of the memory channel [12]

$$\underline{C}_n := \frac{\chi_G(\Phi_n)}{n}. \tag{8}$$

[4]Such a convention was chosen to be consistent with the ordering (1) and the symplectic form (4).

[5]Contrarily to the original definition [16], in this paper, we incorporate the maximum over input states in the Holevo function.

[6]As far as we consider only classical channel capacity, it will be often called simply the capacity.

Taking the limit over n, we can as well define the lower bound[7]

$$\underline{C} := \lim_{n\to\infty} \underline{C}_n. \tag{9}$$

Since the capacity (in sense of aforementioned definitions) in continuous variables case turns out to be infinite, some physically motivated constraints must be specified to avoid meaningless results. A typical choice in the framework of Gaussian channels is to impose a restriction on the maximal average input energy per channel use. As far as we are considering the system of n single-mode oscillators (see Section II) with channel uses corresponding to oscillators modes, this constraint reads[8]

$$\frac{1}{2n(2\pi)^n}\int\left(\int W_\alpha(\mathbf{x})P_\alpha d\alpha\right)\mathbf{x}^2 d\mathbf{x} \leqslant N+\frac{1}{2} \tag{10}$$

where N represents the maximum number of excitations (photons) per mode in average.

Finally, let us consider *Gaussian encoding* W_α, P_α used to calculate χ_G. For n uses of the quantum channel, we fix a reference n-mode Gaussian state, with zero mean, which is described by the Wigner function $\{0, V_{\rm in}\}$ [see definition (2)]. A classical variable α will be encoded by applying a displacement operation on the reference state, thus obtaining Wigner function $\{\sqrt{2}\alpha, V_{\rm in}\}$. We assume the stochastic variable α to be itself distributed according to the Gaussian probability density distribution with zero mean:

$$P_\alpha = \frac{1}{(2\pi)^n\sqrt{\det V_{\rm mod}}}e^{-\left(\alpha, V_{\rm mod}^{-1}\alpha\right)}.$$

Hence, the corresponding ensemble state

$$\int W_\alpha P_\alpha d\alpha$$

is also Gaussian and described by a Wigner function $\{0, \bar{V}_{\rm in}\}$, where

$$\bar{V}_{\rm in} = V_{\rm in} + V_{\rm mod}. \tag{11}$$

Quadratures covariance matrices of output state and output average state below will be labeled by $V_{\rm out}$ and $\bar{V}_{\rm out}$, respectively:

$$\begin{aligned} V_{\rm out} &\leftrightarrow \Phi_n\left(W_\alpha\right) \\ \bar{V}_{\rm out} &\leftrightarrow \int \Phi_n\left(W_\alpha\right) P_\alpha \, d\alpha. \end{aligned} \tag{12}$$

The restriction to Gaussian states, which are mapped into Gaussian states by Gaussian channels, dramatically simplifies the problem, since the complexity of specifying Gaussian states is polynomial in the number n of modes [see (2)]. Moreover, Gaussian states are conjectured to be optimal inputs for Gaussian channels [17], [42]–[44].

[7]Throughout this paper, for the sake of simplicity, we will often refer to this lower bound as simply the capacity.

[8]We assume quantum states to have zero mean, i.e., $\langle \mathbf{x} \rangle = 0$.

The von Neumann entropy S of an n-mode Gaussian state $\{\mathbf{a}, V\}$ is function of symplectic eigenvalues ν_k of matrix V[4], [46]:

$$S(V) = \sum_{k=1}^{n} g\left(\nu_k - \frac{1}{2}\right) \tag{13}$$

where g is defined as

$$g(v) := (v+1)\log_2(v+1) - v\log_2 v.$$

The Holevo-χ quantity for the set G of Gaussian states can be derived from (7) and (13). It equals [3]

$$\chi_n = \max_{V_{\rm in}, V_{\rm mod}} \sum_{k=1}^{n}\left[g\left(\bar{\nu}_k - \frac{1}{2}\right) - g\left(\nu_k - \frac{1}{2}\right)\right] \tag{14}$$

where χ_n is a shorthand notation for $\chi(\Phi_n)$. In turn, the quantities $\bar{\nu}_k$ and ν_k are the symplectic eigenvalues of $\bar{V}_{\rm out}$ and $V_{\rm out}$, respectively. Finally, the input energy constraint (10) for Gaussian states can be written in terms of the covariance matrices as

$$\frac{{\rm Tr}\bar{V}_{\rm in}}{2n} \leqslant N + \frac{1}{2}. \tag{15}$$

A. Estimating the Classical Capacity

As we have seen, the evaluation of the classical capacity practically reduces to the evaluation of the function (13). Notice that $g(v)$ is not analytic in the neighborhood of zero where its asymptotic value is $-v\log_2 v$. Also, the function $g\left(v-\frac{1}{2}\right)$ is not analytic in the neighborhood of infinity, where its asymptotic value is $\log_2 v$. By subtracting this logarithm part, we get the analytic function in the region $v \geqslant \frac{1}{2}$ which has its Laurent series (see also [30])

$$g\left(v-\frac{1}{2}\right) = \log_2 v + \frac{1}{\ln 2}\left[1 - \frac{1}{2}\sum_{j=1}^{\infty}\frac{(2v)^{-2j}}{j(2j+1)}\right] \tag{16}$$

written in the neighborhood of infinity. In particular, to the zeroth-order approximation, it is

$$g\left(v-\frac{1}{2}\right) = \log_2 v + \frac{1}{\ln 2} \tag{17}$$

where we have neglected terms of the order $O\left(v^{-2}\right)$. Allowing perturbation of logarithm by the first terms in the series (16) we can also construct next-order approximations.

In what follows, it will be convenient to introduce the function

$$g_j(v) := v^j g^{(j)}\left(v-\frac{1}{2}\right) \tag{18}$$

where $j = 0, 1, 2, \ldots$. Thus

$$\begin{aligned} g_0(v) &= g\left(v - \frac{1}{2}\right) \\ g_1(v) &= vg'\left(v - \frac{1}{2}\right) = v \log_2 \frac{v + \frac{1}{2}}{v - \frac{1}{2}} \\ g_2(v) &= v^2 g''\left(v - \frac{1}{2}\right) = -\frac{v^2}{\left(v^2 - \frac{1}{4}\right)\ln 2} \end{aligned} \tag{19}$$

and so on. It also has simple rules for derivatives, e.g.,

$$g_1'(v) = \frac{g_1(v) + g_2(v)}{v}, \quad g_2'(v) = \frac{2g_2(v) + g_3(v)}{v}.$$

In particular, we have $g_1(v) \equiv (\ln 2)^{-1}$ to zeroth-order approximation and

$$g_1(v) = \frac{1}{\ln 2}\left[1 + \frac{1}{12v^2}\right] \tag{20}$$

to first-order approximation. Notice that by using (17), we have, at the lowest order

$$\chi_n^{(\log)} = \max_{V_{\rm in}, V_{\rm mod}} \sum_{k=1}^{n} \log_2 \frac{\bar{\nu}_k}{\nu_k}. \tag{21}$$

The value $\underline{C}_n$ calculated through approximation (21) below will be denoted as $\underline{C}_n^{(\log)}$ and called *logarithmic approximation to capacity*. In turn, the quantity $\underline{C}_n$ will be called *zeroth-order approximation to capacity* and denoted by $\underline{C}_n^{(0)}$, if actual maximum over $V_{\rm in}$ and $V_{\rm mod}$ is not taken in (14), but symplectic eigenvalues ν_k and $\bar{\nu}_k$ are chosen instead to be those at which the maximum in (21) is achieved. Thus, $\underline{C}_n^{(0)}$ is given by substitution of the approximate symplectic eigenvalues into the exact relation for Holevo-χ quantity.

B. Examples of Gaussian Channels

There are two types of noises that are mostly relevant for experimental setups: *attenuation* and *addition of classical noise*. The so-called *lossy (bosonic) channels* describe the attenuation, while the *additive (classical) noise channels* take into account only the addition of classical noise. For a discussion of the capacity of the other classes of Gaussian channels, in the single-mode case, see [31]. The lossy channels play a prominent role and below we will focus our attention to them. They are characterized by the map (5) with the matrices

$$X = \sqrt{\eta}\,\mathbb{I}_{2n}, \quad Y = (1 - \eta)V_{\rm env}. \tag{22}$$

Here, $V_{\rm env}$ denotes the $2n \times 2n$ covariance matrix of the channel environment that "contaminates" the input signal, which is attenuated by the channel's *transmissivity* $\eta \in [0, 1]$. In particular, the lossy bosonic channel acts as a rotation (beam splitter) on the canonical quadratures and gives rise to the following relation among the covariance matrices [6]:

$$V_{\rm out} = \eta\, V_{\rm in} + (1 - \eta)\, V_{\rm env} \tag{23}$$

$$\bar{V}_{\rm out} = \eta\,(V_{\rm in} + V_{\rm mod}) + (1 - \eta)\, V_{\rm env}. \tag{24}$$

In fact, these transformations follow from the definitions (5), (12), and (22). Next [see (112)], it will be shown that the capacity is a monotonically increasing function of the average number of input photons per mode (channel use) N; therefore, we shall constrain the input energy using the equality in (15), i.e.,

$$\frac{1}{2n}{\rm Tr}(V_{\rm in} + V_{\rm mod}) = N + \frac{1}{2}. \tag{25}$$

The additive noise channels are described by similar transformations [6]

$$V_{\rm out} = V_{\rm in} + V_{\rm env} \tag{26}$$

$$\bar{V}_{\rm out} = V_{\rm in} + V_{\rm mod} + V_{\rm env} \tag{27}$$

following from (5) if $X = \mathbb{I}_{2n}$ and $Y = V_{\rm env}$, where $V_{\rm mod}$ and $V_{\rm env}$ correspond to classical distribution, while $V_{\rm in}$ should satisfy the uncertainty relation. Notice that similarity between (26), (27) and (23), (24) makes the extension of the method we are going to develop to the additive noise channel straightforward. In particular, a similar approach has been recently used in [22].

C. Heterodyne and Homodyne Rates

As far as the general optimization approach to find the Holevo function (14) is also applicable to information transmission rates, we are going to consider these as well and compare them with the capacity.

Suppose that the matrices $V_{\rm in}$, $V_{\rm mod}$, and $V_{\rm env}$ are block diagonal, i.e., can be written in the form

$$V_{\rm ind} = \begin{pmatrix} V_{{\rm ind},qq} & \mathbb{O}_n \\ \mathbb{O}_n & V_{{\rm ind},pp} \end{pmatrix} \tag{28}$$

where $\mathbb{O}_n$ was defined by (4) and "ind" may stand for "in," "mod," or "env." Moreover, let us assume that their diagonal blocks mutually commute (including blocks taken from different matrices). In such a case by considering the average information accessible by performing *heterodyne* measurement on each single channel output (joint measurement of q and p quadratures), one can get the *heterodyne rate* [11]

$$R^{(\rm het)} := \lim_{n\to\infty} R_n^{(\rm het)} \tag{29}$$

$$R_n^{(\rm het)} = \frac{1}{2n} \max_{V_{\rm in}, V_{\rm mod}} \log_2 \det \left[\left(\bar{V}_{\rm out} + \frac{\mathbb{I}_{2n}}{2}\right)\left(V_{\rm out} + \frac{\mathbb{I}_{2n}}{2}\right)^{-1}\right]. \tag{30}$$

Analogously, by considering *homodyne* measurement on each single-channel output (measurement of $u_\star$ quadrature, where $u_\star$ is a placeholder for q or p), one can find the *homodyne rate* [11]

$$R^{(\rm hom)} := \lim_{n\to\infty} R_n^{(\rm hom)}$$

$$R_n^{(\rm hom)} = \frac{1}{2n} \max_{V_{\rm in}, V_{\rm mod}} \log_2 \det \left[\bar{V}_{{\rm out},u_\star u_\star} V_{{\rm out},u_\star u_\star}^{-1}\right] \tag{31}$$

where notations of matrix blocks are the same as in (28).

IV. Single Channel Use

Let us consider single use (single mode) of the lossy bosonic channel. Its description requires the consideration of 2×2 co-

variance matrices of the general form to solve the optimization problem. However, all the properties can be found by taking all involved matrices in the diagonal form. This can be done thanks to the following *input purity theorems*:

Theorem 1: For the single use of the lossy bosonic channel, the 2×2 matrices $V_{\rm in}$ and $V_{\rm mod}$, at which the maximum of the Holevo function over Gaussian states is achieved, are simultaneously diagonalizable together with $V_{\rm env}$. Moreover, the optimal matrix $V_{\rm in}$ corresponds to a pure state.

Proof: The proof[9] is reported in Appendix A. ■

Theorem 2: Let us consider the single use of the lossy bosonic channel characterized by 2×2 diagonal covariance matrices $V_{\rm env}$, $V_{\rm in}$, and $V_{\rm mod}$; then, the maxima for both heterodyne and homodyne rates are provided by pure input states.[10]

Proof: The proof is reported in Appendix B. ■

Let us discuss these theorems in the context of rates. Remember that in the case of 2×2 matrices, the assumptions used to derive general relations (30) and (31) are equivalent to diagonality of all involved matrices; therefore, optimality of pure input states for rates is guaranteed by theorem 2. Moreover, if one conjectures that the relations (30) and (31) hold also for 2×2 matrices of general form (i.e., nondiagonal), then commutativity of matrices together with input purity are guaranteed by theorem 1, whose extension to the case of rates is straightforward.

Thus, below, it is always assumed without loss of generality that all the matrices are already diagonalized and the input state is pure. Furthermore, unless otherwise stated, in the following, it is assumed[11] that $0 < \eta < 1$.

A. System of Notations

Let us introduce the system of notations that will be used hereafter. Any single-mode state labeled by index "ind" will be referred to by its quadratures covariance matrix $V_{\rm ind}$ parametrized by $\mathcal{N}_{\rm ind} \in \mathbb{R}_+$ and $s_{\rm ind} \in \mathbb{R}$ as

$$V_{\rm ind} := V(\mathcal{N}_{\rm ind}, s_{\rm ind}) = \left[\mathcal{N}_{\rm ind} + \frac{1}{2}\right] \begin{pmatrix} e^{s_{\rm ind}} & 0 \\ 0 & e^{-s_{\rm ind}} \end{pmatrix}. \tag{32}$$

In particular, "ind" may stand for "in," "mod," "env," or "out" for the cases of input, modulation, environment, or output covariance matrices, respectively. The quantity $s_{\rm ind}$ will be referred to as *squeezing* in "ind." The quantity $\mathcal{N}_{\rm ind}$ will always be written in "Lucida Calligraphy" font and called *average amount of thermal photons* in the state "ind." We also define the *average amount of photons* $N_{\rm ind}$ in the state "ind" as

$$\frac{1}{2}{\rm Tr}(V_{\rm ind}) = N_{\rm ind} + \frac{1}{2} \tag{33}$$

which is equivalent to the relation

$$N_{\rm ind} = \left(\mathcal{N}_{\rm ind} + \frac{1}{2}\right) \cosh s_{\rm ind} - \frac{1}{2}. \tag{34}$$

In the following, we will usually omit the word "average" referring to the quantities $\mathcal{N}_{\rm ind}$ and $N_{\rm ind}$. All the quantities related to some overlined matrix will be also overlined, i.e., $\bar{V}_{\rm ind}$ equals $V(\overline{\mathcal{N}}_{\rm ind}, \bar{s}_{\rm ind})$ and has amount of photons $\bar{N}_{\rm ind}$. In order to indicate that some channel parameters are related with homodyne or heterodyne rates (they are defined later in Section IV-B) the upper indices "(hom)" and "(het)" will be used. The only exceptions from the previous rules are: the index "env" will be omitted for quantities which represent the squeezing (or its particular values) in channel environment, e.g., $s \equiv s_{\rm env}$; the index "in" and overlining will be omitted for the quantities which represent the average amount of photons (or its particular values, e.g., thresholds) in averaged input state $\bar{V}_{\rm in}$ [see (11)] and its "heterodyne analog" $\bar{V}_{\rm in}^{(\rm het)}$, e.g., $N \equiv \bar{N}_{\rm in} \equiv \bar{N}_{\rm in}^{(\rm het)}$.

Notice that the state $V(\mathcal{N}_{\rm ind}, s_{\rm ind})$ is *pure* if $\mathcal{N}_{\rm ind} = 0$ and *mixed* otherwise, is *squeezed* if $s_{\rm ind} \neq 0$, is *thermal* if $\mathcal{N}_{\rm ind} \neq 0$ and $s_{\rm ind} = 0$, is *thermal squeezed* if both $\mathcal{N}_{\rm ind} \neq 0$ and $s_{\rm ind} \neq 0$, and is *vacuum* if both $\mathcal{N}_{\rm ind} = 0$ and $s_{\rm ind} = 0$.

The eigenvalues of each matrix will be denoted by the first character of matrix index. Then, the eigenvalue which is the first diagonal element corresponds to quadrature q; therefore, it will be labeled by index q (analogously, by p for the second diagonal element). However, as far as both quadratures enter all the relations in the same way, instead of specifying the quadrature q or p usually, we will use index u as a placeholder for q or p. Also, we will use the rule: if $u = q$, then $u_\star = p$, and vice versa. In particular, we will refer to the eigenvalues of matrices $V_{\rm in}$, $V_{\rm mod}$, $V_{\rm env}$, $V_{\rm out}$, and $\bar{V}_{\rm out}$ as i_u, m_u, e_u, o_u, and $\bar{o}_u$, respectively. For instance, we have $V_{\rm env} = {\rm diag}(e_q, e_p)$ for the environment matrix. Also, without loss of generality, in the following, it is always assumed that if environment eigenvalues are nonequal, then $e_u > e_{u_\star}$. As far as only the single-mode case is discussed in this section, index k will be omitted for symplectic eigenvalues ν_k and $\bar{\nu}_k$ [they were introduced in (14)]. Also, index n will be omitted for χ- and $\underline{C}$- and R-quantities [e.g., see (8), (14), (21), (30), and (31)]. To simplify the notations, in what follows, we allow each of these quantities to stand either for the result of the maximization or for the function to maximize, depending on context.

Taking into account that the symplectic eigenvalue for 2×2 matrix V is $\sqrt{\det V}$, we have for the matrices $V_{\rm out}$ and $\bar{V}_{\rm out}$ the relations

$$\nu = \sqrt{o_u o_{u_\star}}, \quad \bar{\nu} = \sqrt{\bar{o}_u \bar{o}_{u_\star}} \tag{35}$$

where

$$\begin{aligned} o_u &= \eta\, i_u + (1-\eta)\, e_u \\ \bar{o}_u &= \eta\, (i_u + m_u) + (1-\eta)\, e_u \\ o_{u_\star} &= \eta\, i_{u_\star} + (1-\eta)\, e_{u_\star} \\ \bar{o}_{u_\star} &= \eta\, (i_{u_\star} + m_{u_\star}) + (1-\eta)\, e_{u_\star}. \end{aligned} \tag{36}$$

[9] In the generic setting, the optimality of pure input states has been proven in [15]. However, in our case, the Holevo function has to be optimized under the constraint of Gaussian input states and energy restriction. For these reasons, it is worth proving this property explicitly for the considered setting.

[10] Notice that extension of Theorem 2 to the case of Holevo function is straightforward, being it a particular case of Theorem 1.

[11] This is done because the limit case $\eta = 1$ (noiseless channel) is considered separately in Section IV-I and the limit case $\eta = 0$ (infinitely noisy channel) is trivial giving zero capacity and rates.

B. Heterodyne Variables

In the following, it will be convenient to introduce the *heterodyne environment matrix*

$$V_{\rm env}^{(\rm het)} := V_{\rm env} + \frac{\mathbb{I}_2}{2(1-\eta)}$$

whose eigenvalues are

$$e_u^{(\rm het)} = e_u + \frac{1}{2\,(1-\eta)}, \quad e_{u_\star}^{(\rm het)} = e_{u_\star} + \frac{1}{2\,(1-\eta)}. \quad (37)$$

Replacing $V_{\rm env}$ by $V_{\rm env}^{(\rm het)}$ in the relations (23) and (24), one can also define the "heterodyne version" of the other matrices:

$$V_{\rm out}^{(\rm het)} = \eta\, V_{\rm in}^{(\rm het)} + (1-\eta)\, V_{\rm env}^{(\rm het)} \quad (38)$$

$$\bar{V}_{\rm out}^{(\rm het)} := \eta \left(V_{\rm in}^{(\rm het)} + V_{\rm mod}^{(\rm het)} \right) + (1-\eta)\, V_{\rm env}^{(\rm het)} \quad (39)$$

where the eigenvalues of matrices $V_{\rm out}$, $\bar{V}_{\rm out}$, $V_{\rm out}^{(\rm het)}$, and $\bar{V}_{\rm out}^{(\rm het)}$ are related as follows:

$$o_u^{(\rm het)} = o_u + \frac{1}{2}, \quad o_{u_\star}^{(\rm het)} = o_{u_\star} + \frac{1}{2},$$
$$\bar{o}_u^{(\rm het)} = \bar{o}_u + \frac{1}{2}, \quad \bar{o}_{u_\star}^{(\rm het)} = \bar{o}_{u_\star} + \frac{1}{2}.$$

Then, one can define symplectic eigenvalues in the heterodyne setting (similarly to (35)) by the relations

$$\nu^{(\rm het)} = \sqrt{o_u^{(\rm het)} o_{u_\star}^{(\rm het)}}, \quad \bar{\nu}^{(\rm het)} = \sqrt{\bar{o}_u^{(\rm het)} \bar{o}_{u_\star}^{(\rm het)}}. \quad (40)$$

The average amount of photons $N_{\rm env}^{(\rm het)}$ in the heterodyne environment

$$V_{\rm env}^{(\rm het)} = V\left(\mathcal{N}_{\rm env}^{(\rm het)}, s^{(\rm het)} \right)$$

[see (32)] can be introduced using the standard relation (33). The parameters of the environment matrices $V_{\rm env} = V(\mathcal{N}_{\rm env}, s)$ and $V_{\rm env}^{(\rm het)}$ are related by

$$\left[\mathcal{N}_{\rm env}^{(\rm het)} + \frac{1}{2} \right]^2 = \left[\mathcal{N}_{\rm env} + \frac{1}{2} + \frac{1}{2\,(1-\eta)} \right]^2 + \frac{N_{\rm env} - \mathcal{N}_{\rm env}}{1-\eta} \quad (41)$$

$$s^{(\rm het)} = \frac{1}{2} \ln \frac{1 + (1-\eta)(2\,\mathcal{N}_{\rm env} + 1)\, e^{s}}{1 + (1-\eta)(2\,\mathcal{N}_{\rm env} + 1)\, e^{-s}}, \quad (42)$$

$$s = \frac{1}{2} \ln \frac{1 - (1-\eta)\left(2\,\mathcal{N}_{\rm env}^{(\rm het)} + 1 \right) e^{s^{(\rm het)}}}{1 - (1-\eta)\left(2\,\mathcal{N}_{\rm env}^{(\rm het)} + 1 \right) e^{-s^{(\rm het)}}} \quad (43)$$

$$N_{\rm env}^{(\rm het)} = N_{\rm env} + \frac{1}{2\,(1-\eta)}. \quad (44)$$

In particular, for thermal environment $V(\mathcal{N}_{\rm env}, 0)$, we have $N_{\rm env}^{(\rm het)} = \mathcal{N}_{\rm env}^{(\rm het)}$ and

$$\mathcal{N}_{\rm env}^{(\rm het)} = \mathcal{N}_{\rm env} + \frac{1}{2\,(1-\eta)}.$$

Notice that the heterodyne environment $V_{\rm env}^{(\rm het)}$ is squeezed if and only if $V_{\rm env}$ is squeezed.

The quantities with upper index "het" defined in this section will allow us to simplify the relations for the heterodyne rate. We shall refer to them as *heterodyne variables*. The latter, which are eigenvalues, will be also called *heterodyne eigenvalues* to distinguish them from *standard* eigenvalues (of $V_{\rm in}$, $V_{\rm env}$, $V_{\rm out}$, etc.).

C. Heterodyne and Homodyne Rates

Let us consider the homodyne rate (31). It corresponds to a measurement of the $u_\star$-quadrature, which is the less noisy according to the convention $e_u > e_{u_\star}$ (obviously, there is no difference in the choice of quadrature if $e_u = e_{u_\star}$). Such a choice gives higher rate in comparison with the measurement of u-quadrature. In what follows (see Section IV-E), it will be shown that this case corresponds to eigenvalue $m_u = 0$ be optimal for homodyne rate. In explicit form, it is

$$R^{(\rm hom)} = \frac{1}{2} \log_2 \frac{\bar{o}_{u_\star}}{o_{u_\star}} \quad (45)$$

which coincides with $\log_2 (\bar{\nu}/\nu)$ if $m_u = 0$. This property gives rise to the relation [see (21) and (35)]

$$R^{(\rm hom)} = \underline{C}^{(\log)} \quad (46)$$

if the optimal m_u is zero for logarithmic approximation to capacity[12] (we equalize the quantities $R^{(\rm hom)}$ and $\underline{C}^{(\log)}$ for the same channel parameters). This holds true for small values of N [see (81)]. Thus, in this case, the homodyne rate coincides with the logarithmic approximation to capacity.

Analogously, (30) gives

$$R^{(\rm het)} = \log_2 \frac{\bar{\nu}^{(\rm het)}}{\nu^{(\rm het)}} \quad (47)$$

for heterodyne measurement [see (40)], i.e., the heterodyne rate is equal to the logarithmic approximation to capacity calculated with $V_{\rm env}^{(\rm het)}$. One can also get for a fixed s that

$$\lim_{\mathcal{N}_{\rm env} \to \infty} R^{(\rm het)} = \underline{C}^{(\log)}. \quad (48)$$

Equation (46) and (48) define the values of parameters s and $\mathcal{N}_{\rm env}$ for which the rates approach the capacity (the comparison between capacity, homodyne and heterodyne rates was discussed earlier in [7]).

The simple form of (47) explains why the description of heterodyne rate using heterodyne variables introduced in Section IV-B is the most natural one. Keep in mind that the heterodyne rate can be described using both approaches: standard variables used for capacity and homodyne rate, or heterodyne variables. Despite, we shall usually work with heterodyne variables, sometimes standard variables will be used.

As far as quantities (30) and (47) are identical as functions of input and modulation eigenvalues, the latter do not depend on representation (type of variables) used for $R^{(\rm het)}$. It means that upper indices "(het)" written for input and modulation eigenvalues are used only to indicate that they are optimal for heterodyne rate (to distinguish them from those optimal for capacity and homodyne rate). However, index "het" written for environment, output, and average output eigenvalues indicate both different variables used and optimality for heterodyne rate.

[12]It will be shown in Section IV-F that if $m_u = 0$ is optimal for one of the quantities $\underline{C}$ and $\underline{C}^{(\log)}$, then it is optimal also for the other. Also, remember (see Section III-A) that the optimal eigenvalues for $\underline{C}^{(\log)}$ and $\underline{C}^{(0)}$ are always the same by definition.

Loosely speaking, $i_u^{(\mathrm{het})} = i_u$ and $m_u^{(\mathrm{het})} = m_u$, while $e_u^{(\mathrm{het})} \neq e_u, o_u^{(\mathrm{het})} \neq o_u, \bar{o}_u^{(\mathrm{het})} \neq \bar{o}_u$ $(u \in \{q,p\})$ *as abstract variables*, but in our convention *all* of them are different, because $i_u^{(\mathrm{het})}$ and $m_u^{(\mathrm{het})}$ are used *only* for heterodyne case and are optimal for it.[13]

In the following, we shall usually write the relations for capacity and then explain which replacements should be applied to get analogous relations for rates. These replacements can be some of the following:

$$i_u \to i_u^{(\mathrm{het})}, \qquad i_{u_\star} \to i_{u_\star}^{(\mathrm{het})} \tag{49}$$
$$m_u \to m_u^{(\mathrm{het})}, \qquad m_{u_\star} \to m_{u_\star}^{(\mathrm{het})} \tag{50}$$
$$e_u \to e_u^{(\mathrm{het})}, \qquad e_{u_\star} \to e_{u_\star}^{(\mathrm{het})} \tag{51}$$
$$o_u \to o_u^{(\mathrm{het})}, \qquad o_{u_\star} \to o_{u_\star}^{(\mathrm{het})} \tag{52}$$
$$\bar{o}_u \to \bar{o}_u^{(\mathrm{het})}, \qquad \bar{o}_{u_\star} \to \bar{o}_{u_\star}^{(\mathrm{het})} \tag{53}$$
$$N_{\mathrm{env}} \to N_{\mathrm{env}}^{(\mathrm{het})}, \qquad \mathcal{N}_{\mathrm{env}} \to \mathcal{N}_{\mathrm{env}}^{(\mathrm{het})} \tag{54}$$
$$\nu \to \nu^{(\mathrm{het})}, \qquad \bar{\nu} \to \bar{\nu}^{(\mathrm{het})} \tag{55}$$
$$g_1 \to \tfrac{1}{\ln 2}, \qquad g_2 \to -\tfrac{1}{\ln 2}. \tag{56}$$

Each of the above numbered lines specifies two replacements. However, only those replacements, which correspond to *explicit* variables of the relation (subjected to replacements) must be applied. Finally, when discussing about the rates, if we refer to relations written for the capacity, we should first apply the proper replacements.

D. Optimization Problem

The optimization problem for the heterodyne rate can be formulated as follows. One needs to find the matrices $V_{\mathrm{in}}^{(\mathrm{het})}$ and $V_{\mathrm{mod}}^{(\mathrm{het})}$ [see (38) and (39)], which provide the maximum for the function (47) and satisfy the energy constraint

$$\frac{1}{2}\mathrm{Tr}\left(\bar{V}_{\mathrm{in}}^{(\mathrm{het})}\right) = N + \frac{1}{2} \tag{57}$$

where

$$\bar{V}_{\mathrm{in}}^{(\mathrm{het})} = V_{\mathrm{in}}^{(\mathrm{het})} + V_{\mathrm{mod}}^{(\mathrm{het})}.$$

By substituting (38) into (33) written for $\bar{V}_{\mathrm{out}}^{(\mathrm{het})}$ and taking into account the energy constraint (57), we get the amount of photons in the average output state

$$\bar{N}_{\mathrm{out}}^{(\mathrm{het})} = \eta N + (1-\eta) N_{\mathrm{env}}^{(\mathrm{het})}. \tag{58}$$

Analogously, for the case of capacity, the relations (24) and (25) give

$$\bar{N}_{\mathrm{out}} = \eta N + (1-\eta) N_{\mathrm{env}}. \tag{59}$$

Notice that Theorems 1 and 2 allow us to exclude the variables $i_{u_\star}$ and $i_{u_\star}^{(\mathrm{het})}$ from the optimization problems due to the purity of the input states:

$$i_u i_{u_\star} = \frac{1}{4}, \quad i_u^{(\mathrm{het})} i_{u_\star}^{(\mathrm{het})} = \frac{1}{4}.$$

[13]Writing, e.g., $i_u^{(\mathrm{het})} = i_u$ would be misleading, as i_u are those eigenvalues optimal for capacity, but not optimal for heterodyne rate. This is less problematic for homodyne rate, because its optimal eigenvalues coincide in some cases with that of the logarithmic approximation to capacity [see (46)] and therefore can be treated as a particular case of eigenvalues optimal for capacity.

Then, the optimization problems for the single-mode channel can be formulated as follows. One needs to find the maxima of functions [see definitions (8), (14), (45), and (47)]

$$\underline{C} = g\left(\bar{\nu} - \frac{1}{2}\right) - g\left(\nu - \frac{1}{2}\right) \tag{60}$$
$$R^{(\mathrm{het})} = \log_2 \bar{\nu}^{(\mathrm{het})} - \log_2 \nu^{(\mathrm{het})} \tag{61}$$
$$R^{(\mathrm{hom})} = \frac{1}{2}\left[\log_2 \bar{o}_{u_\star} - \log_2 o_{u_\star}\right] \tag{62}$$

over the variables i_u, m_u, and $m_{u_\star}$ in the case of $\underline{C}$ and $R^{(\mathrm{hom})}$, and over the variables $i_u^{(\mathrm{het})}$, $m_u^{(\mathrm{het})}$, $m_{u_\star}^{(\mathrm{het})}$ in the case of $R^{(\mathrm{het})}$, taking into account the constraints

$$i_u > 0 \tag{63}$$
$$m_u, m_{u_\star} \geqslant 0 \tag{64}$$
$$i_u + \frac{1}{4i_u} + m_u + m_{u_\star} = 2N + 1 \tag{65}$$

in the case of $\underline{C}$ and $R^{(\mathrm{hom})}$, and the constraints (63)–(65) after the replacements (49) and (50) in the case of $R^{(\mathrm{het})}$. In Sections IV-F and IV-G, we shall solve it using the Lagrange multipliers method.

It is interesting to note that the relations for symplectic eigenvalues (35) and (40) allow the capacity (60) and heterodyne rate (61) to be represented as

$$\underline{C} = g\left(\overline{\mathcal{N}}_{\mathrm{out}}\right) - g\left(\mathcal{N}_{\mathrm{out}}\right) \tag{66}$$
$$R^{(\mathrm{het})} = \log_2\left(\overline{\mathcal{N}}_{\mathrm{out}}^{(\mathrm{het})} + \frac{1}{2}\right) - \log_2\left(\mathcal{N}_{\mathrm{out}}^{(\mathrm{het})} + \frac{1}{2}\right) \tag{67}$$

where $\overline{\mathcal{N}}_{\mathrm{out}}$, $\mathcal{N}_{\mathrm{out}}$, $\overline{\mathcal{N}}_{\mathrm{out}}^{(\mathrm{het})}$, and $\mathcal{N}_{\mathrm{out}}^{(\mathrm{het})}$ are the amounts of thermal photons for the states $\bar{V}_{\mathrm{out}}$, V_{out}, $\bar{V}_{\mathrm{out}}^{(\mathrm{het})}$, and $V_{\mathrm{out}}^{(\mathrm{het})}$, respectively.

E. Solution Stages

Let us consider the capacity and the homodyne rate. In Sections IV-F and IV-G, it will be shown that all the solutions of Lagrange equations, associated to the optimization problem stated in Section IV-D, give positive i_u, i.e., $m_u, m_{u_\star} \geqslant 0$ are the only inequalities to satisfy. This allows us to classify the solutions depending on the amount of positive optimal m-eigenvalues. The following terminology is used for this purpose.

Definition 1: The solution belongs to the *first stage* if the optimal m_u, $m_{u_\star}$ are both equal to zero, to the *second stage* if the optimal m_u, $m_{u_\star}$ are one equal to zero and the other is positive, and to the *third stage* if the optimal $m_u, m_{u_\star}$ are both positive.

As far as $R^{(\mathrm{hom})}$ does not depend on m_u, due to the condition (65) the maximum is achieved for $m_u = 0$, which shows the absence of the third stage in homodyne rate. In other words, energy N should not be wasted in the quadrature unused for information transmission.

The first stage holds if and only if capacity is equal to zero, which can only be if $N = 0$ (if $N \neq 0$ one can always get nonzero capacity and rates by taking $i_u = \frac{1}{2}, m_u = m_{u_\star} = N$). In particular, (65) applied for the first stage gives $i_u = \frac{1}{2}$. The same consideration holds true also for the homodyne rate.

Proposition 1: Given $\bar{o}_u \neq \bar{o}_{u_\star}$ in the second stage, the eigenvalues $m_u = 0$ and $m_{u_\star} > 0$ are optimal for capacity[14] if and only if $\bar{o}_u > \bar{o}_{u_\star}$.

Proof: Suppose that $m_{u_\star} = 0$ and $m_u > 0$ are optimal in the case of $\bar{o}_u > \bar{o}_{u_\star}$. The energy constraint (65) is preserved by the change of variables $m'_u = m'_{u_\star} = m_u/2$, $i'_u = i_u$. The new variables do not change the second term in (60) but increase the first term.[15] Thus, they give higher maximum for capacity. Similarly, one can prove that $m_u = 0$ and $m_{u_\star} > 0$ are not optimal if $\bar{o}_u < \bar{o}_{u_\star}$. Hence, the proposition is proved by contradiction. ■

Proposition 2: If $e_u > e_{u_\star}$, then in the second stage, $m_u = 0$ and $m_{u_\star} > 0$ are optimal for capacity.

Proof: The proof is reported in Appendix C. ■

It follows from Propositions 1 and 2 that the case of $e_u > e_{u_\star}$ requires $o_u = \bar{o}_u$ and

$$o_u \geqslant \bar{o}_{u_\star} > o_{u_\star} \tag{68}$$

in the second stage.

Similar consideration gives $\bar{o}_u = \bar{o}_{u_\star}$ in the third stage (by supposing $\bar{o}_u \neq \bar{o}_{u_\star}$ one can always redistribute the energy N among m-eigenvalues so to decrease the difference $|\bar{o}_u - \bar{o}_{u_\star}|$ thus giving higher maximum for capacity). Taking into account (65), we get in this case

$$\bar{o}_u = \bar{o}_{u_\star} = \eta\left(N + \frac{1}{2}\right) + (1-\eta)\left(N_{\rm env} + \frac{1}{2}\right). \tag{69}$$

The equality $\bar{o}_u = \bar{o}_{u_\star}$ is equivalent to the equation $\overline{\mathcal{N}}_{\rm out} = \bar{N}_{\rm out}$, where the latter is given by (59). Thus, for the third stage, the first term in the relation (66) is already found.

Notice that the previous considerations for the capacity [including definition 1, Propositions 1 and 2, (68) and (69)] hold true also for the heterodyne rate if the replacements (49)–(54) and $g \to \log_2$ are applied, and if (58), (61), and (67) are mentioned instead of (59), (60), and (66), respectively. In the following, the solutions for the third and second stages are presented.

F. Third Stage

In the case of third stage, the Lagrange multipliers method applied to the function $\underline{C}$ with the constraint (65) leads to the following system of equations [see definition of g_k in (18)]:

$$\frac{\partial L}{\partial i_u} = \frac{\eta}{2}\Bigg[g_1(\bar{\nu})\left(\frac{1}{\bar{o}_u} - \frac{1}{4i_u^2\bar{o}_{u_\star}}\right) - g_1(\nu)\left(\frac{1}{o_u} - \frac{1}{4i_u^2 o_{u_\star}}\right)\Bigg] - \varkappa\left[1 - \frac{1}{4i_u^2}\right] = 0 \tag{70}$$

$$\frac{\partial L}{\partial m_u} = \frac{\eta}{2}\frac{g_1(\bar{\nu})}{\bar{o}_u} - \varkappa = 0 \tag{71}$$

$$\frac{\partial L}{\partial m_{u_\star}} = \frac{\eta}{2}\frac{g_1(\bar{\nu})}{\bar{o}_{u_\star}} - \varkappa = 0 \tag{72}$$

where the Lagrange function is

$$L = \underline{C} - \varkappa\left(i_u + \frac{1}{4i_u} + m_u + m_{u_\star} - 2N - 1\right)$$

with $\varkappa$ the Lagrange multiplier.

Equations (71) and (72) give $\bar{o}_u = \bar{o}_{u_\star}$ which was obtained earlier from qualitative considerations. By substituting (71) and (72) into (70), one can find that squeezing in input $s_{\rm in}$ equals that of environment s and output $s_{\rm out}$:

$$\frac{i_{u_\star}}{i_u} = \frac{e_{u_\star}}{e_u} = \frac{o_{u_\star}}{o_u} \tag{73}$$

which allows us to find optimal input eigenvalues

$$i_u = \frac{1}{2}\sqrt{\frac{e_u}{e_{u_\star}}}, \qquad i_{u_\star} = \frac{1}{2}\sqrt{\frac{e_{u_\star}}{e_u}}. \tag{74}$$

Thus, given the environment state $V_{\rm env} = V(\mathcal{N}_{\rm env}, s)$, the optimal input state is $V_{\rm in} = V(0, s)$. Combining (69) with (74), one can obtain optimal m-eigenvalues

$$\begin{aligned} m_u &= N + \frac{1}{2} - i_u + \frac{1-\eta}{\eta}\left(N_{\rm env} + \frac{1}{2} - e_u\right) \\ m_{u_\star} &= N + \frac{1}{2} - i_{u_\star} + \frac{1-\eta}{\eta}\left(N_{\rm env} + \frac{1}{2} - e_{u_\star}\right). \end{aligned} \tag{75}$$

In order to get analogous relations for the heterodyne rate, the replacements (49)–(54) and (56) must be applied to (70)–(72) and (73)–(75). In particular, it gives

$$s_{\rm in}^{(\rm het)} = s^{(\rm het)} = s_{\rm out}^{(\rm het)}$$

and $V_{\rm in}^{(\rm het)} = V(0, s^{(\rm het)})$. Notice that (37) and (44) give

$$\begin{aligned} N_{\rm env}^{(\rm het)} + \frac{1}{2} - e_u^{(\rm het)} &= N_{\rm env} + \frac{1}{2} - e_u \\ N_{\rm env}^{(\rm het)} + \frac{1}{2} - e_{u_\star}^{(\rm het)} &= N_{\rm env} + \frac{1}{2} - e_{u_\star} \end{aligned}$$

for the relations (75).

Finally, the explicit relations for capacity and heterodyne rate in the third stage read

$$\underline{C} = g\left[\eta N + (1-\eta)N_{\rm env}\right] - g\left[(1-\eta)\mathcal{N}_{\rm env}\right] \tag{76}$$

$$R^{(\rm het)} = \log_2\left[\eta N + (1-\eta)N_{\rm env}^{(\rm het)} + \frac{1}{2}\right] - \log_2\left[(1-\eta)\mathcal{N}_{\rm env}^{(\rm het)} + \frac{1}{2}\right] \tag{77}$$

where (77) becomes

$$R^{(\rm het)} = \log_2\left[1 + \frac{\eta N}{1 + (1-\eta)\mathcal{N}_{\rm env}}\right] \tag{78}$$

for the case of thermal nonsqueezed environment. Relation (76) (originally was found in [12]) generalizes the one obtained for lossy bosonic channel with vacuum environment $g(\eta N)$[7] and, later, with thermal nonsqueezed environment [10]. In turn, (77) generalizes the relation for the heterodyne rate,

[14]This proposition holds for both cases $e_u > e_{u_\star}$ and $e_u < e_{u_\star}$.

[15]The area of a rectangle with fixed perimeter is higher if the length of sides differs less. In the considered case, $\bar{o}'_u + \bar{o}'_{u_\star} = \bar{o}_u + \bar{o}_{u_\star}$ but $|\bar{o}'_u - \bar{o}'_{u_\star}| < |\bar{o}_u - \bar{o}_{u_\star}|$. In addition, g is monotonically increasing and concave function.

$\log_2(1+\eta N)$, found in [32] for vacuum environment (see also discussion in [7]).

By comparing (21), (60), and (76), we get the logarithmic approximation to the capacity[16]

$$\underline{C}^{(\log)} = \log_2\left[\eta N + (1-\eta)N_{\rm env} + \frac{1}{2}\right] - \log_2\left[(1-\eta)\mathcal{N}_{\rm env} + \frac{1}{2}\right] \quad (79)$$

which coincides with the heterodyne rate (77) after the replacements (54) (it follows from (41) and (44) that the limits of the ratios $N_{\rm env}^{(\rm het)}/N_{\rm env}$ and $\mathcal{N}_{\rm env}^{(\rm het)}/\mathcal{N}_{\rm env}$ for $\mathcal{N}_{\rm env}\to\infty$ are equal to one). Thus, the limit (48) actually holds. Notice, that eigenvalues (74) and (75) are optimal also for the quantity $\underline{C}^{(\log)}$; therefore, we have $\underline{C}\equiv\underline{C}^{(0)}$ in the third stage.

In the case of pure environment, the capacity (76) can be written as

$$\underline{C} = g(\bar{N}_{\rm out}) \quad (80)$$

where $\bar{N}_{\rm out}$ is given by (59). The form of the relation (80) provides the most natural generalization of the noiseless channel capacity $g(N)$. Thus, in the third stage, the capacity of the channel with pure environment is completely defined by the average amount of photons contained in the channel (i.e., in the system "environment plus input"), where probability weights η and $1-\eta$ specify the contribution of input and environment states into the channel capacity.

Previously, it was proved (see proposition 2) that $m_{u_\star}\neq 0$ is optimal for the chosen convention ($e_u > e_{u_\star}$); therefore, the third stage holds if $m_u > 0$. This is the case for the capacity (quantities $\underline{C}$, $\underline{C}^{(\log)}$, and $\underline{C}^{(0)}$) if the amount N of input photons is higher than the threshold[17]

$$N_{2\to 3} = i_u - \frac{1}{2} - \frac{1-\eta}{\eta}\left(N_{\rm env}+\frac{1}{2}-e_u\right) \quad (81)$$

where i_u is defined by the first of (74). It is equivalent to the restriction $s < s_{2\to 3}$ for given values of η, N and $\mathcal{N}_{\rm env}$, where

$$s_{2\to 3} = -\ln\left[\sqrt{1+\phi_0+(N+1/2)^2\phi_0^2}-(N+1/2)\phi_0\right]$$

with

$$\phi_0 := \frac{\eta}{(1-\eta)\left(\mathcal{N}_{\rm env}+\frac{1}{2}\right)}. \quad (82)$$

Notice that the quantity $s_{2\to 3}$ has the limits

$$\lim_{\eta\to 1} s_{2\to 3} = \ln(2N+1) \quad (83)$$
$$\lim_{\eta\to 0} s_{2\to 3} = 0.$$

The threshold (81) holds also for the heterodyne rate if the replacements (49) and $N_{2\to 3}\to N_{2\to 3}^{(\rm het)}$ are applied, where $i_u^{(\rm het)}$ expressed through the standard eigenvalues reads

$$i_u^{(\rm het)} = \frac{1}{2}\sqrt{\frac{1+2(1-\eta)e_u}{1+2(1-\eta)e_{u_\star}}}. \quad (84)$$

[16]Remember that according to (17), $g(v)\approx\log_2\left(v+\frac{1}{2}\right)$.

[17]A similar optimization problem considered in [30], [45] also has different types of solutions depending on the relation between the amount of input photons and the parameters of the channel environment.

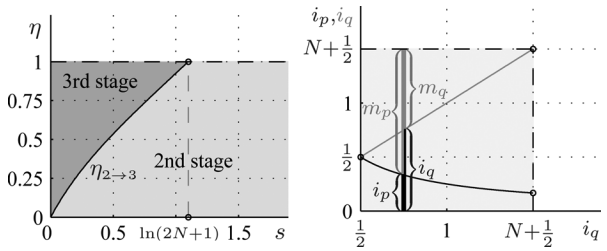

Fig. 1. (Left) Two regions of the plane (s,η) corresponding to the third (darker background) and the second stage for $N=1$ and $\mathcal{N}_{\rm env}=1$. The regions are separated by the curve $\eta_{2\to 3}$ [see (85)] plotted versus s (black curve); it splits the whole plane into two regions marked with different gray-scale backgrounds (the darker background corresponds to third stage). The curve $\eta_{2\to 3}$ reaches the value $\eta=1$ at squeezing value $s=\ln(2N+1)$. The horizontal dashed line plotted for $\eta=1$ corresponds to noiseless channel. (Right) Eigenvalues i_p and i_q for the noiseless channel are plotted versus i_q for $N=1$. The area of the square of gray color is equal to $\bar{\nu}^2=\left(N+\frac{1}{2}\right)^2$ which defines the capacity $g\left(\sqrt{\bar{\nu}^2}-\frac{1}{2}\right)=g(N)$. Depicted braces show that each value of i_q corresponds to two different methods to distribute the energy $N+\frac{1}{2}$ between input and modulation quadratures.

The threshold $N_{2\to 3}$ is a nonnegative number which equals zero only for the vacuum environment. As far as the third stage holds only if $N > N_{2\to 3}$ and the first stage holds only if $N=0$, the second stage must correspond to values $0 < N \leqslant N_{2\to 3}$. Thus, the type of solution increases its stage in sequence starting from the first stage and ending to the third one if N grows from zero to infinity. This explains the origin of the adopted term "stage." Also, it can be interpreted as "the third stage is always the most preferable if energy N is sufficiently high, otherwise the second stage should be taken, and the first stage holds if only both the third and the second stage fail to satisfy the constraint." This mnemonic rule, although trivial for the single-mode channel, will be useful when applied to the multimode memory channel. The previous consideration is also valid for the heterodyne threshold $N_{2\to 3}^{(\rm het)}$.

Similarly to the quantity $s_{2\to 3}$, given the values of s, N, and $\mathcal{N}_{\rm env}$, the relation for transmissivity $\eta_{2\to 3}$ corresponding to transition from the second to third stages can be written as

$$\eta_{2\to 3}^{-1} = 1 - \frac{N+\frac{1}{2}-i_u}{N_{\rm env}+\frac{1}{2}-e_u} \quad (85)$$

where $0 < s \leqslant \ln(2N+1)$ and i_u is defined by the first of (74). Taking into account that $s_{\rm in}=s$, $s\geqslant 0$, the limit (83) and monotonicity of $\eta_{2\to 3}$ with respect to s, one can see that

$$\frac{1}{2} \leqslant i_u \leqslant N+\frac{1}{2} \quad (86)$$

where higher values of i_u correspond to higher values of $\eta_{2\to 3}$. The transmissivity $\eta_{2\to 3}$ is plotted versus s in Fig. 1(left).

G. Second Stage

One can show that the Lagrange equations for the capacity (and heterodyne rate) in the second stage can be obtained from the system (70)–(72) by substituting $m_u=0$ ($m_u^{(\rm het)}=0$) in all equations and by removing (71) corresponding to derivative with respect to m_u ($m_u^{(\rm het)}$). This is because unknown variables enter in the Lagrange equations as linear combinations. For the homodyne rate, the Lagrange equations are the same as for the capacity in the second stage if the replacement (56) is applied.

Then, solving the Lagrange equations for the homodyne rate, one can find the ratio

$$\frac{i_{u_\star}}{i_u} = \frac{o_{u_\star}}{\bar{o}_{u_\star}} \tag{87}$$

which also holds for the heterodyne rate after replacements (49), (52), and (53). For the capacity, the Lagrange equations give a *mode transcendental equation* on i_u

$$\mathcal{F}(i_u) = 0 \tag{88}$$

where

$$\mathcal{F} := g_1(\bar{\nu}) \left[\frac{1}{o_u} - \frac{1}{\bar{o}_{u_\star}}\right] - g_1(\nu) \left[\frac{1}{o_u} - \frac{1}{4i_u^2 o_{u_\star}}\right]. \tag{89}$$

Notice that (88) results to (87) if the g_1 function is taken to zeroth-order approximation (i.e., $g_1 \equiv (\ln 2)^{-1}$). Remember that in the second stage, the optimal eigenvalues for $\underline{C}^{(\log)}$, $\underline{C}^{(0)}$, and $R^{(\hom)}$ [see (21) and (46)] are the same. They follow from (87) solved for the variable i_u and equal to

$$m_u = 0 \tag{90}$$

$$m_{u_\star} = 2N + 1 - i_u - \frac{1}{4i_u} \tag{91}$$

$$i_u = \frac{1}{2}\left[\sqrt{1 + (2N+1)\phi + (\phi/2)^2} - \phi/2\right] \tag{92}$$

$$i_{u_\star} = \frac{1}{4i_u} \tag{93}$$

where

$$\phi = \frac{\eta}{1-\eta} e_{u_\star}^{-1} \tag{94}$$

is equal to ϕ_0 [see (82)] in the case of thermal environment ($s = 0$). The exact values of the optimal eigenvalues for the capacity $\underline{C}$ are given by (88), (90), (91), and (93). As far as eigenvalues (90)–(93) are optimal for the quantity $\underline{C}^{(0)}$, later, we will call them as *the zeroth-order solution* (or *the zeroth-order eigenvalues*) for capacity. Thus, similar to the third stage, in the second stage, the quantity $\underline{C}^{(0)}$ is also expressed in an explicit form. In turn, the condition $m_{u_\star} > 0$ [see (91)] restricts the admissible region for i_u to the interval

$$N + \frac{1}{2} - \sqrt{N^2 + N} < i_u < N + \frac{1}{2} + \sqrt{N^2 + N}.$$

The optimal eigenvalues for the heterodyne rate are given by the same relations (90)–(93) if the replacements (49), (50) and

$$\phi \to \phi^{(\mathrm{het})} \tag{95}$$

with

$$\phi^{(\mathrm{het})} = \frac{\eta}{1-\eta}\left[e_{u_\star}^{(\mathrm{het})}\right]^{-1} \tag{96}$$

are applied.

By comparing (62) with (87), one can get the homodyne rate

$$\begin{aligned} R^{(\hom)} &= \log_2(2i_u) \\ &= \log_2\left[\sqrt{1 + (2N+1)\phi + (\phi/2)^2} - \phi/2\right]. \end{aligned} \tag{97}$$

Remember that $R^{(\hom)} \equiv \underline{C}^{(\log)}$ [see (46)] in the second stage. Then, similarly, by comparing (61) and (87), we get the same relation (97) for the heterodyne rate if the replacements (49) and (95) are applied to it.

The first-order approximation for mode transcendental (88) can be obtained by replacing the function g_1 with its first-order approximation (20). Since (88) cannot be exactly solved within this approximation, we will solve it in the neighborhood of the zeroth-order solution (90)–(93) as linear perturbation. In particular, by denoting input zeroth-order eigenvalue (92) as $i_u^{(0)}$ and substituting i_u with $i_u^{(0)} + \varepsilon_u$ in the first-order approximation of (88), we get a linear equation for small deviation ε_u. Its solution is

$$\varepsilon_u = \frac{\eta \bar{o}_{u_\star} o_u i_u^{(0)} m_{u_\star} (\bar{o}_{u_\star} - o_u)}{2\left[\eta^2 (o_u^2 + \bar{o}_{u_\star}^2 - \bar{o}_{u_\star} o_u)\, i_u^{(0)} m_{u_\star} - \bar{o}_{u_\star}^2 o_u^2 (12\nu^2 + 1)\right]} \tag{98}$$

whose variables are the zeroth-order eigenvalues. Thus, we have found *the first-order solution*[18] $i_u^{(1)} = i_u^{(0)} + \varepsilon_u$. Remember that in the second stage, by virtue of (90), (91), and (93), the only degree of freedom is represented by i_u. Hence, it is sufficient to specify its value in order to have the complete solution of the optimization problem.

Similar to the quantity $\underline{C}^{(0)}$ whose variables are the zeroth-order eigenvalues (90)–(93), the first-order solution has to be substituted into the exact[19] relation (60) instead of its first-order approximation which was used to derive the first-order eigenvalues. Otherwise, the loss in accuracy becomes significant. In particular, although input and modulation eigenvalues calculated through exact and approximate approaches essentially differ each other, they give rise to almost equal values for capacity. This can be explained by the fact that the quantity (60), considered as a function of only one unknown variable[20] i_u, has zero derivative in the neighborhood of its optimal value (i.e., the deviation of i_u affects the maximum of capacity only in the second order). The quantity (60) considered as a function of the first-order eigenvalues below will be called *the first-order approximation to capacity* $\underline{C}^{(1)}$.

The homodyne rate $\log_2 \sqrt{1 + 4\eta N}$ was found in [32] by supposing both the environment and input states to be vacuum (see also the discussion in [7]). Indeed, it can be obtained without solving the optimization problem, by substituting in (62) $i_u = i_{u_\star} = e_u = e_{u_\star} = 1/2$ and $m_{u_\star} = 2N$ as it follows from the constraint (65). However, since optimal input state is never vacuum according to (92), that rate holds (approximately) only if the value of N is close to zero.

H. $\bar{O}_{u_\star}$ Representation

We have solved the problem of finding the optimal eigenvalues i_u, $i_{u_\star}$, m_u, and $m_{u_\star}$ for given values of e_u, $e_{u_\star}$, η, and N. It is interesting to note that the eigenvalue $\bar{o}_{u_\star}$ can be used

[18]Similarly, another first-order solution can be obtained if exact relation for g_1 function is used instead of approximation (20).

[19]Notice that in order to get the zeroth-order and the first-order approximate solutions we replaced the exact g function and its derivatives (everywhere in optimization problem) by their zeroth-order and first-order approximations, respectively.

[20]The other input and modulation eigenvalues have to be expressed through i_u using (90), (91), and (93).

as the equivalent replacement[21] of the quantity N. In fact, (69) makes it evident in the third stage. Let us show this also for the second stage. Combining (36), (91), (93), and (94), one can get the relation

$$2N+1 = i_u + \frac{\bar{o}_{u_\star}}{\eta} - \frac{1}{\phi}. \tag{99}$$

By substituting it into (92) and then solving the latter for i_u, one can obtain

$$i_u = \frac{1}{2}\left[\sqrt{(\phi/4)^2 + \bar{o}_{u_\star}\phi/\eta} - \phi/4\right]. \tag{100}$$

Hence, (97) can be equivalently rewritten through variable $\bar{o}_{u_\star}$ as

$$R^{(\mathrm{hom})} = \log_2\left[\sqrt{(\phi/4)^2 + \bar{o}_{u_\star}\phi/\eta} - \phi/4\right] \tag{101}$$

which coincides with the quantity $\underline{C}^{(\log)}$ in the second stage. Notice that eigenvalue $m_{u_\star}$ can be expressed through $\bar{o}_{u_\star}$ as

$$m_{u_\star} = \frac{\bar{o}_{u_\star}}{\eta} - \frac{1}{\phi} - \frac{1}{4i_u}. \tag{102}$$

Thus, the eigenvalues (90), (93), (100), and (102) are optimal for the quantities $R^{(\mathrm{hom})}$, $\underline{C}^{(\log)}$, and $\underline{C}^{(0)}$ in the second stage and expressed through the quantity $\bar{o}_{u_\star}$ instead of N. Equations (99)–(102) hold also for the heterodyne rate if the replacements (49), (50), (53), and (95) are applied.

Similarly, the mode transcendental equation (88) also does not depend on N if eigenvalue $\bar{o}_{u_\star}$ is assumed to be a known constant. In this case, the admissible region for the eigenvalue i_u [root of (88)] can be estimated using inequalities $\bar{\nu} > \frac{1}{2}$ and $m_{u_\star} > 0$ [see (102)], which can be rewritten as

$$i_u > \frac{1}{\eta}\left[\frac{1}{4\bar{o}_{u_\star}} - (1-\eta)e_u\right]$$

and

$$i_u > \frac{1}{4}\left[\frac{\bar{o}_{u_\star}}{\eta} - \frac{1}{\phi}\right]^{-1}$$

respectively. Analogous to (98), by expressing N through $\bar{o}_{u_\star}$ in (88) and using approximation (20), one can get the first-order solution $i_u^{(1)} = i_u^{(0)} + \varepsilon_u$ in terms of $\bar{o}_{u_\star}$. In this case, ε_u is given by the relation

$$\begin{aligned}\varepsilon_u = {} & (\bar{o}_{u_\star} - o_u)(\bar{o}_{u_\star} - o_{u_\star})\, o_u i_u^{(0)} \\ & \times \Big\{\left(2\left[o_u^2 + \bar{o}_{u_\star}^2 - (o_u + o_{u_\star})\,\bar{o}_{u_\star}\right] + \left[12\,o_u^2 + 1\right]\nu^2\right) i_u^{(0)}\eta \\ & - 2\left[12\,\nu^2 + 1\right] o_u^2\,\bar{o}_{u_\star}\Big\}^{-1}\end{aligned} \tag{103}$$

whose variables are the zeroth-order eigenvalues (93), (100) and (102). Notice that despite (92) and (100) are equivalent (one can be obtained from another), this is not the case for relations (98) and (103).

I. Noiseless Channel

Let us demonstrate the aforementioned results on the particular case of noiseless (i.e., ideal) channel ($\eta = 1$). Its capacity equals $C = g(N)$ [47]. The optimal eigenvalues for its homodyne rate can be found from (87), (91), and (93) by substituting $\eta = 1$, which gives

$$i_u = N + \frac{1}{2} \tag{104}$$

$$m_{u_\star} = N\left(1 + \frac{1}{2N+1}\right) = \sinh(\ln(2N+1))). \tag{105}$$

The optimal eigenvalues for its heterodyne rate can be obtained from (75) and (84) by substituting $\eta = 1$, which results in $i_u^{(\mathrm{het})} = i_{u_\star}^{(\mathrm{het})} = \frac{1}{2}$ and $m_u^{(\mathrm{het})} = m_{u_\star}^{(\mathrm{het})} = N$. Hence, we have $N_{2\to3}^{(\mathrm{het})} = 0$ (see (81)), i.e., the second stage does not exist in this case.

Relations (78) and (97) applied to the noiseless channel give the inequalities [7]

$$R^{(\mathrm{het})} < R^{(\mathrm{hom})} < C \tag{106}$$

where $R^{(\mathrm{hom})} = \log_2(2N+1)$ and $R^{(\mathrm{het})} = \log_2(N+1)$ [32]. It means that both heterodyne and homodyne rates never achieve the capacity for finite N even for the noiseless channel. [22] In particular, for large values of N, inequalities (106) read

$$\log_2 N < \log_2 N + 1 < \log_2 N + \frac{1}{\ln 2}$$

where the ratio between the rates and the capacity disappears in the limit $N \to \infty$. In addition, both capacity and rates of the noiseless channel are always higher than their values in the presence of losses (environment), i.e., when $\eta < 1$.

One can also notice that despite optimal input and modulation eigenvalues are unique for heterodyne and homodyne rate; this is not the case for noiseless channel capacity. The latter has infinite amount of solutions [30], which can be shown as follows. At first, since Theorem 1 holds also for $\eta = 1$, the optimal input state must be pure. At second, any pure input state zeros the second term in Holevo-χ quantity. As far as the area of a rectangle with fixed perimeter is maximal if and only if rectangle's sides are equal (see proof of Proposition 2), we have the system of equations

$$\begin{aligned} i_u + m_u &= N + \frac{1}{2} \\ \frac{1}{4i_u} + m_{u_\star} &= N + \frac{1}{2} \end{aligned} \tag{107}$$

where the energy restriction (65) is the "perimeter." Thus, by taking any input eigenvalue from the interval

$$\frac{1}{4\left(N + \frac{1}{2}\right)} \leqslant i_u \leqslant N + \frac{1}{2} \tag{108}$$

and obtaining the eigenvalues $i_{u_\star}$, m_u, and $m_{u_\star}$ from the relations (93) and (107), we arrive at the same value of capacity $g(N)$.

Taking into account that the capacity is symmetric over quadratures and considering as usual only positive values of s_{in}, we can parametrize the interval (108) as [see similarity with (86)] $s_{\mathrm{in}} = \sigma\ln(2N+1)$, where $\sigma \in [0,1]$ [30]. Notice that $\sigma = 1$ is the only solution corresponding to second stage

[21] This fact will be used in Section VI for discussing memory channels.

[22] It is discussed in [32] that the capacity of the noiseless channel can be achieved by using Fock states for encoding and photon counting measurement for decoding.

in this interval. Then, the optimal eigenvalues can be expressed as functions of σ as

$$\begin{aligned} i_u &= \frac{1}{2}(2N+1)^{\sigma} \\ i_{u_\star} &= \frac{1}{2}(2N+1)^{-\sigma} \\ m_u &= N + \frac{1}{2}\left[1-(2N+1)^{\sigma}\right] \\ m_{u_\star} &= N + \frac{1}{2}\left[1-(2N+1)^{-\sigma}\right] \end{aligned} \tag{109}$$

The set of eigenvalues optimal for noiseless channel are plotted in Fig. 1(right). The black point at the left part of the graph corresponds to well-known solution $i_u = i_{u_\star} = \frac{1}{2}$, $m_u = m_{u_\star} = N$ which is the particular case of $\sigma = 0$ in (109). Two black points at the right part of the graph correspond to solution (104), (105) following from (109) for $\sigma = 1$. Thus if $\sigma = 1$, then the same input and modulation eigenvalues are optimal for both the capacity and the homodyne rate [30]. Moreover, this case corresponds to the maximum signal-to quantum noise ratio [30], [48]:

$$\frac{\bar{o}_{u_\star} - o_{u_\star}}{o_{u_\star}} = \frac{m_{u_\star}}{i_{u_\star}} = 4N(N+1)$$

Let us consider how the solution (i.e., the optimal input and modulation eigenvalues) changes if noise in the channel disappears ($\eta \to 1$). The loci (s, η) corresponding to different stages are shown in Fig. 1(left). One can see that if s belongs to the interval $(0, \ln(2N+1))$, then by increasing η from 0 to 1, we always change the second stage to the third one. As far as $s_{\text{in}} = s$ in the third stage, the solutions for different values of s for noisy channel tend to different solutions for noiseless channel and remain in the third stage. These solutions of noiseless channel correspond to the interval $\sigma \in [0, 1)$. Then, all solutions for $s \geqslant \ln(2N+1)$ of noisy channel tend to the same solution of the noiseless channel which corresponds to the second stage and to $\sigma = 1$.

J. Universal Limit

Let us analyze the behavior of the capacity and rates in the limit of infinite environment squeezing ($s \to \infty$) if channel parameters η, N, and $\mathcal{N}_{\text{env}}$ are fixed. Notice that only the second stage is possible in this case according to (81). By substituting eigenvalues (90), (91), and (93) into mode transcendental equation (88) and then solving it for i_u in the case of $s \to \infty$, one can get the result (104). Thus, the eigenvalues maximizing the capacity in the limit of $s \to \infty$ are the same as for the noiseless channel and given by (104) and (105). Substituting them into (35), one can see that both symplectic eigenvalues ν and $\bar{\nu}$ tend to infinity if $s \to \infty$. This allows us to use the logarithmic approximation to the capacity to find the limit. Hence, by comparing (46), (97), and (104), we obtain the result [12]

$$\lim_{s\to\infty} \underline{C}(s, \eta, N, \mathcal{N}_{\text{env}}) = \log_2(2i_u) = \log_2(2N+1) \tag{110}$$

which will be called below as *the universal limit*.

As far as $\lim_{\phi\to\infty} i_u$ [see (92)] gives the relation (104), the limit (110) also holds for homodyne rate $\lim_{s\to\infty} R^{(\text{hom})}$ [24]. Analogously, taking into account that $\lim_{s\to\infty} \phi^{(\text{het})} = 2\eta$ [see (96)], we get the limit

$$\lim_{s\to\infty} R^{(\text{het})} = \log_2\left[\sqrt{1+2(2N+1)\eta+\eta^2} - \eta\right]. \tag{111}$$

Notice that the limiting value (110) of the capacity equals the homodyne rate in the case of perfect (noiseless) channel [see (106)]. This fact can be understood by considering that, for $s \to \infty$, the quadrature u becomes infinitely noisy while the quadrature $u_\star$ becomes noiseless. Thus, by encoding the information in the quadrature $u_\star$, the information transmission becomes noiseless.

K. Concavity of Solution

The concavity over N for the capacity and rates will be essential below for discussing multiple channels uses. It is also the important property allowing to show additivity of the capacity and rates for the memoryless channels. Let us show the concavity of the function $\underline{C}(N)$. In the second stage, the latter can be represented as $\underline{C}(N, i_u(N))$; therefore, the first derivative with respect to N is

$$\frac{d\underline{C}}{dN} = \frac{\partial \underline{C}}{\partial N} + \frac{\partial \underline{C}}{\partial i_u}\frac{\partial i_u}{\partial N}.$$

However, since only the eigenvalues maximizing $\underline{C}$ are of interest, we have $\partial\underline{C}/\partial i_u = (\eta/2)\mathcal{F} = 0$ [see definition (89)]; therefore

$$\frac{d\underline{C}}{dN} = \frac{\partial \underline{C}}{\partial N}.$$

Then, one can show that for all values of N and for both second and third stages

$$\frac{d\underline{C}}{dN} = \frac{\eta}{\bar{o}_{u_\star}} g_1(\bar{\nu}) > 0 \tag{112}$$

which proves that $\underline{C}(N)$ is a monotonically increasing function of its argument. Notice that

$$\max_N \frac{\partial \underline{C}}{\partial N} = \lim_{N\to 0} \frac{\partial \underline{C}}{\partial N} \leqslant \infty \tag{113}$$

where equality is achieved only by the pure environment state ($e_u = e_{u_\star} = 1/2$).

It is shown in Appendix E that

$$\frac{d^2\underline{C}}{dN^2} < 0. \tag{114}$$

Then, we deduce from (112) and (114) that the function $\underline{C}(N)$ is concave on the whole region of $N \in [0, \infty)$. Thus, the single-mode (one-shot) capacity for fixed values of $e_u, e_{u_\star}$ and η can be considered as the concave function:

$$N \longrightarrow \boxed{\underline{C} = \underline{C}(N)} \longrightarrow \underline{C} \tag{115}$$

i.e., as a "blackbox" returning the value of $\underline{C}$ upon "input" N while respecting the concavity property.

Derivative (112) holds also for rates if the replacement (56) is applied. Besides it, for the heterodyne rate, the replacements (53) and (55) must be applied. The concavity of both rates and

logarithmic approximation to capacity can be deduced from explicit relations (77), (79), and (97). Hence, both heterodyne and homodyne rates are also concave functions which can be treated in the same "blackbox" form.

L. λ-Representation

As far as the function $\underline{C}(N)$ is concave and monotonically increasing, the value of the derivative (112) can be used as the equivalent replacement for the amount of photons N granted for the channel input. Such an approach below will be called the *λ-representation* to distinguish it from the standard approach using the quantity N (*N-representation*). Thus, we can specify an input energy for capacity using

$$\lambda(N) := \frac{\partial \underline{C}}{\partial N} = \frac{\eta}{\bar{o}_{u_\star}} g_1(\bar{\nu}). \tag{116}$$

(116) can be equivalently rewritten[23] in the form of Planck distribution[24]

$$\overline{\mathcal{N}}_{\rm out} = \frac{1}{e^{\,\omega/T} - 1} \tag{117}$$

where $\overline{\mathcal{N}}_{\rm out} = \bar{\nu} - 1/2$, $T := \eta/(\lambda \ln 2)$ ("temperature"), and $\omega := \bar{\nu}/\bar{o}_u$ ("frequency"). We will also use the "temperature" for the ideal channel

$$T_1 := (\lambda \ln 2)^{-1} \tag{118}$$

obtained from the relation for T with $\eta = 1$.

In the third stage, $\omega = 1$ and $\overline{\mathcal{N}}_{\rm out} = \bar{N}_{\rm out}$ (see Section IV-E), i.e., the quantities λ and η completely define the average amount of photons (59) contained in channel and, if the environment is pure, its capacity [see (80)]. Moreover, the dependence $N(\lambda)$ given by (117) is expressible in explicit form:

$$N = \frac{1}{\eta}\left[\frac{1}{e^{\,1/T} - 1} - (1-\eta) N_{\rm env}\right]. \tag{119}$$

Let us now consider the second stage. Following [22], one can substitute $g_1(\bar{\nu}) = \bar{o}_{u_\star}\lambda/\eta$ [see (116)] in the relation (88). That leads to

$$\omega = \sqrt{1 + \frac{\eta g_1(\nu)}{\lambda}\left[\frac{1}{o_u} - \frac{1}{4 i_u^2 o_{u_\star}}\right]} \tag{120}$$

where we used the relation $\omega^2 = \bar{o}_{u_\star}/o_u$ (remember, that in the second stage we have $\bar{o}_u = o_u$). Then, by substituting (120) and the relation $\bar{\nu} = \omega o_u$ in (117), we get a transcendental equation which relates λ and i_u. Hence, (117) (after all substitutions) becomes the mode transcendental equation (88) written in λ-representation. If the value of i_u is found for a given value of λ, the input energy N reads

$$N = \frac{1}{2}\left[\frac{o_u\,\omega^2}{\eta} - \frac{1}{\phi} + i_u - 1\right] \tag{121}$$

which is the relation (99) with $\bar{o}_{u_\star} = o_u \omega^2$. Thus, in any representation (N-, $\bar{o}_{u_\star}$-, or λ-representation), we have to solve only a single transcendental equation to find all variables.

Similar to the threshold value $N_{2\to 3}$ defined by (81), one can consider the threshold $N_{1\to 2} = 0$ which defines the amount of photons corresponding to the transition from the first to second stage. These thresholds in the λ-representation will be denoted by $\lambda_{2\to 3}$ and $\lambda_{1\to 2}$ and can be obtained as follows.

The threshold $\lambda_{1\to 2}$ is the limit of λ for $N \to 0$. Remember that $N = 0$ is the case of the first stage with optimal eigenvalues $i_u = i_{u_\star} = \frac{1}{2}$ and $m_u = m_{u_\star} = 0$ (see Section IV-E). Then, the convention $e_u > e_{u_\star}$ means for the first stage that u is the quadrature corresponding to $m_u = 0$ for infinitesimal nonzero values of N. Hence, the general relation (116) gives

$$\lambda_{1\to 2} \equiv \lim_{N\to 0} \lambda = \frac{\eta}{o_{u_\star}} g_1(\nu) = \eta \sqrt{\frac{o_u}{o_{u_\star}}}\, g'\left(\nu - \frac{1}{2}\right) \tag{122}$$

where the input eigenvalues are those of vacuum. Analogously

$$\lambda_{2\to 3} \equiv \lambda\left(N_{2\to 3}\right) = \eta g_1(\bar{\nu})/\bar{\nu} = \eta\, g'\left[\eta\left(i_u - \frac{1}{2}\right) + (1-\eta)\left(e_u - \frac{1}{2}\right)\right] \tag{123}$$

where i_u is given by (74).

Proposition 3: The function $\lambda_{1\to 2}(e_u, e_{u_\star})$ is monotonically decreasing over each of its arguments.

Proof: The dependence $\lambda_{1\to 2}(e_u)$ is proportional to the function $g_1(\nu)$, and the dependence $\lambda_{1\to 2}(e_{u_\star})$ is proportional to the function $g_1(\nu)/\nu^2$. Both these functions are monotonically decreasing over the argument ν. In turn, ν is monotonically increasing over o_u and $o_{u_\star}$ which are linear functions of e_u and $e_{u_\star}$, respectively. Taking into account that the composition of monotonically decreasing and monotonically increasing functions is monotonically decreasing, the proposition is proved. ■

Using the zeroth-order approximation for the g_1-function in (116), one can consider the quantity

$$\lambda^{(0)} = \frac{\eta}{\bar{o}_{u_\star} \ln 2} \tag{124}$$

which will play the role of λ for both[25] the approximated quantities $\underline{C}^{(0)}$ and $\underline{C}^{(1)}$. Analogous to (118), we will use the notation

$$T_1^{(0)} := \left(\lambda^{(0)} \ln 2\right)^{-1}.$$

Then, the thresholds $\lambda_{1\to 2}^{(0)}$ and $\lambda_{2\to 3}^{(0)}$ can be defined like the quantities (122) and (123).

Similar to capacity (the derivatives $dR^{(\rm hom)}/dN$ and $dR^{(\rm het)}/dN$ were defined in Section IV-K), one can introduce the quantities

$$\lambda^{(\rm hom)} := \frac{dR^{(\rm hom)}}{dN} = \frac{\eta}{\bar{o}_{u_\star} \ln 2} \tag{125}$$

$$\lambda^{(\rm het)} := \frac{dR^{(\rm het)}}{dN} = \frac{\eta}{\bar{o}_{u_\star}^{(\rm het)} \ln 2} \tag{126}$$

[23]Here, we use the property: if $g'(v) = y$, then $v = 1/(e^{\,y \ln 2} - 1)$.

[24]Similar result was presented in [32] for a number-state channel, where the optimal photon-number distribution is the Planck distribution parametrized by a Lagrange multiplier.

[25]Our purpose is to get (as much as possible) analytical relation for capacity in multimode setting discussed in Section VI. If the first-order approximation for g_1 function is used [see (20)], then the inversion of the dependence $\lambda(N)$ given by (116) gives rise to algebraic equation of high order; therefore, we use the quantity $\lambda^{(0)}$ also to derive $\underline{C}^{(1)}$.

for homodyne and heterodyne rates, respectively. Their threshold values will be denoted as $\lambda_{1\to 2}^{(\mathrm{hom})}$, $\lambda_{1\to 2}^{(\mathrm{het})}$, and $\lambda_{2\to 3}^{(\mathrm{het})}$. The "temperatures" for rates can be defined analogously to (118) as

$$T_1^{(\mathrm{hom})} := \left[\lambda^{(\mathrm{hom})} \ln 2\right]^{-1}, \quad T_1^{(\mathrm{het})} := \left[\lambda^{(\mathrm{het})} \ln 2\right]^{-1}. \tag{127}$$

Then, in the third stage, the quantities N and $\lambda^{(\mathrm{het})}$ are related by

$$N = T_1^{(\mathrm{het})} - \frac{1-\eta}{\eta} N_{\mathrm{env}} - \frac{1}{\eta}.$$

It follows from (99) and (100) that in the second stage, N depends on $\lambda^{(0)}$ (for capacity $\underline{C}^{(0)}$) as

$$N = \frac{1}{2}\left[T_1^{(0)} - \phi^{-1} + i_u - 1\right] \tag{128}$$

where

$$i_u = \frac{1}{2}\left[\sqrt{(\phi/4)^2 + \phi\, T_1^{(0)}} - \phi/4\right]. \tag{129}$$

Notice the similarity between (121) and (128). In fact, the first term in (121) is equal to $\bar{o}_{u_\star}/\eta$, which can be rewritten as [see (116)] $(g_1(\bar{\nu})/\eta)T \ln 2$. The latter is equal to T_1 if the replacement (56) is applied and η is set to 1. Taking into account the definitions (125)–(127), one can see that (128) and (129) hold also for rates if $T_1^{(0)}$ is replaced by $T_1^{(\mathrm{hom})}$ or $T_1^{(\mathrm{het})}$, ϕ is given by (94) or replaced by $\phi^{(\mathrm{het})}$ [see (96)], for homodyne and heterodyne rate, respectively.

M. Stage Transition and Quantum Water Filling

Finally, let us discuss the point of stage transition. As far as different stages correspond to solutions of different systems of Lagrange equations, it is natural that some properties (e.g., smoothness; see (192) and (194) in Appendix E) are violated at this point. In fact, this can be seen from Fig. 2(left), where the loci $(\bar{o}_q, \bar{o}_p)$ and (o_q, o_p) are plotted for different values of N and fixed values of s, η, and $\mathcal{N}_{\mathrm{env}}$. The dependence of $\bar{o}_p$ versus $\bar{o}_q$ given by the locus $(\bar{o}_q, \bar{o}_p)$ has a kink in the point of transition from second to third stage. Similarly, the function $\lambda(N)$ has a kink and the function $d\lambda/dN = d^2\underline{C}/dN^2$ is discontinuous at this point (see Fig. 3). However, the function $\underline{C}(N)$ is smooth at the point of stage transition, because its derivative (112) is continuous [see Fig. 2(right)].

In the third stage, we have equality (69), which can be written as

$$\eta(i_u + m_u) + (1-\eta)\, e_u = \eta(i_{u_\star} + m_{u_\star}) + (1-\eta) e_{u_\star}.$$

It means that the energy spent for modulation is distributed between quadratures in a way to equalize the eigenvalues of the state $\bar{V}_{\mathrm{out}}$. This type of solution is typical for optimization problems and it appears also for classical channels [35], where it was called "water filling." Later, such a solution was shown to hold for some parameters also for quantum channel with additive noise [22], [30], [36], where it was called "quantum water filling." For the case of lossy channel, this type of solution was presented in [12].

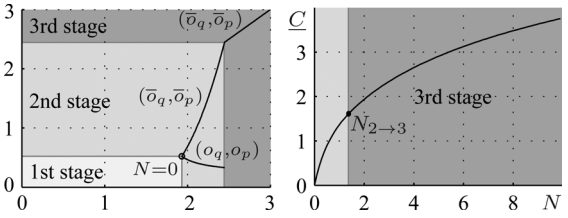

Fig. 2. (Left) Loci $(o_q(N), o_p(N))$ (bottom curve) and $(\bar{o}_q(N), \bar{o}_p(N))$ (top curve) for values of $N \in (0, 3)$ are plotted. The values of other parameters are $\mathcal{N}_{\mathrm{env}} = s = 1$ and $\eta = 0.6$. Different gray-scale backgrounds indicate the parameters' regions corresponding to different stages for given curves (the higher the stage, the darker the color). The first stage is a single point at $N = 0$, where $(o_q, o_p) = (\bar{o}_q, \bar{o}_p)$. In the third stage, the locus (o_q, o_p) is mapped into a single point (situated at the border between the second and the third stages) for all values of N, since V_{in} does not depend on N. In turn, the locus $(\bar{o}_q, \bar{o}_p)$ in the third stage is the line $\bar{o}_p = \bar{o}_q$. On the right, the quantity $\underline{C}$ is plotted versus N. One can see that the dependence $\underline{C}(N)$ is actually concave. The values of $N \in (0, N_{2\to 3}]$ (marked using light gray color) corresponds to the second stage, and the values of $N \in (N_{2\to 3}, 10)$ (marked with dark gray color) corresponds to the third stage.

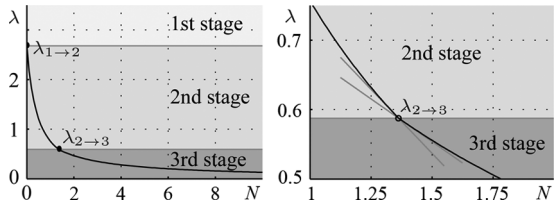

Fig. 3. Quantity λ is plotted versus N (the right is a magnification of the stage transition point $\lambda_{2\to 3}$). The values of other parameters are $s = 1, \eta = 0.7$, and $\mathcal{N}_{\mathrm{env}} = 0.5$. One can see that $\lambda_{1\to 2} = \lambda(N = 0) < \infty$. On the right, the left and right tangents are plotted at the point of $\lambda_{2\to 3} = \lambda(N_{2\to 3})$ (the left and right derivatives are different as it follows from (192) and (194) in Appendix E).

Quite generally, one can call "quantum water filling" all types of solutions for the optimal distribution of input energy between quadratures. It will be shown later in Section VI for memory channels that the input energy has to be distributed between many modes. In addition, all modes belonging to the third stage must possess equal average number of photons $\bar{N}_{\mathrm{out}}$, and for all of them equality $\bar{o}_u = \bar{o}_{u_\star}$ must hold. Furthermore, if almost all modes are in the third stage, the solution can be interpreted as a small perturbation of water filling. Thus, the term "quantum water filling" used for all types of solutions underlines the "physical" meaning of the performed optimization.

V. Role of Channel Parameters

In this section, we discuss the dependence from parameters of capacity and rates found in Section IV (i.e., for single channel use). Apart from characterizing the one-shot capacity, this study is also relevant for the case of multiple channel uses and additivity problem discussed below in Section VI.

It is evident that both capacity and rates must be monotonic functions of parameters η, N, and $\mathcal{N}_{\mathrm{env}}$. In fact, higher transmissivity and input energy cannot result to less capacity or rates from physical point of view. In addition, it was explicitly shown in Section IV-K that both capacity and rates are monotonic concave functions of N.

In turn, monotonic dependence of capacity from $\mathcal{N}_{\mathrm{env}}$ can be shown as follows. Given the value $\mathcal{N}'_{\mathrm{env}} > \mathcal{N}_{\mathrm{env}}$ the lossy channel for the parameters s, η, and $\mathcal{N}'_{\mathrm{env}}$ can be represented

as a channels composition $\mathcal{G}_N \circ \mathcal{G}_{\rm L}$, where $\mathcal{G}_{\rm L}$ is a lossy channel with parameters s, η, $\mathcal{N}_{\rm env}$ and $\mathcal{G}_N$ is an additive (classical) noise channel [see (26) and (27)] with environment matrix

$$V_{\rm env} = (1-\eta)(\mathcal{N}'_{\rm env} - \mathcal{N}_{\rm env}) \begin{pmatrix} e^s & 0 \\ 0 & e^{-s} \end{pmatrix}.$$

Since the capacity of the composition of two channels cannot exceed that of each individual channel, we deduce that the capacity is nonincreasing function of $\mathcal{N}_{\rm env}$. Furthermore, the following *environment purity theorem* states that the optimal $\mathcal{N}_{\rm env}$ is zero:

Theorem 3: The maximum of capacity on the set of environment states $\{V_{\rm env}\}$ whose elements have the same average amount of photons $N_{\rm env}$ is achieved on pure environment state, i.e., $e_u e_{u_\star} = 1/4$.

Proof: Proof is given in Appendix D. ■

Extension of this theorem to the case of rates is straightforward.

Thus, the only parameter which can make capacity and rates nonmonotonic is the environment squeezing s. In this section, we investigate this nonmonotonic dependence. Next, Sections V-B and V-C are mainly devoted to definitions, properties, and numerical results on channel parameters, while the other subsections contain analytical results justifying the numerics.

A. Role of Input and Environment Squeezing

Using representation (32) for input covariance matrix $V_{\rm in} = V(\mathcal{N}_{\rm in}, s_{\rm in})$, one can relate the optimal degree of input squeezing $s_{\rm in}$ to the degree of environment squeezing s. It follows from (73) and (92) that $s_{\rm in} = s$ for the third stage (for $\underline{C}$, $\underline{C}^{(0)}$, $\underline{C}^{(1)}$, and $\underline{C}^{(\log)}$) and

$$s_{\rm in} = \ln\left[\sqrt{1+(2N+1)\phi+\phi^2/4} - \phi/2\right] \qquad (130)$$

for the second stage (for $\underline{C}^{(0)}$ and $\underline{C}^{(\log)}$). Analogously, it follows from (73) that $s_{\rm in} = s^{(\rm het)}$ [see (42)] for the heterodyne rate in the third stage. In the second stage, both homodyne and heterodyne rates result to the same relation (130), where the replacement (95) must be applied for the heterodyne case. At the transition point between different stages, there is a *kink* in the function $s_{\rm in}(s)$ [see Fig. 4(left)]. It reflects the fact that different stages correspond to solution of different systems of equations. The dependence $i_q(s)$ is shown in Fig. 4(right) (this is discussed in the following sections in a more detailed way).

The capacity $\underline{C}$ found by the exact analytical solution is shown in Fig. 5 for fixed N as function of s and for different values of η (at left) and $\mathcal{N}_{\rm env}$ (at right). One can see that the squeezed environment ($s \neq 0$) may result to capacity enhancement. This phenomenon shows similarity with the improvement of the signal to noise ratio achieved by squeezed vacuum injection in an optical waveguide tap [33]. The highest enhancement occurs at either finite value of s or at $s \to \infty$ depending on the value of η. In any case, the capacity in the limit of large s becomes only function of the energy constraint N [see (110)] explaining why all curves $\underline{C}(s)$ flow together

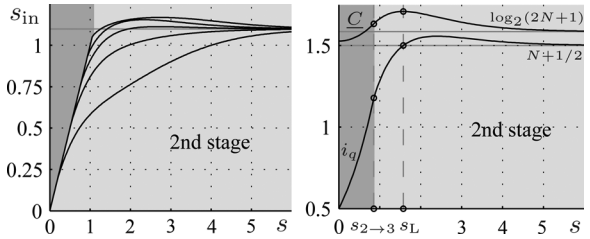

Fig. 4. (Left) Optimal input squeezing $s_{\rm in}$ is plotted versus s, for values of η going from 0.1 (bottom curve) to 0.9 (top curve) with step 0.2. The values of the other parameters are $N = 1$ and $\mathcal{N}_{\rm env} = 0$. (Right) Both the capacity $\underline{C}$ and optimal input eigenvalue i_q are plotted versus s. The value of the other parameters are $\mathcal{N}_{\rm env} = 0$, $N = 1$, and $\eta = 0.6$.

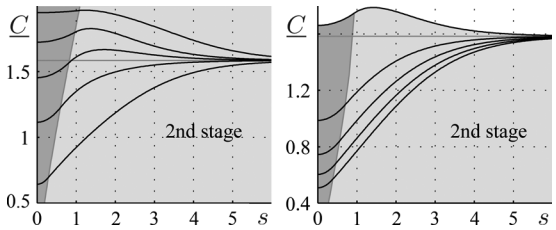

Fig. 5. (Left) Capacity $\underline{C}$ versus s, for values of η going from 0.15 (bottom curve) to 0.95 (top curve) with step 0.2. The values of the other parameters are $N = 1$ and $\mathcal{N}_{\rm env} = 0$. (Right) Capacity $\underline{C}$ versus s for values of $\mathcal{N}_{\rm env}$ going from 0 (top curve) to 4 (bottom curve) with step 1. The values of the other parameters are $\eta = 0.7$ and $N = 1$.

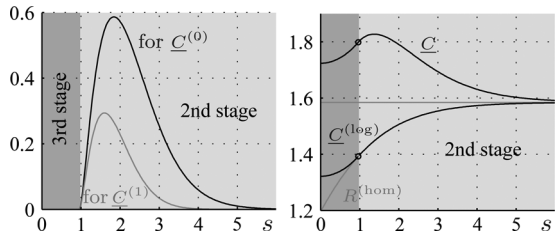

Fig. 6. (Left) Quantities $[(\underline{C} - \underline{C}^{(0)})/\underline{C}] \times 100\%$ (black) and $[(\underline{C} - \underline{C}^{(1)})/\underline{C}] \times 100\%$ (gray) are plotted versus s for $\eta = 0.75$, $N = 1$, and $\mathcal{N}_{\rm env} = 0$. (Right) Quantities $\underline{C}$, $\underline{C}^{(\log)}$, and $R^{(\rm hom)}$ are plotted versus s for $\eta = 0.75$, $N = 1$, and $\mathcal{N}_{\rm env} = 0$.

to the same value[26] when $s \to \infty$. Similarly, $s_{\rm in}$ tends to the value (104) for $s \to \infty$ because it follows from (130) (see also Fig. 4).

The difference among quantities $\underline{C}^{(0)}$, $\underline{C}^{(1)}$ and $\underline{C}$ is shown in Fig. 6(left). In Fig. 6(right), the quantities $\underline{C}$, $\underline{C}^{(\log)}$, and $R^{(\rm hom)}$ are shown together. One can see that $\underline{C}^{(\log)}$ coincides with homodyne rate in the second stage [see (46)].

The rates $R^{(\rm hom)}$ and $R^{(\rm het)}$ together with the exact solution for capacity are shown in Fig. 7 for fixed N as functions of s and for different values of η. One can see that in the second stage, both rates are monotonically growing functions of s which is in agreement with (97). In the third stage, the heterodyne rate may be nonmonotonic achieving its minimum. As it can be seen from Fig. 7, the optimal heterodyne rate is achieved at either $s \to \infty$ or $s = 0$. Analytical description of this behavior is given in Section V-J. A similar (to Fig. 7) family of curves can be obtained if $R^{(\rm het)}$ or $R^{(\rm hom)}$ is plotted versus s for different

[26]This behavior originally was observed in [11] for the capacity of particular memory channel found as maximum over a small subset of Gaussian states.

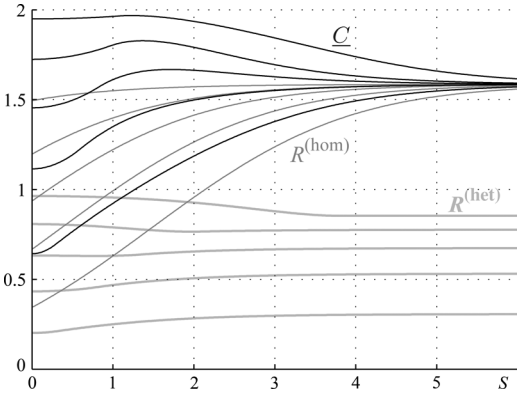

Fig. 7. Classical capacity $\underline{C}$ (solid curves), homodyne $R^{(\mathrm{hom})}$ (thin gray curves), and heterodyne $R^{(\mathrm{het})}$ (bold gray curves) rates versus s, for values of η going from 0.15 (bottom curve) to 0.95 (top curve) with step 0.2. The values of the other parameters are $N = 1$ and $\mathcal{N}_{\mathrm{env}} = 0$.

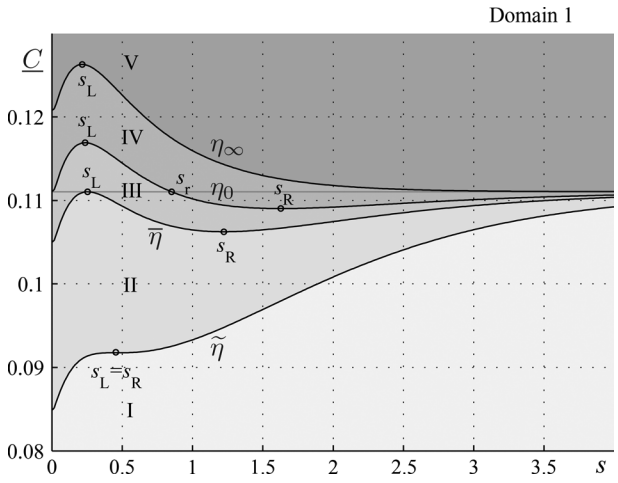

Fig. 8. Dependence $C(s)$ for channel parameters N and $\mathcal{N}_{\mathrm{env}}$ belonging to the *first domain* ($N = 0.04,\ \mathcal{N}_{\mathrm{env}} = 0.001$) is plotted for values of transmissivity $\eta = 0.28, 0.359, 0.384$, and 0.424 (from bottom to top), which approximately correspond to border values between different *regimes* ($\tilde{\eta}$, $\bar{\eta}$, η_0, and η_∞, respectively). Regimes are indicated with roman numbers (I–V) and different gray scale colors. Any curve $C(s)$ corresponding to a particular regime would completely lie in the area with the background color corresponding to that regime.

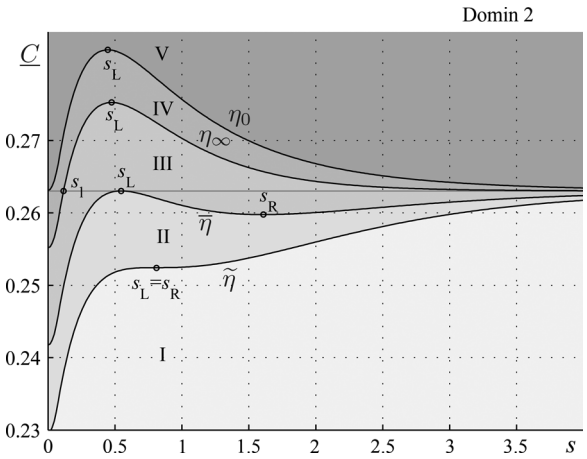

Fig. 9. Dependence $C(s)$ for channel parameters N and $\mathcal{N}_{\mathrm{env}}$ belonging to the *second domain* ($N = 0.1,\ \mathcal{N}_{\mathrm{env}} = 0$) is plotted for values of transmissivity $\eta = 0.369, 0.394, 0.423, 0.44$ (from bottom to top), which approximately correspond to border values between different *regimes* ($\tilde{\eta}$, $\bar{\eta}$, η_∞, and η_0, respectively). Regimes are indicated with roman numbers (I–V) and different gray scale colors. Any curve $C(s)$ corresponding to a particular regime would completely lie in the area with the background color corresponding to that regime.

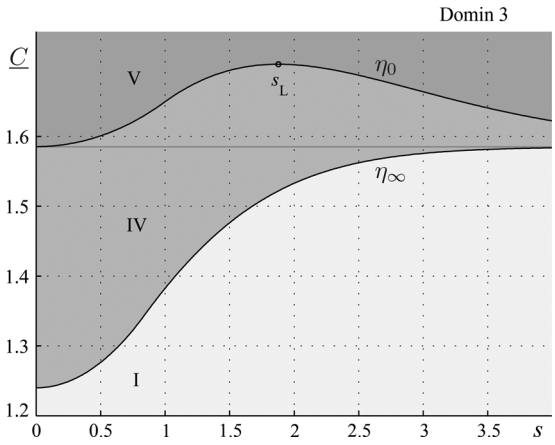

Fig. 10. Dependence $C(s)$ for channel parameters N and $\mathcal{N}_{\mathrm{env}}$ belonging to the *third domain* ($N = 1,\ \mathcal{N}_{\mathrm{env}} = 1$) is plotted for values of transmissivity $\eta = 0.808$ (bottom curve) and 0.919 (top curve), which approximately correspond to border values between different *regimes* (η_∞ and η_0, respectively). Regimes are indicated with roman numbers (I, IV, and V: other regimes do not exist in the third domain) and different gray scale colors. Any curve $C(s)$ corresponding to particular regime would completely lie in the area with the background color corresponding to that regime.

values of $\mathcal{N}_{\mathrm{env}}$ and fixed η. One can see that the universal limit (110) holds also for this case.

Despite the behavior shown in Fig. 5 is the most typical, there are parameters values giving more complicated dependence for $\underline{C}(s)$ (all possible cases are plotted in Figs. 8–11). In particular, the capacity may have both minimum and maximum each of them attained at finite environment squeezing $0 < s < \infty$. Such behavior and the parameters related with its description are discussed in the following sections.

B. Role of Transmissivity for Capacity

It was shown in Fig. 5 that both η and $\mathcal{N}_{\mathrm{env}}$ can be chosen to parametrize the family of curves $\underline{C}(s)$. In order to completely characterize how capacity depends on squeezing we will use η. All "qualitative" possibilities for the dependence $\underline{C}(s)$ are shown in Figs. 8–11. Such a dependence can be interpreted as crossing different *regimes* by increasing η from zero to one. In turn, the set of regimes depend on the *domain* which N and $\mathcal{N}_{\mathrm{env}}$ values belong to [see Fig. 11(bottom-right)]. Let us consider this behavior in more detail (in the relations below, the argument of $\underline{C}$ is assumed to be s).

Let us define the specific values of squeezing and transmissivity in a formal way. First, supported numerical calculations we state the following.

Proposition 4: The function $\underline{C}(s)$ may have at maximum two extrema for the values of squeezing $0 < s < \infty$.

Evidently, if the function $\underline{C}(s)$ has two extrema, then one of them must be maximum and the other minimum. They can be formally defined as follows.

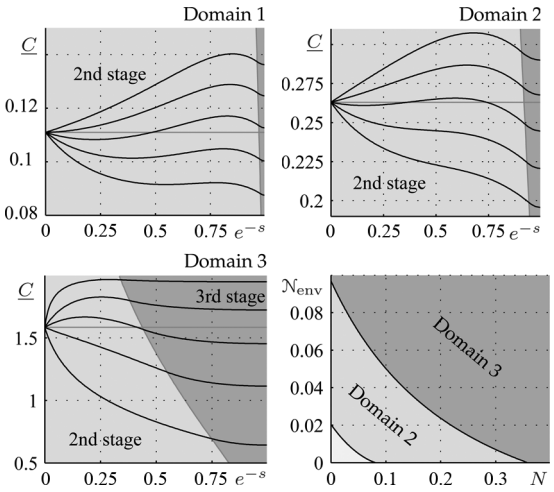

Fig. 11. Dependence $\underline{C}(e^{-s})$ for different values of η and fixed values of N and $\mathcal{N}_{\rm env}$. In particular, $N = 0.04$ and $\mathcal{N}_{\rm env} = 0$ (corresponding to the first domain), η goes from 0.275 (bottom) to 0.475 (top) with step 0.05 (top-left figure); $N = 0.1$ and $\mathcal{N}_{\rm env} = 0$ (corresponding to the second domain), η goes from 0.3 (bottom) to 0.5 (top) with step 0.05 (top-right figure); $\mathcal{N}_{\rm env} = 0$ and $N = 1$ (corresponding to the third domain), η goes from 0.15 (bottom) to 0.95 (top) with step 0.2 (bottom-left figure). The parts corresponding to different backgrounds belongs to different stages (lighter color states for second stage, and darker color states for third stage). Bottom-right: the loci $(N_0, \mathcal{N}_{\rm env,0})$ (bottom curve) and $(\widetilde{N}, \widetilde{\mathcal{N}}_{\rm env})$ (top curve), corresponding to transitions between different channel domains. The points $(N, \mathcal{N}_{\rm env})$ belonging to the area between these curves correspond to the domains indicated with different gray scale backgrounds colors.

Definition 2: The finite positive value of squeezing s will be denoted by $s_{\rm L}$ or $s_{\rm R}$ if the function $\underline{C}(s)$ has its local maximum or minimum at that values, respectively:

$$\underline{C}'(s_{\rm L}) = 0, \quad \underline{C}''(s_{\rm L}) < 0$$
$$\underline{C}'(s_{\rm R}) = 0, \quad \underline{C}''(s_{\rm R}) > 0.$$

One of our purpose is to study the value of squeezing giving highest capacity, which can be defined as written below.

Definition 3: The value of squeezing s will be denoted by $s_\star$ and called *optimal* if it corresponds to global maximum of the function $\underline{C}(s)$:

$$\underline{C}(s_\star) = \max_{0 \leqslant s \leqslant \infty} \underline{C}(s).$$

Finite values of squeezing providing the same value of capacity as infinite squeezing can exist.

Definition 4: The finite positive value of squeezing s will be denoted by s_l $(s_{\rm r})$ if both the value of function $\underline{C}(s)$ at that squeezing coincides with the value at infinity and $\underline{C}(s)$ is an increasing (decreasing) function at this point:

$$\underline{C}(s_l) = \underline{C}(\infty), \quad \underline{C}'(s_l) > 0$$
$$\underline{C}(s_{\rm r}) = \underline{C}(\infty), \quad \underline{C}'(s_{\rm r}) < 0.$$

As far as $\underline{C}(s)$ belongs to the third stage for small values of s and $\underline{C}(s)$ is always increasing function of s in the third stage, the extremum corresponding to the smallest value of squeezing must be the maximum. Hence, the minimum must correspond to higher value of squeezing which exists only if the maximum does. This also makes the function $\underline{C}(s)$ increasing in s_l and decreasing in $s_{\rm r}$. Thus, if both extrema exist, we have $s_{\rm L} < s_{\rm R}$ and $s_l < s_{\rm r}$ which explains the notations introduced in the definitions 2 and 4). In the general case, it follows from numerical results that the function $\underline{C}(s)$ in the interval $0 < s < \infty$ can be one of the following:

1) monotonic function without stationary points;
2) monotonic function with single saddle-point;
3) function with one maximum;
4) function with one maximum and one minimum.

In order to study the case with the saddle-point, we define the following transmissivity:

Definition 5: The transmissivity η will be denoted by $\tilde{\eta}$ and called *saddle-point transmissivity* if $\underline{C}(s)$ has saddle-point in some finite positive value of squeezing:

$$\exists\ \tilde{s} \in (0, \infty) | \underline{C}'(\tilde{s}) = \underline{C}''(\tilde{s}) = 0.$$

It follows from the results of numerical study that $\tilde{\eta}$ exists if and only if the following transmissivity does.

Definition 6: The transmissivity η will be denoted by $\bar{\eta}$ and called $\bar{\eta}$*-transmissivity* if a finite positive value of squeezing exists such that $\underline{C}(s)$ has maximum at that squeezing and the value of maximum is equal to $C(\infty)$:

$$\exists\ \bar{s} \in (0, \infty) | \underline{C}(\bar{s}) = \underline{C}(\infty),\ \underline{C}'(\bar{s}) = 0,\ \underline{C}''(\bar{s}) < 0.$$

Then, by considering the behavior of $\underline{C}(s)$ for zero and infinite squeezings, the following definitions can be introduced.

Definition 7: The transmissivity η will be denoted by η_0 and called η_0*-transmissivity* if the values of $\underline{C}(s)$ for zero and infinite squeezing coincide: $\underline{C}(0) = \underline{C}(\infty)$.

Definition 8: The transmissivity η will be denoted by η_∞ and called η_∞*-transmissivity* if $\underline{C}'(\infty) = 0$, i.e., in the neighborhood of infinite squeezing $\underline{C}(s)$ is decreasing for $\eta > \eta_\infty$ and increasing for $\eta < \eta_\infty$.

One can note that some properties (e.g., saddle-point) can be observed only for particular "domains" of the parameters N and $\mathcal{N}_{\rm env}$, which requires to introduce further classification. It follows from the results of numerical study that the following definitions allow us to divide the quadrant $(N > 0, \mathcal{N}_{\rm env} \geqslant 0)$ into three nonoverlapping *domains* [see Fig. 11(bottom-right)], thus providing consistent classification of all possible cases.

Definition 9: The parameters $(N, \mathcal{N}_{\rm env})$ belong to the *first* or to the *second domain* if $\eta_0 < \eta_\infty$ or $\eta_0 > \eta_\infty$, respectively.

Definition 10: The parameters $(N, \mathcal{N}_{\rm env})$ belong to the *third domain* if the function $\underline{C}(s)$ has at maximum one extremum in the interval $0 < s < \infty$ for all values of transmissivity $\eta \in (0, 1)$.

These domains correspond to the following relations between transmissivities:

1) *First domain*: $\tilde{\eta} < \bar{\eta} < \eta_0 < \eta_\infty$;
2) *Second domain*: $\tilde{\eta} < \bar{\eta} < \eta_\infty < \eta_0$;

3) *Third domain*: $\eta_\infty < \eta_0$ ($\tilde{\eta}$ and $\bar{\eta}$ do not exist).

In order to characterize the transitions from one domain to another, we will use the following definitions.

Definition 11: The value of N will be denoted by N_0 and called *supercritical* for a given value of $\mathcal{N}_{\rm env}$, if the point $(N_0, \mathcal{N}_{\rm env})$ corresponds to the transition from first to second domain. Similarly, the value of $\mathcal{N}_{\rm env}$ will be denoted by $\mathcal{N}_{{\rm env},0}$ and called *supercritical* for a given value of N, if the point $(N, \mathcal{N}_{{\rm env},0})$ corresponds to transition from first to second domain.

Definition 12: The value of N will be denoted by $\widetilde{N}$ and called *supercritical* for a given value of $\mathcal{N}_{\rm env}$, if the point $(\widetilde{N}, \mathcal{N}_{\rm env})$ corresponds to transition from second to third domain. Similarly, the value of $\mathcal{N}_{\rm env}$ will be denoted by $\widetilde{\mathcal{N}}_{\rm env}$ and called *supercritical* for a given value of N, if the point $(N, \widetilde{\mathcal{N}}_{\rm env})$ corresponds to transition from second to third domain.

Definition 13: The function $f(N, \mathcal{N}_{\rm env}) = 0$ will be denoted by f_0 and called *supercritical* if it corresponds to the boundary between the first and second domains. Similarly, the function $f(N, \mathcal{N}_{\rm env}) = 0$ will be denoted by $\tilde{f}$ and called *supercritical* if it corresponds to the boundary between the second and third domain.

As far as the boundary between domains characterizes the critical parameters (transmissivities), e.g., appearance of some critical parameters or the relations between them, the term "supercritical" was used in Definitions 11–13. One can also say that supercritical parameters are those critical parameters which characterize the other critical parameters.

The mnemonic rule to remember the notations used for the critical and supercritical parameters is the following. The quantities η_0 and η_∞ are defined by considering the behavior of capacity at the points of zero and infinite squeezing; therefore, these values are used as subscripts. The supercritical values N_0 and $\mathcal{N}_{{\rm env},0}$ correspond to transition between the domains which have different relations between η_0 and η_∞; therefore, subscript zero is used. The $\tilde{\eta}$-transmissivity corresponds to the case when $\underline{C}(s)$ decays into maximum to the left and minimum to the right if transmissivity η is slightly above the value $\tilde{\eta}$, i.e., $\underline{C}(s)$ forms a "wave" in such a case. This explains the usage of tilde sign. The transmissivity $\bar{\eta}$ corresponds to the case when the curve $\underline{C}(s)$ "touches" the upper line $\underline{C}(s) = \log_2(2N+1)$; therefore, overlining is used. Finally, the transition from the third to the second domain corresponds to the appearance of the quantity $\tilde{\eta}$, i.e., "wave" behavior of the curve $\underline{C}(s)$; therefore, the tilde sign is used for supercritical parameters $\widetilde{N}$ and $\widetilde{\mathcal{N}}_{\rm env}$.

Thus, we have defined four critical transmissivities ($\tilde{\eta}$, $\bar{\eta}$, η_0, and η_∞) and four specific values of squeezing ($s_{\rm R}$, $s_{\rm L}$, $s_{\rm r}$, and s_l). Similarly, by considering the family of functions $\underline{C}(s)$ parametrized by $\mathcal{N}_{\rm env}$ (for fixed values of η and N) or by N (for fixed values of η and $\mathcal{N}_{\rm env}$), the corresponding critical values for environment thermal or input photons can be considered, respectively. All these approaches can be generalized and considered as particular cases of *critical functions*. The latter are functions of the form $\delta(\eta, N, \mathcal{N}_{\rm env}) = 0$, where any of the parameters η, N, and $\mathcal{N}_{\rm env}$ is critical if the others are considered to be constants. In particular, by assuming N and $\mathcal{N}_{\rm env}$ to be constants and using notations for critical functions similarly to transmissivities, we get the following relations:

$$\begin{aligned}
&\tilde{\delta}(\tilde{\eta}, N, \mathcal{N}_{\rm env}) = 0\\
&\bar{\delta}\,(\bar{\eta}, N, \mathcal{N}_{\rm env}) = 0\\
&\delta_0(\eta_0, N, \mathcal{N}_{\rm env}) = 0\\
&\delta_\infty(\eta_\infty, N, \mathcal{N}_{\rm env}) = 0.
\end{aligned}$$

Now, once we have introduced all necessary definitions we can discuss how $\underline{C}(s)$ is varying by increasing η from zero to one. As one can see from Figs. 8–11, it passes in sequence the following five *regimes*:

I. $0 < \eta \leqslant \tilde{\eta}$ (for the third domain one can consider η_∞ instead of $\tilde{\eta}$).
Capacity is monotonically increasing function of $s \in \mathbb{R}_+$ and tends to its universal limit (110) from the bottom. Optimal squeezing $s_\star$ is equal to ∞. In particular, when $\eta = \tilde{\eta}$, capacity has its saddle-point for the value of squeezing $s = s_{\rm L} = s_{\rm R}$.

II. $\tilde{\eta} < \eta \leqslant \bar{\eta}$ (this regime does not exist for the third domain).
The saddle-point decays into two extrema—the capacity maximum to the left at the point of $s = s_{\rm L}$ and the capacity minimum to the right at the point of $s = s_{\rm R}$, where it is

$$\underline{C}(0) < \underline{C}(s_{\rm R}) < \underline{C}(s_{\rm L}) < \underline{C}(s_\star) = \underline{C}(\infty).$$

Higher values of η correspond to lower values $s_{\rm L}$ and to higher values of $s_{\rm R}$. Thus, despite we still have $s_\star = \infty$, the value of $s = s_{\rm L}$ could be more preferable because it is finite. When $\eta = \bar{\eta}$, the local maximum at the point $s = s_{\rm L}$ reaches the value of global maximum:

$$\underline{C}(s_{\rm L}) = \underline{C}(s_\star) = \underline{C}(\infty) = \log_2(2N+1).$$

III. $\bar{\eta} < \eta < \eta_0$ or $\bar{\eta} < \eta \leqslant \eta_\infty$ for the first and the second domains, respectively (this regime does not exist for the third domain).
Optimal squeezing $s_\star$ becames finite and equal to $s_{\rm L}$. Two values of squeezing s_l and $s_{\rm r}$ providing the same capacity as in the universal limit appear:

$$\underline{C}(s_l) = \underline{C}(s_{\rm r}) = \underline{C}(\infty).$$

Higher values of η correspond to higher $s_{\rm r}$ and lower s_l. Capacity approaches its universal limit from the bottom: $\underline{C}(0 \ll s < \infty) < \underline{C}(s = \infty)$.

a) *The first domain*. With the increasing of η the value of s_l is decreasing. It tends to zero when η tends to η_0 and then disappears (does not exist for $\eta \geqslant \eta_0$). The global capacity minimum for $\eta \to \eta_0 - 0$ is achieved at the value $s_{\rm R}$.

b) *The second domain*. When $\eta \to \eta_\infty$ both values of $s_{\rm r}$ and $s_{\rm R}$ tend to infinity, i.e.,

$$\underline{C}(s_{\rm r}) = \underline{C}(s_{\rm R}) = \underline{C}(\infty)$$

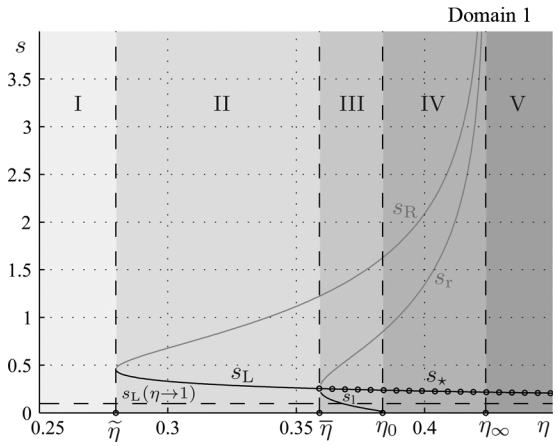

Fig. 12. Dependence of the quantities $s_{\rm r}$, s_l, $s_{\rm R}$, $s_{\rm L}$, and $s_\star$ versus η for capacity $\underline{C}$. The value of the other parameters are $N = 0.04$ and $\mathcal{N}_{\rm env} = 0.001$ (corresponding to the first domain). Different gray scale backgrounds corresponds to transmissivities η from different regimes (indicated with roman numbers). Vertical asymptotes are plotted for the critical transmissivities, and the horizontal asymptote shows the limit $\lim_{\eta\to 1} s_{\rm L}$. The part of the curve $s_{\rm L}(\eta)$ coinciding with $s_\star(\eta)$ is shown with dots. At the point $\eta = \bar{\eta}$ the quantity $s_\star$ jumps to infinity and for all values of $\eta \leqslant \bar{\eta}$ is equal to infinity.

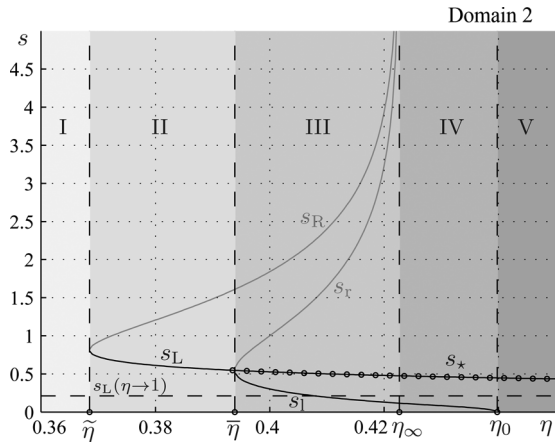

Fig. 13. Dependence of the quantities $s_{\rm r}$, s_l, $s_{\rm R}$, $s_{\rm L}$, and $s_\star$ versus η for capacity $\underline{C}$. The value of the other parameters are $N = 0.1$ and $\mathcal{N}_{\rm env} = 0$ (corresponding to the second domain). Different gray scale backgrounds corresponds to transmissivities η from different regimes (indicated with roman numbers). Vertical asymptotes are plotted for the critical transmissivities, and the horizontal asymptote shows the limit $\lim_{\eta\to 1} s_{\rm L}$. The part of the curve $s_{\rm L}(\eta)$ coinciding with $s_\star(\eta)$ is shown with dots. At the point $\eta = \bar{\eta}$ the quantity $s_\star$ jumps to infinity and for all values of $\eta \leqslant \bar{\eta}$ is equal to infinity.

and one of capacity extrema disappears. The global capacity minimum is still achieved at $s = 0$; therefore, any squeezed environment is still more preferable.

IV. $\eta_0 \leqslant \eta \leqslant \eta_\infty$ (for the first domain) or $\eta_\infty < \eta \leqslant \eta_0$ (for the second and the third domains).
   a) *The first domain*. The capacity has two minima at values of zero and $s = s_{\rm R}$, where $\underline{C}(0) > \underline{C}(s_{\rm R})$. When η tends to η_∞, both $s_{\rm r}$ and $s_{\rm R}$ tend to infinity and the right extremum of $\underline{C}(s)$ disappears.
   b) *The second and the third domains*. The capacity has two minima at values of zero and infinite squeezing, where $\underline{C}(0) < \underline{C}(\infty)$. Starting from this regime it will have only one extremum for finite nonzero values of s which is maximum at $s = s_{\rm L}$. When η reaches η_0, we have

$$\underline{C}(0) = \underline{C}(\infty) = \log_2(2N+1).$$

V. $\eta > \eta_\infty$ (for the first domain) or $\eta > \eta_0$ (for the second and the third domains).
   The global capacity minimum is at infinite squeezing, i.e., $\underline{C}(\infty) < \underline{C}(0)$.

The notion of regime can be also clarified by considering specific values of squeezing as functions of transmissivity for fixed values of N and $\mathcal{N}_{\rm env}$. In fact, one can see that these values of squeezing appear and disappear at some critical values of transmissivity which can also correspond to asymptotic lines (see Figs. 12–14). In particular, the optimal squeezing equals

$$s_\star = \begin{cases} \infty, & \text{if} \quad 0 < \eta < \eta' \\ s_{\rm L}, & \text{if} \quad \eta' < \eta < 1 \end{cases} \tag{131}$$

where $\eta' = \bar{\eta}$ for the case of first and second domains and $\eta' = \eta_\infty$ for the case of third domain. Moreover, the optimal squeezing asymptotically tends to infinity for the case of third domain, but discontinuously jumps to infinity for first and second domains. This transition behavior of optimal squeezing is shown in Fig. 15(left) and Fig. 16(left), where $s_\star < \infty$ is plotted as function of η for different values of $\mathcal{N}_{\rm env}$ and N, respectively. The capacity corresponding to these finite values of $s_\star$ is plotted in Fig. 15(right) and Fig. 16(right), respectively.

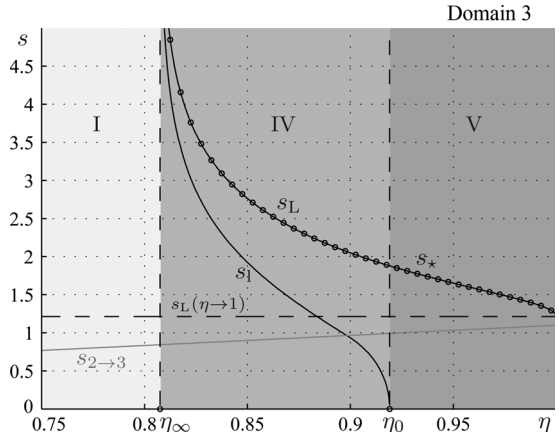

Fig. 14. Dependence of the quantities $s_{\rm r}$, s_l, $s_{\rm R}$, $s_{\rm L}$, $s_\star$, and $s_{2\to 3}$ versus η for capacity $\underline{C}$. The value of the other parameters are $N = 1$ and $\mathcal{N}_{\rm env} = 1$ (corresponding to the third domain). Different gray scale backgrounds correspond to transmissivities η from different regimes (indicated with roman numbers, the second and third regimes do not exist). Vertical asymptotes are plotted for the critical transmissivities, and the horizontal asymptote shows the limit $\lim_{\eta\to 1} s_{\rm L}$. The part of the curve $s_{\rm L}(\eta)$ coinciding with $s_\star(\eta)$ is shown with dots [$s_\star$ coincides with $s_{\rm L}$ on the whole region of transmissivities where $s_{\rm L}$ is defined, i.e., for $\eta \in (\eta_\infty, 1)$, and $s_\star$ equals infinity if $\eta \in (0, \eta_\infty)$]. At the point $\eta = \eta_\infty$, the quantity $s_\star$ together with $s_{\rm L}$ asymptotically tends to infinity. Also notice that $s_{2\to 3} \neq s_{\rm L}$ in the limit $\eta \to 1$.

Finally, let us consider how critical transmissivities depend on N and $\mathcal{N}_{\rm env}$. One can see that η_∞ does not depend on N and has nontrivial minimum for $\mathcal{N}_{\rm env} = 0$ [see Fig. 17(top-right)]. Then, both $\tilde{\eta}$ and $\bar{\eta}$ (we have always $\tilde{\eta} < \bar{\eta} < \eta_\infty$) are monotonically growing functions of $N \in (0, \widetilde{N})$ which disappear for the values of $N \geqslant \widetilde{N}$ and tend to η_∞ if N tends to $\widetilde{N}$ from the left. Notice that the values of $\tilde{\eta}$ and $\bar{\eta}$ do not tend to zero for $N \to 0$ if $\mathcal{N}_{\rm env} > 0$.

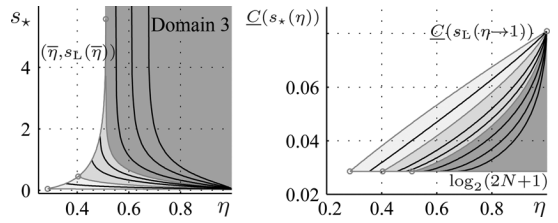

Fig. 15. Optimal environment squeezing $s_\star$ (left) and capacity $\underline{C}(s_\star(\eta))$ (right) are plotted versus η for values of $\mathcal{N}_{\rm env}$ equal to 0, 0.0055, 0.0165, 0.0413, 0.066, 0.0898, 0.1403, 0.2393, and 0.3879 (from bottom to top at left, and from top to bottom at right). The value of the other parameter is $N = 0.01$. Curves corresponding to different backgrounds belongs to different domains (darker background corresponds to higher domain). The curves corresponding to transition between different domains are plotted using gray color. (Left) Each curve belonging to the first or the second domain jumps to infinity at some finite value and equals infinity for all transmissivities to the left of that jump. Then, curves, corresponding to the third domain tend asymptotically to infinity and are equal to infinity for all values of η which are to the left of that asymptote. The whole region occupied by the finite dependences $s_\star(\eta)$ is bounded to the left by the locus $(\bar\eta, s_{\rm L}(\bar\eta))$. The values of $s_\star(\min\eta) < \infty$ corresponding to borders between different domains are indicated with gray points. It is interesting to note that the area corresponding to the second domain is bounded by finite value from the top, i.e., for the values of N and $\mathcal{N}_{\rm env}$ corresponding to transition from second to third domain, the value of $s_\star$ is still finite at the point $\eta = \bar\eta$. The area occupied by curves is bounded from the bottom by the curve $s_\star(\eta)$ for $\mathcal{N}_{\rm env} = 0$ which is not zero. (Right) Whole region occupied by family of possible curves $\underline{C}(s_\star(\eta))$ is bounded from the bottom by the limit (110). Here, we plotted capacity corresponding to finite values of $s_\star$ (for small values of η, we have $s_\star = \infty$; therefore, each curve $\underline{C}(s_\star(\eta))$ is equal to $\log_2(2N+1)$—this is not plotted). By increasing η from zero to one, we reach the point of $\eta = \bar\eta$ (for the first and second domains) or $\eta = \eta_\star$ (for the third domain) where the curve $\underline{C}(s_\star(\eta))$ is detached from horizontal line $\log_2(2N+1)$. And finally, when η tends to 1, all curves $\underline{C}(s_\star(\eta))$ tend to the same value $\lim_{\eta\to 1}\underline{C}(s_{\rm L}(\eta))$. One can see from numerics that this value does not depend on $\mathcal{N}_{\rm env}$.

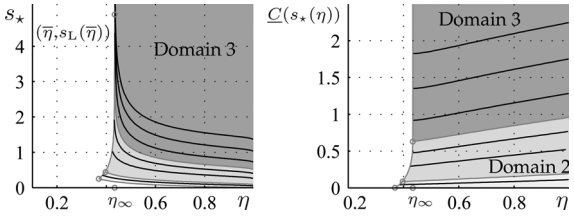

Fig. 16. Optimal environment squeezing $s_\star$ (left) and capacity $\underline{C}(s_\star(\eta))$ (right) are plotted versus η for values of N equal to 10^{-6}, 0.0149, 0.0298, 0.1127, 0.1956, 0.2755, 0.4443, 0.7760, and 1.2734 (from bottom to top for both: left and right graphs). The value of the other parameter is $\mathcal{N}_{\rm env} = 0.01$. Curves corresponding to different backgrounds belongs to different domains (darker background corresponds to higher number of domain). The curves corresponding to transition between different domains are plotted using gray color. (Left) Each curve belonging to the first or the second domain jumps to infinity at some finite value and equals infinity for all transmissivities which are to the left of that value. Then, curves corresponding to the third domain tend asymptotically to infinity (when η tends to η_∞ from the right) and are equal to infinity to the left of that asymptote. The whole region occupied by the finite dependences $s_\star(\eta)$ is bounded to the left by the locus $(\bar\eta, s_{\rm L}(\bar\eta))$. The values of $s_\star(\min\eta) < \infty$ corresponding to borders between different domains are indicated with gray points. It is interesting to note that the area corresponding to the second domain is bounded by the finite value from the top, i.e., for the values of N and $\mathcal{N}_{\rm env}$ corresponding to transition from the second to third domains, the value of $s_\star$ is still finite at the point $\eta = \bar\eta$. The area occupied by curves is bounded from the bottom by the curve $s_\star(\eta)$ for $N \to 0$ which is not zero. One can see that in the third domain the value of $\eta = \eta_\infty$ is the same for all curves. This is in fact in agreement with the analytical result (obtained in subsequent subsections) that η_∞ does not depend on N. (Right) Whole region occupied by family of possible curves $\underline{C}(s_\star(\eta))$ is bounded from the bottom by the zero. Here, we plotted the capacity corresponding to finite values of $s_\star$ (for small values of η we have $s_\star = \infty$; therefore, each curve $\underline{C}(s_\star(\eta))$ should be continued horizontally to the left being at the same level as in left border—this is not plotted).

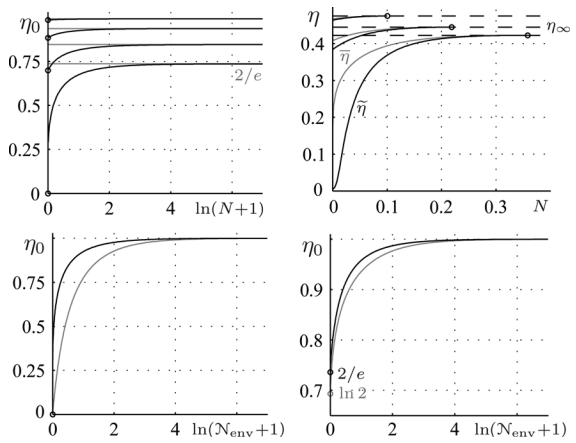

Fig. 17. (Top-left) Quantity η_0 is plotted versus $\ln(N+1)$ for the values of $\mathcal{N}_{\rm env}$ equal to 0, 0.2, 1, 10 (from bottom to top). (Top-right) Quantities $\tilde\eta$ (black solid), $\bar\eta$ (gray), and η_∞ (horizontal dashed black lines) are plotted versus N for the values $\mathcal{N}_{\rm env}$ equal to 0, 0.02, and 0.05 (from bottom to top for all curves). The points where $\tilde\eta$ and $\bar\eta$ touch the line corresponding to η_∞ are indicated with bold points. (Bottom-left) Function $\lim_{N\to 0}\eta_0$ versus $\ln(\mathcal{N}_{\rm env}+1)$ as exact [black curve; see (142)] and approximate [gray curve; see (145)] quantities. (Bottom-right) Function $\lim_{N\to\infty}\eta_0$ as exact [black curves; see (146)] and approximate [gray curve; see (148)] quantities. The values of all the quantities for all the graphs for zero argument are shown by bold point.

The η_0-transmissivity is plotted versus $\ln(N+1)$ for different values of $\mathcal{N}_{\rm env}$ in Fig. 17(top-left). One can see that η_0 has nontrivial limits for the values of N tending to zero and infinity. These limits are plotted in Fig. 17(left) and (right), respectively. It is interesting to note that the quantity $\eta_0(N \to \infty)$ also has nontrivial minimum.

The next sections will be devoted to analytical estimation of critical and supercritical parameters as well as to estimation of the specific values of squeezing. This will eventually allow us to prove most of their properties discussed in this section.

C. Stationary Points for Capacity

Let us consider the quantities $s_{\rm L}$, $s_{\rm R}$, δ_∞, and $\tilde\delta$ analytically. The critical function δ_∞ which characterize the behavior of the channel in the neighborhood of infinite environment squeezing $s \to \infty$ can be found as follows. We first note that only eigenvalues maximizing $\underline{C}$ are of interest; therefore, it is $\partial\underline{C}/\partial i_u = (\eta/2)\mathcal{F} = 0$, where $\mathcal{F} = 0$ is the mode transcendental (88). This allows us to simplify the derivative over s as

$$\frac{d\underline{C}}{ds} = \frac{\partial\underline{C}}{\partial s} + \frac{\partial\underline{C}}{\partial i_u}\frac{\partial i_u}{\partial s} = \frac{\partial\underline{C}}{\partial s}.$$

Its asymptotic behavior is

$$\frac{\partial\underline{C}}{\partial s} = \frac{\left[2N+1-(2N+1)^{-1}\right]\delta_\infty}{\eta(1-\eta)\left(\mathcal{N}_{\rm env}+\frac{1}{2}\right)\ln 2}e^{-s}$$

where

$$\delta_\infty = (1-\eta)^2\left(\mathcal{N}_{\rm env}+\frac{1}{2}\right)^2 - \frac{1}{12}. \tag{132}$$

Thus, η and $\mathcal{N}_{\rm env}$ are the only parameters which define how capacity tends to its universal limit (110). In particular, given a

value of $\mathcal{N}_{\rm env}$, the capacity tends to this limit from the top if $\eta > \eta_\infty$ and from the bottom if $\eta < \eta_\infty$, where η_∞ transmissivity can be found from the relation

$$(1-\eta_\infty)\left(\mathcal{N}_{\rm env}+\frac{1}{2}\right)=\frac{1}{\sqrt{12}}. \tag{133}$$

In particular, for the vacuum environment, it is

$$\eta_\infty = 1-\frac{1}{\sqrt{3}} \approx 0.42265.$$

Analogously, if the value of η is fixed, the capacity tends to the universal limit (110) from the top or bottom depending on the value of $\mathcal{N}_{\rm env}$, which follows from (133). Consequently, this value plays a role similar to critical transmissivity if the family of curves $\underline{C}(s)$ parametrized by $\mathcal{N}_{\rm env}$ for fixed η and N is considered [compare the curves in Fig. 5(left) and (right)]. It is interesting to note that this effect also exists for additive noise Gaussian channel where the quantity $\mathcal{N}_{\rm env}$ has the same meaning and its critical value equals $1/\sqrt{12}$ [34]. Thus, the critical parameters and the behavior shown in Fig. 5 may be relevant for a general Gaussian channel.

In order to specify the region where environment squeezing increases the capacity, in the following, we estimate the values of s corresponding to extrema of function $\underline{C}(s)$. Following [34], let us consider the system of equations[27] $\partial\underline{C}/\partial s = 0$, $\partial\underline{C}/\partial i_u = 0$ taken for the eigenvalues maximizing $\underline{C}$ and belonging to the second stage [extremum cannot be in the third stage since $\partial\underline{C}/\partial s \neq 0$ according to (76)]. Its solution results to the value $i_u = N+1/2$ and the value of s defined by

$$\mathcal{P}(s)=0 \tag{134}$$

where

$$\mathcal{P}=\frac{g_1(\bar\nu)}{\bar\nu^2}\sinh s-\frac{g_1(\nu)}{\nu^2}\frac{\sinh(s-\ln(2N+1))}{2N+1}.$$

Thus, we have the same value of i_u for both local extrema of $\underline{C}(s)$ and the point of $s=\infty$.

Solving (134) in the neighborhood of zero or infinite values of s one can estimate both its roots ($s_{\rm L}$ and $s_{\rm R}$). In particular, after the expansion of (134) in powers of e^{-s} in the neighborhood of $s\to\infty$, where terms higher than the second order are neglected, it takes the form $z_2(e^{-s})=0$ with $z_2(e^{-s})=be^{-2s}+ce^{-s}$ (b and c are some constants). The function $z_2(e^{-s})$ is the partial sum for Laurent series of the function $Z(e^{-s})$, where $Z=0$ is the (134). Both functions $z_2(e^{-s})$ and $Z(e^{-s})$ are concave in the neighborhood of $s\to\infty$ [see Fig. 18(top-right)]; therefore, their nontrivial[28] roots are close each other. The latter property explains why the approximation $z_2(e^{-s})=0$ is applicable and leads to the result

$$s_{\rm R}=\ln\frac{\left[1+(2N+1)^2\right]\left[\delta_\infty^2+\frac{1}{180}\right]-\frac{\eta^2}{6}\left[N+\frac{1}{2}\right]^2}{\eta\,(1-\eta)\left(N+\frac{1}{2}\right)\left(\mathcal{N}_{\rm env}+\frac{1}{2}\right)\delta_\infty} \tag{135}$$

[27]Since in the second stage all input and modulation eigenvalues are the explicit functions of i_u, by substituting them in the relation for capacity one can represent it as function of only one variable $\underline{C}(i_u)$. Then, as the dependence on squeezing is also analyzed, we consider the capacity as function $\underline{C}(s,i_u)$.

[28]The trivial solution which we imply is $e^{-s}=0$ corresponding to $s=\infty$.

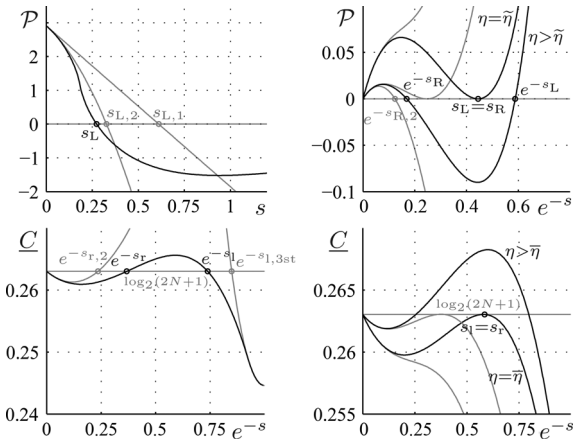

Fig. 18. Top-left (analytical method of estimation of $s_{\rm L}$): quantity $\mathcal{P}$ versus s together with its linear and quadratic approximations at the point $s=0$. The value of parameters are $\eta=0.8$, $N=0.1$, and $\mathcal{N}_{\rm env}=0$. Top-right (analytical method of estimation of $\bar\eta$): quantity $\mathcal{P}$ versus e^{-s} for the values $\eta=0.3985$ (bottom black curve, its quadratic and cubic approximations at point $e^{-s}=0$ through partial Taylor sum—gray color) and $\eta=0.3685$ (top black curve and its third approximation at point $e^{-s}=0$—gray color). The value of other parameters are $N=0.1$ and $\mathcal{N}_{\rm env}=0$. The points, where quadratic and linear approximations cross the line $\mathcal{P}=0$, defines quadratic and liner approximations for the corresponding s-quantities: approximations $s_{\rm L,2}$ and $s_{\rm L,1}$ for the quantity $s_{\rm L}$, and approximation $s_{\rm R,2}$ for the quantity $s_{\rm R}$. Similarly, the value of transmissivity at which cubic approximation has two roots (touches the line $\mathcal{P}=0$) defines approximation for $\bar\eta$. Bottom-left (method of estimation of s_l and $s_{\rm r}$): $\underline{C}$ versus e^{-s} for the values of $\eta=0.4$, $N=0.1$, and $\mathcal{N}_{\rm env}=0$. Bottom-right (method of estimation of $\bar\eta$): $\underline{C}$ versus e^{-s} for the values of $\eta=0.3939$ (bottom black curve) and $\eta=0.4062$ (top black curve). The value of other parameters are $N=0.1$ and $\mathcal{N}_{\rm env}=0$. For the top black curve, its cubic approximation gives an estimation for the quantity $\bar\eta$.

where critical function δ_∞ is given by (132) and characterizes the "criticality" of the given channel parameters (their vicinity to the transition point). Notice that according to estimation (135), we have

$$\lim_{\eta\to\eta_\infty} s_{\rm R}=\lim_{\delta_\infty\to 0} s_{\rm R}=\infty.$$

Analogously, considering the next-order approximation for (134), one can construct the function $z_3(e^{-s})=ae^{-3s}+be^{-2s}+ce^{-s}$ and find the condition when both nontrivial roots of the equation $z_3(e^{-s})=0$ coincide. This is the case of $s_{\rm L}=s_{\rm R}$ (both $s_{\rm L}$ and $s_{\rm R}$ are taken from approximation z_3, see Fig. 18), i.e., the saddle-point of the curve $\underline{C}(s)$ where both the derivatives $\partial\underline{C}/ds$ and $\partial^2\underline{C}/ds^2$ equal zero. In Section V-A, this approach will be used in order to provide analytical estimation of the saddle-point transmissivity $\tilde\eta$.

Similarly, expanding (134) in powers of s in the neighborhood of $s=0$, we get an equation of the form $as^3+bs^2+cs=0$ (a, b, and c are some constants depending on channels parameters), whose nontrivial root is an estimation for the left extremum $s_{\rm L}$ (see Section V-E for its value and derivation).

Analyzing the equation $\underline{C}(s)=0$ instead of (134) and applying the same method (expansion in powers of e^{-s} in the neighborhood of $s=\infty$ and in powers of s in the neighborhood of $s=0$), one can estimate both left (s_l) and right ($s_{\rm r}$) roots. In particular, one can get the relation

$$s_{\rm r}=s_{\rm R}-\ln 2.$$

Estimation of s_l is given in Section V-G. The case when s_l and $s_{\rm r}$ (considered for this approximation) coincide corresponds to $\bar{\eta}$ transmissivity, which is estimated in Section V-H.

D. Estimation of $s_{\rm L}$

Let us estimate the quantity $s_{\rm L}$. Our purpose is to solve (134) in the neighborhood of $s = 0$ taking into account that all eigenvalues in extrema points are known. At first, notice that squares of symplectic eigenvalues as functions of s in the extrema points read

$$\nu_{\rm e}^2(s) = \mathcal{Q}\left[\frac{\eta}{2}, (1-\eta)\left(\mathcal{N}_{\rm env}+\frac{1}{2}\right), s - \ln(2N+1)\right]$$
$$\bar{\nu}_{\rm e}^2(s) = \mathcal{Q}\left[\eta\left(N+\frac{1}{2}\right), (1-\eta)\left(\mathcal{N}_{\rm env}+\frac{1}{2}\right), s\right]$$

where

$$\mathcal{Q}(a,b,\varphi) := a^2 + b^2 + 2ab\cosh(\varphi).$$

In the following, we use the notations $\nu_{\rm e,0} = \nu_{\rm e}(0)$ and $\bar{\nu}_{\rm e,0} = \bar{\nu}_{\rm e}(0)$. Let us define the function

$$\boldsymbol{y}(x_1, x_2) = \frac{x_1}{\nu_{\rm e,0}^2} + \frac{x_2}{\left(\nu_{\rm e,0}^2 - \frac{1}{4}\right) g_1(\nu_{\rm e,0})}$$

and introduce the following notations:

$$\mathcal{X} := \frac{\eta}{2}(1-\eta)\left(\mathcal{N}_{\rm env}+\frac{1}{2}\right)$$
$$\mathfrak{cn} := \cosh(\ln(2N+1))$$
$$\mathfrak{sn} := \sinh(\ln(2N+1)).$$

By representing (134) as $\mathcal{P}(s) = as^2 + bs + c = 0$, we can find both linear (supposing $a = 0$) and quadratic ($a \neq 0$) approximations. They result as estimations of squeezing in left extremum of $C(s)$ (denoted as $s_{\rm L,1}$ for linear approximation and $s_{\rm L,2}$ for quadratic one):

$$s_{\rm L,1}^{-1} = \mathcal{K}_1, \qquad s_{\rm L,2}^{-1} = \frac{1}{2}\left(\sqrt{\mathcal{K}_1^2 - 2\mathcal{K}_2} + \mathcal{K}_1\right)$$

where

$$\mathcal{K}_1 = \frac{\mathfrak{cn}}{\mathfrak{sn}} - \mathcal{X}\boldsymbol{y}(1,1)\,\mathfrak{sn} - \frac{(2N+1)}{\mathfrak{sn}}\frac{\nu_{\rm e,0}^2}{\bar{\nu}_{\rm e,0}^2}\frac{g_1(\bar{\nu}_{\rm e,0})}{g_1(\nu_{\rm e,0})} \tag{136}$$

$$\mathcal{K}_2 = 1 - 3\mathcal{X}\boldsymbol{y}(1,1)\,\mathfrak{cn} + \mathfrak{sn}^2\mathcal{X}^2\boldsymbol{y}\left(3\boldsymbol{y}(1,1), \frac{2}{\nu_{\rm e,0}^2 - \frac{1}{4}}\right). \tag{137}$$

Approximation $s_{\rm L,1}$ is applicable only if $\mathcal{K}_1 > 0$ and $s_{\rm L,2}$ is applicable only if $\mathcal{K}_1^2 > 2\mathcal{K}_2$ (it is equivalent to $N < \left(\sqrt{2}\right)^{-1}$ if $\eta \to 1$). These regions of applicability follow from the condition that proper equations must have their roots positive.

Let us consider the limit $\lim_{\eta\to 1} s_{\rm L}$. First, note that both second and third terms in relations (136) and (137) disappear when $\eta \to 1$; therefore, we have

$$\lim_{\eta\to 1} s_{\rm L,1} = \frac{\mathfrak{sn}}{\mathfrak{cn}} = \frac{2N(N+1)}{2N(N+1)+1} = \frac{1}{1+\phi_{s_{\rm L}}} \tag{138}$$

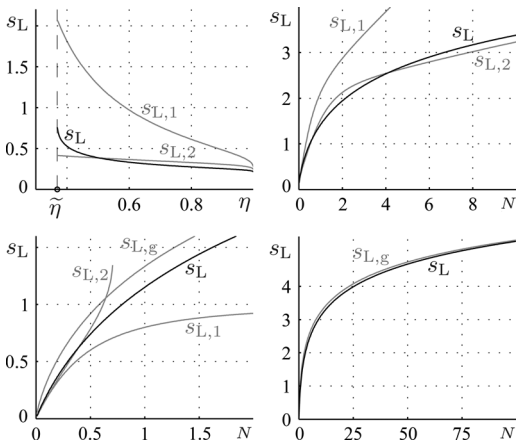

Fig. 19. Top: Dependence of the quantities $s_{\rm L}$, $s_{\rm L,1}$, and $s_{\rm L,2}$ versus η (left) and versus N (right). The value the other parameters are: $N = 0.1$ and $\mathcal{N}_{\rm env} = 0$ (left), $\eta = 0.9$ and $\mathcal{N}_{\rm env} = 0.1$ (right). Bottom (left and right): the quantity $\lim_{\eta\to 1} s_{\rm L}$ versus N (the value of $\mathcal{N}_{\rm env}$ was set to zero, but numerically this limit does not depend on $\mathcal{N}_{\rm env}$). To the left it is plotted together with the approximations $s_{\rm L,1}$, $s_{\rm L,2}$, $s_{\rm L,g} = \frac{2}{3}g(N)$, and to the right it is plotted together only with $s_{\rm L,g} = \frac{2}{3}g(N)$ [see (138) and (139)]. Approximations $s_{\rm L,1}$ and $s_{\rm L,2}$ are plotted only for those values of the argument where they are applicable.

where

$$\phi_{s_{\rm L}} = \frac{1}{2N(N+1)}.$$

The quantity $\lim_{\eta\to 1} s_{\rm L,1}$, in turn, tends to 1 for $N \to \infty$ and to zero for $N \to 0$. Analogously

$$\lim_{\eta\to 1} s_{\rm L,2}^{-1} = \frac{1}{2}\left(1 + \phi_{s_{\rm L}} + \sqrt{\phi_{s_{\rm L}}^2 + 2\phi_{s_{\rm L}} - 1}\right). \tag{139}$$

Notice that approximations (138) and (139) do not depend on thermal photons $\mathcal{N}_{\rm env}$. This is an argument in support of the behavior observed numerically in Fig. 15 for the exact limit.

The dependence of $s_{\rm L}$ and its approximation from parameters is shown in Fig. 19. One can see that $s_{\rm L}$ is monotonically decreasing function of η, which indeed has nontrivial limit for $\eta \to 1$.

E. Estimation of η_0

As it follows from Definition 7, the transmissivity η_0 is given by

$$\mathcal{O}(\eta) = 0 \tag{140}$$

where

$$\mathcal{O}(\eta) := g\left[\eta N + (1-\eta)\mathcal{N}_{\rm env}\right] - g\left[(1-\eta)\mathcal{N}_{\rm env}\right] - \log_2(2N+1). \tag{141}$$

Note that for $s = 0$, we have the case of the third stage and $N_{\rm env} = \mathcal{N}_{\rm env}$. We can have the following cases: $\eta_0 < \eta_\infty$ (see Fig. 8), $\eta_0 > \eta_\infty$ (see Fig. 9), and $\eta_0 = \eta_\infty$. The latter case corresponds to transition from first to second domain and defines the locus $(N, \mathcal{N}_{\rm env})$ where equality $\eta_0 = \eta_\infty$ holds. One can see from Fig. 11(bottom-right) that the limit value $\mathcal{N}_{\rm env} = \mathcal{N}_{\rm env,0}$, which still can have $\eta_0 = \eta_\infty$, is achieved at $N = 0$. However, since (140) is satisfied by any values of η and $\mathcal{N}_{\rm env}$ if

$N = 0$, we have to solve it for the limit $N \to 0$. By expanding (140) over N, we get the equation $N\partial\mathcal{O}/\partial N = 0$. Then, by substituting $N = 0$ into $\partial\mathcal{O}/\partial N = 0$, we get

$$\eta_0 \ln\left(1 + \frac{1}{(1-\eta_0)\mathcal{N}_{\rm env}}\right) = 2. \tag{142}$$

The joint solution of the system of (142), (133), and $\eta_0 = \eta_\infty$ results to

$$\left(1 - \frac{1}{\sqrt{3}\,(2\mathcal{N}_{\rm env}+1)}\right) \ln\left(1 + \frac{\sqrt{3}\,(2\mathcal{N}_{\rm env}+1)}{N_{\rm env}}\right) = 2.$$

Its solution is the supercritical value

$$\mathcal{N}_{{\rm env},0}(N=0) \approx 0.0204.$$

Limit Values of $\mathcal{N}_{\rm env}$: For high values of $\mathcal{N}_{\rm env}$, (140) has its asymptotic behavior given by the relation

$$\log_2 \frac{\eta N + (1-\eta)\,\mathcal{N}_{\rm env} + \frac{1}{2}}{(1-\eta)\,\mathcal{N}_{\rm env} + \frac{1}{2}} = \log_2(2N+1)$$

from which one can get

$$(1-\eta)(1+2\mathcal{N}_{\rm env}) = 0$$

i.e.,

$$\lim_{\mathcal{N}_{\rm env}\to\infty} \eta_0 = 1. \tag{143}$$

In the case of pure (i.e., $\mathcal{N}_{\rm env} = 0$), environment η_0 is equal to [see (140)]

$$\eta_0 = \frac{1}{N} g^{-1}\left[\log_2(2N+1)\right]. \tag{144}$$

In turn, by supposing $\eta_0 = \eta_\infty$, we get the equation for N

$$\frac{1}{N} g^{-1}\left[\log_2(2N+1)\right] = 1 - \frac{1}{\sqrt{3}}$$

whose solution is the supercritical value

$$N_0(\mathcal{N}_{\rm env} = 0) \approx 0.0817.$$

Thus, $\eta_0 > \eta_\infty$ if $N > N_0(0)$, and $\eta_0 < \eta_\infty$ if $N < N_0(0)$ (see examples in Figs. 8–10). In other words, if and only if $N \geqslant N_0(0)$, we have

$$\forall s \quad C(s, \eta \geqslant \eta_0) \geqslant \log_2(2N+1).$$

In particular, if the environment is pure, $\eta > \eta_0$ and $N \geqslant N_0(0)$, then the universal limit gives the global minimum for $C(s)$, and $s_{\rm L}$ gives the global maximum:

$$\min_{0\leqslant s\leqslant\infty} C(s) = \log_2(2N+1)$$
$$\max_{0\leqslant s\leqslant\infty} C(s) = C(s_{\rm L}).$$

The Case $N \to 0$: By considering (142) for $\mathcal{N}_{\rm env} \gg 0$, we obtain, to linear approximation in $\mathcal{N}_{\rm env}^{-1}$, that

$$\lim_{N\to 0} \eta_0(\mathcal{N}_{\rm env} \gg 0) = \frac{2\mathcal{N}_{\rm env}}{2\mathcal{N}_{\rm env}+1}. \tag{145}$$

Using (144), we get for pure environment

$$\lim_{N\to 0} \eta_0(\mathcal{N}_{\rm env} = 0) = 0.$$

The Case $N \to \infty$: By taking the limit $N \to \infty$ in (140) (we use expansion of g-function), one can get that it is equivalent to

$$\log_2 \frac{\eta e}{2} - g\left[(1-\eta)\mathcal{N}_{\rm env}\right] = 0. \tag{146}$$

In particular, for pure environment, we get

$$\lim_{N\to\infty} \eta_0(\mathcal{N}_{\rm env} = 0) = \frac{2}{e}. \tag{147}$$

The function $g(x)$ behaves like $-x\log_2 x$ for small values of x. Using this property and expanding the logarithm in the first term of (146) in powers of $\varepsilon := 1 - \eta$ up to the first order, one can obtain the equation

$$\ln\frac{e}{2} - \varepsilon + \varepsilon\mathcal{N}_{\rm env}\ln(\varepsilon\mathcal{N}_{\rm env}) = 0.$$

Its solution gives an estimation of $\lim_{N\to\infty}\eta_0$:

$$\lim_{N\to\infty}\eta_0 = 1 - \left[\mathcal{N}_{\rm env} W_{-1}\left(e^{-\mathcal{N}_{\rm env}^{-1}}\ln\frac{2}{e}\right)\right]^{-1}\ln\frac{2}{e} \tag{148}$$

where W_{-1} is -1 branch of Lambert W function which is solution of $W(z)e^{W(z)} = z$ and whose properties are well known [37]. One can show that the approximation (148) has the limits

$$\lim_{\mathcal{N}_{\rm env}\to\infty}\lim_{N\to\infty}\eta_0 = 1$$
$$\lim_{\mathcal{N}_{\rm env}\to 0}\lim_{N\to\infty}\eta_0 = \ln 2. \tag{149}$$

The first limit coincides with the exact value [see (143)], but the second one is different [see (147)]. Maximal error of estimation (148) is about 5% and achieved by $\mathcal{N}_{\rm env} = 0$. As far as $\lim_{N\to\infty}\eta_0$ is monotonic over $\mathcal{N}_{\rm env}$ [see (148)], (147) gives its minimum:

$$\lim_{N\to\infty}\eta_0 \geqslant \frac{2}{e}.$$

Equation (149) can be obtained as follows. First, note that the following limit holds:

$$\lim_{z\to 0-0}\frac{\ln(-z)}{W_{-1}(z)} = 1. \tag{150}$$

It can be obtained by applying logarithm to both parts of equation

$$-W_{-1}(z)e^{W_{-1}(z)} = -z, \quad z < 0$$

and then dividing it by $W_{-1}(z)$. Notice that $W_{-1}(z) < 0$ for $z \in \left[-e^{-1}, 0\right]$ and has the limit

$$\lim_{z\to 0-0} W_{-1}(z) = -\infty.$$

Let us define a new variable $x < 0$ to be equal to the argument of W_{-1} in (148) and consider the limit of (148) for $x \to 0 - 0$ which corresponds to $\mathcal{N}_{\rm env} \to 0$. Taking into account (150), we arrive at the result (149).

The dependence of η_0 on parameters is shown in Fig. 17.

F. Estimation of s_l

The definition $C(s_l) = \log_2(2N+1)$ results to

$$\cosh s_l = \frac{g^{-1}\left[\log_2(2N+1) + g((1-\eta)\,\mathcal{N}_{\rm env})\right] - \eta\left(N+\frac{1}{2}\right)+\frac{1}{2}}{(1-\eta)\left(\mathcal{N}_{\rm env}+\frac{1}{2}\right)}$$

which for pure environment reads

$$\cosh s_l = 1 + \frac{2N(\eta_0-\eta)}{1-\eta} \tag{151}$$

where $\eta_0 = \eta_0(\mathcal{N}_{\rm env}=0)$ is given by (144). In particular, it is clear from (151) that

$$\lim_{\eta\to\eta_0-0} s_l = 0$$

which is in full correspondence with the definition and properties of s_l.

G. Full-Channel Characterization

Let us summarize the results that we obtained for channel characterization. We started from the point that squeezing s is the only parameter which gives rise to nonmonotonic dependence of capacity $\underline{C}$. We have analyzed this behavior for typical values of N and $\mathcal{N}_{\rm env}$ (see Fig. 5) and found that $\underline{C}(s)$ has maximum in the interval $0<s<\infty$ if $\eta>\eta_\infty$, and is monotonic otherwise. Then, we have shown that the family of curves $\underline{C}(s)$ can be considered also for different values of $\mathcal{N}_{\rm env}$ and fixed η. Both these cases can be described using the parameter δ_∞ [see (132)]. Thus, we get the pair of parameters $(\eta_\infty, \mathcal{N}_{\rm env})$ characterizing the behavior of $\underline{C}(s)$ in the neighborhood of infinity. Then, we considered also other critical parameters, namely, $\tilde\eta$, $\bar\eta$, and η_0 by analyzing the family of curves $\underline{C}(s)$ for different values of η and fixed $\mathcal{N}_{\rm env}$. However, by considering the family of curves $\underline{C}(s)$ for different values of $\mathcal{N}_{\rm env}$ (or N) and fixed η one can also introduce analogous critical parameters as the values of $\mathcal{N}_{\rm env}$ (or N). Hence, we finally have four triads of critical parameters to characterize the channel. After that we have analyzed how these critical parameters depend on N and $\mathcal{N}_{\rm env}$ by introducing supercritical parameters.

On the other hand, one can also say that critical parameters have allowed us to split the total space $(0\leqslant\eta\leqslant 1,\ 0\leqslant N\leqslant\infty,\ 0\leqslant\mathcal{N}_{\rm env}\leqslant\infty)$ into *regimes* with different properties of the dependence $\underline{C}(s)$, while supercritical parameters have allowed us to split the total space $(0\leqslant N\leqslant\infty,\ 0\leqslant\mathcal{N}_{\rm env}\leqslant\infty)$ into *domains* with different properties of the critical parameters. Finally, note that given the type of domain, regime, and stage for parameters η, N, $N_{\rm env}$, one can qualitatively plot the family of curves $\underline{C}(s)$ (for different values of η) without numerical calculations and put forward all important points and extrema of these curves.

This classification completely characterizes the role of environment squeezing. For example, "supernonmonotonic" behavior of $\underline{C}(s)$ (when it has two extrema in the interval $0<s<\infty$) is only possible in the first and second domains, since in the third domain, $\underline{C}(s)$ has at maximum a single extremum. Most of practically interesting channel parameters belong to the third domain; however, this classification is useful, as it provides exact conditions *when it is so* (expected behavior of $\underline{C}(s)$ from the third domain). The global optimal squeezing $s_\star$ has sudden jump to infinity at $\bar\eta$ in the first and second domains, but tends asymptotically to infinity in the third domain.

It is quite nontrivial that despite this difficult classification scheme the existence of supercritical parameters can be shown analytically (see Section V-H). Moreover, in some important cases, they can be found exactly and analytically (being expressed through radicals). Thus, despite we have started from numerical analysis of the dependence $\underline{C}(s)$, there are analytical results which support the found properties (see Section V-H).

H. Supercritical Parameters

First, we have to remember that $\tilde\eta$ tends to η_∞ when channel passes from second to third domain [see Fig. 17(top-right)]. In particular, the limits

$$\lim_{(N,\mathcal{N}_{\rm env})\to(\widetilde{N},\widetilde{\mathcal{N}}_{\rm env})}\ \lim_{\eta\to\tilde\eta^+} s_{\rm L}(\eta) = \infty \tag{152}$$

$$\lim_{(N,\mathcal{N}_{\rm env})\to(\widetilde{\mathcal{N}},\widetilde{N}_{\rm env})}\ \lim_{\eta\to\tilde\eta^+} s_{\rm R}(\eta) = \infty \tag{153}$$

are supported by numerical calculations (here, the notation "$(N,\mathcal{N}_{\rm env})\to(\widetilde{N},\widetilde{\mathcal{N}}_{\rm env})$" means that we consider the values $(N,\mathcal{N}_{\rm env})$ belonging to the second domain and tending to the border between second and third domain). Relations (152) and (153) are equivalent to the following statement: the value of squeezing corresponding to saddle-point transmissivity tends to infinity if the values of the channel parameters $(N,\mathcal{N}_{\rm env})$ tend to those from the third domain. Consequently, in this case, the quantities $e^{-s_{\rm L}}, e^{-s_{\rm R}}$ tend to zero. Thus, we can say that the transition between second and third domains is completely characterized by the behavior of the function (134) in the neighborhood of the point $e^{-s}=0$ [remember, that $e^{-s_{\rm L}}$ and $e^{-s_{\rm R}}$ are zeros of the function (134)]. Let us now consider the Taylor expansion of (134) in the neighborhood of that point. To the third order, it gives rise to the relation

$$ae^{-3s} + be^{-2s} + ce^{-s} = 0 \tag{154}$$

which is an approximate form of (134) in the neighborhood of $e^{-s}=0$. Remember that the coefficient c is proportional to δ_∞ [see (132)] and defines the transition from "undercritical" to "uppercritical" parameters of transmissivity and thermal photons. If we neglect a constant factor, c is just a denominator of the fraction under logarithm in $s_{\rm R}$ [see (135)]. The case when $\tilde\eta$ disappears corresponds to the case when the function (134) has no roots in the neighborhood of $e^{-s}=0$ except of the point $e^{-s}=0$ itself. As far as (134) in this neighborhood is the polynomial (154), this condition is equivalent to the statement that this polynomial has no other extrema except of the point $e^{-s}=0$. It is exactly so if both $b=c=0$. Thus, by substituting $\delta_\infty=0$ and $\eta=\eta_\infty$ in the relation $b=0$ [up to a constant factor b is a numerator in the fraction under logarithm of (135)], we get

$$\frac{1+(2N+1)^2}{180} - \frac{1}{6}\left[\left[1-\frac{1}{\sqrt{3}(2\mathcal{N}_{\rm env}+1)}\right]\left[N+\frac{1}{2}\right]\right]^2 = 0.$$

This relation between the values of N and $\mathcal{N}_{\rm env}$ is that defined by the function $\tilde{f}(\widetilde{N}, \widetilde{\mathcal{N}}_{\rm env}) = 0$; therefore, it can be rewritten as [see the parallelism with relation (133)]

$$(1-\tilde{\eta}_\infty)\left(\widetilde{\mathcal{N}}_{\rm env}+\frac{1}{2}\right)=\frac{1}{\sqrt{12}}$$

where the *supercritical transmissivity* $\tilde{\eta}_\infty$ is

$$\tilde{\eta}_\infty=\sqrt{\frac{2}{15}\left(\frac{1}{(2\widetilde{N}+1)^2}+1\right)}.$$

The quantity $\widetilde{\mathcal{N}}_{\rm env}$ as a function of $\widetilde{N}$ was plotted in Fig. 11(bottom-right). Finally, let us write down explicitly the aforementioned supercritical values for the particular important cases:

$$\widetilde{\mathcal{N}}_{\rm env}(\widetilde{N}=0)=\frac{1}{2}\left[\left(\sqrt{3}-\frac{2}{\sqrt{5}}\right)^{-1}-1\right]\approx 0.0969 \tag{155}$$

$$\widetilde{N}(\widetilde{\mathcal{N}}_{\rm env}=0)=\frac{1}{2}\left[\sqrt{\frac{3}{2}+\frac{5}{2\sqrt{3}}}-1\right]\approx 0.3578 \tag{156}$$

where the value (155) is the maximum amount of thermal photons admissible in environment which still allows us to obtain effects from first and second domains (e.g., existence of saddle-point transmissivity), and the value (156) is the maximum amount of input photons which still allows to observe the same behavior. These are fundamental constants of lossy bosonic channel providing its description on the top level of "hierarchy of characterization."

Remember that (134) [and hence its approximation (154)] is the derivative of the equation $\underline{C}(s)=0$. Therefore, the analogous expansion of equation $\underline{C}(s)=0$ in the neighborhood of $s\to\infty$ has the form

$$\mathfrak{A}e^{-3s}+\mathfrak{B}e^{-2s}+\mathfrak{C}e^{-s}+\log_2(2N+1)=0 \tag{157}$$

where $\mathfrak{C}=-c$, $\mathfrak{B}=-\frac{b}{2}$ and $\mathfrak{A}=-\frac{a}{3}$. Equation (157) allows to interpret both critical and supercritical parameters in the same framework. In particular, zero-order coefficient $\log_2(2N+1)$ is the universal limit (110), zero-equal linear coefficient ($\mathfrak{C}=0$) defines critical parameter η_∞, and if both linear and quadratic coefficients are zero ($\mathfrak{C}=\mathfrak{B}=0$), we get supercritical parameters $\widetilde{N}$ and $\widetilde{\mathcal{N}}_{\rm env}$. In explicit form, they read

$$\begin{aligned}
\underline{C}&=K_0+K_1\,x+K_2\,x^2+K_3\,x^3\\
K_0&=\log_2(2N+1)\\
K_1&=T_1\,\delta_\infty\\
K_2&=T_2\left[\left(1+M^2\right)\left(\delta_\infty^2+\frac{1}{180}\right)-\frac{\eta^2M^2}{24}\right]\\
K_3&=T_3\left[\left(1+M^2+M^4\right)\left(\delta_\infty^3+\frac{\delta_\infty}{60}-\frac{1}{3780}\right)\right.\\
&\quad+\left(1+M^2\right)\\
&\quad\left.\left(\frac{1}{60}-\frac{\delta_\infty}{4}\right)\frac{\eta^2M^2}{4}-\frac{\eta^4M^4}{64}\right]
\end{aligned}$$

where $M:=2N+1$ and

$$T_j:=\frac{2N(N+1)(-1)^j}{j\left[\eta(1-\eta)\left(N+\frac{1}{2}\right)\left(\mathcal{N}_{\rm env}+\frac{1}{2}\right)\right]^j\ln 2}$$

with $j=1,2,3$. The equation (discriminant)$K_2^2-4K_1K_3=0$ can be rewritten as

$$\begin{aligned}
&\left(1+M^4\right)\left(\frac{1}{900}+\frac{16}{315}\,\delta_\infty-\frac{14}{5}\,\delta_\infty^2-156\,\delta_\infty^4\right)\\
&\quad+M^2\left(\frac{1}{450}+\frac{16}{315}\,\delta_\infty-\frac{12}{5}\,\delta_\infty^2-120\,\delta_\infty^4\right)\\
&\quad-\eta^2M^2\left(1+M^2\right)\left(\frac{1}{60}+\frac{4}{5}\,\delta_\infty-9\,\delta_\infty^2\right)\\
&\quad+\eta^4M^4\left(\frac{1}{16}+3\,\delta_\infty\right)=0
\end{aligned}$$

Similarly, for the function $Z(e^{-s})$ [see (134) and Section V-C] we have decomposition over $x=e^{-s}$, which reads

$$D=K_1'x+K_2'^2x^2+K_3'^3x^3$$

$$K_j'=-\frac{j}{\eta(1-\eta)\left(N+\frac{1}{2}\right)\left(\mathcal{N}_{\rm env}+\frac{1}{2}\right)}K_j.$$

Recall, that $\mathcal{P}$ [see (134)] is equal to derivative $d\underline{C}/ds$ taken on the solution of optimization problem, where the input and modulation eigenvalues are equal to those corresponding to extrema of $\underline{C}(s)$. The equation (discriminant) $K_2'^2-4K_1'K_3'=0$ can be rewritten as

$$\begin{aligned}
&\left(1+M^4\right)\left(\frac{1}{900}+\frac{4}{105}\,\delta_\infty-2\,\delta_\infty^2-108\,\delta_\infty^4\right)\\
&\quad+M^2\left(\frac{1}{450}+\frac{4}{105}\,\delta_\infty-\frac{8}{5}\,\delta_\infty^2-72\,\delta_\infty^4\right)\\
&\quad-\eta^2M^2\left(1+M^2\right)\left(\frac{1}{60}+\frac{3}{5}\,\delta_\infty-6\,\delta_\infty^2\right)\\
&\quad+\eta^4M^4\left(\frac{1}{16}+\frac{9}{4}\,\delta_\infty\right)=0.
\end{aligned}$$

Roots of these discriminants provide approximations for the quantities $\tilde{\eta}$ and $\bar{\eta}$.

Notice that all of these results (universal limit and critical and supercritical parameters) are given by exact explicit analytical relations.

In turn, the supercritical parameters N_0 and $\mathcal{N}_{\rm env,0}$ are found in Section V, where the values

$$\begin{aligned}
N_0(\mathcal{N}_{\rm env,0}=0)&\approx 0.0817\\
\mathcal{N}_{\rm env,0}(N_0=0)&\approx 0.0204
\end{aligned}$$

are obtained as numerical solutions of a transcendental equations.

I. Critical Parameters for Heterodyne Rate

Let us analyze the behavior of the function $R^{(\rm het)}(s)$ versus s (below, the argument of $R^{(\rm het)}$ is assumed to be s) for different values of η and fixed $\mathcal{N}_{\rm env}$ (see Fig. 20). By solving $\partial R^{(\rm het)}/\partial s=0$ in the third stage [see (77)], one can show that $R^{(\rm het)}(s)$ is monotonically increasing function if transmissivity

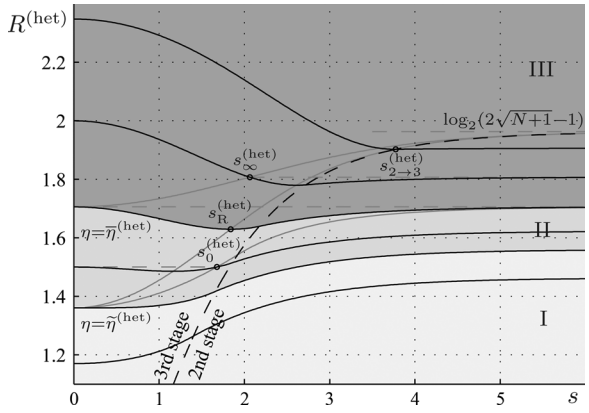

Fig. 20. Heterodyne rate $R^{(\mathrm{het})}$ (black) versus s for the values of η equal to 0.4, 0.4774, 0.5356, 0.623, 0.75, and 0.9 (from bottom to top). The values of other parameters are $N = 5$ and $\mathcal{N}_{\mathrm{env}} = 1$. The gray curves are the loci $(s_0^{(\mathrm{het})}(\eta), R^{(\mathrm{het})}(s_0^{(\mathrm{het})}(\eta)))$, $(s_R^{(\mathrm{het})}(\eta), R^{(\mathrm{het})}(s_R^{(\mathrm{het})}(\eta)))$, and $(s_\infty^{(\mathrm{het})}(\eta), R^{(\mathrm{het})}(s_\infty^{(\mathrm{het})}(\eta)))$, where parameter η is varying over whole definitional domain of the quantities $s_0^{(\mathrm{het})}$, $s_R^{(\mathrm{het})}$, and $s_\infty^{(\mathrm{het})}$, respectively. Dotted black curve divide this quadrant into areas corresponding to different stages. The curves $R^{(\mathrm{het})}(s)$ corresponding to the same regime have the same gray background color (the higher the regime the darker the color).

belongs to the interval[29] $0 < \eta \leqslant \tilde{\eta}^{(\mathrm{het})}$ (we will call this the *first regime* analogously to capacity), where

$$\tilde{\eta}^{(\mathrm{het})} = \left[(2\mathcal{N}_{\mathrm{env}}+1)^2 N - \sqrt{N^2+(2N+1)(2\mathcal{N}_{\mathrm{env}}+1)^2}\right] \times \left[2\mathcal{N}_{\mathrm{env}}(2\mathcal{N}_{\mathrm{env}}+1)\right]^{-1} \quad (158)$$

which is equal to $(N+1)^{-1}$ in the case of squeezed vacuum state [one needs to take the limit $\mathcal{N}_{\mathrm{env}} \to 0$ in (158)]. Then, by equating the heterodyne values taken for $s = 0$ and $s = \infty$ [see (78) and (111)], we obtain the corresponding transmissivity value

$$\bar{\eta}^{(\mathrm{het})} = \left[8\mathcal{N}_{\mathrm{env}}(\mathcal{N}_{\mathrm{env}}+1) + N + 2 - \sqrt{(N+2)^2 + 16\mathcal{N}_{\mathrm{env}}(\mathcal{N}_{\mathrm{env}}+1)(N+1)}\right] \times \left[4\mathcal{N}_{\mathrm{env}}(2\mathcal{N}_{\mathrm{env}}+1)\right]^{-1} \quad (159)$$

which becomes $2(N+2)^{-1}$ in the case of $\mathcal{N}_{\mathrm{env}} = 0$. The latter can be obtained by taking the limit $\mathcal{N}_{\mathrm{env}} \to \infty$ in (159) or by equating the relations $\log_2(1+\eta N)$ and (111).

If $\tilde{\eta}^{(\mathrm{het})} < \eta \leqslant \bar{\eta}^{(\mathrm{het})}$ (the *second regime*), one can consider squeezing value $s_0^{(\mathrm{het})}$ defined by the equality $R^{(\mathrm{het})}\left(s_0^{(\mathrm{het})}\right) = R^{(\mathrm{het})}(0)$. In the second stage, it equals

$$s_0^{(\mathrm{het})} = \ln\left[1 + 2\eta N\left[\phi_0^{(\mathrm{het})}\right]^{-1} \times \left\{\left(2\left[\phi_0^{(\mathrm{het})}\right]^{-1}+1\right)\left(2\eta\left[\phi_0^{(\mathrm{het})}\right]^{-1}-1\right) - N\right\}^{-1}\right]$$

[29]Notations for critical parameters of heterodyne rate are chosen to be similar to those for capacity if saddle-point is imagined at $s = 0$.

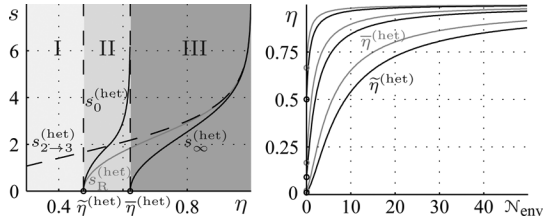

Fig. 21. (Left) Quantities $s_{2\to3}^{(\mathrm{het})}$, $s_0^{(\mathrm{het})}$, $s_\infty^{(\mathrm{het})}$ (black), and $s_R^{(\mathrm{het})}$ (gray) are plotted versus η for $N = 5$ and $\mathcal{N}_{\mathrm{env}} = 1$. (Right) $\bar{\eta}^{(\mathrm{het})}$ and $\tilde{\eta}^{(\mathrm{het})}$ are plotted versus $\mathcal{N}_{\mathrm{env}}$ for the values of N equal to 1, 10, and 100 (from top to bottom).

where $\phi_0^{(\mathrm{het})}$ is defined similarly to ϕ_0 [see (82)] as the value of $\phi^{(\mathrm{het})}$ [see (96)] taken in the point $s = 0$. In explicit form, $\phi_0^{(\mathrm{het})}$ reads

$$\phi_0^{(\mathrm{het})} = \frac{2\eta}{1+(1-\eta)(2\mathcal{N}_{\mathrm{env}}+1)}.$$

In the third stage, $s_0^{(\mathrm{het})}$ is given by the relation

$$s_0^{(\mathrm{het})} = \operatorname{arcosh}\left[\eta N F_0 - 1\right]$$

where

$$F_0 = \frac{8\left[N - \left(\eta\left[\phi_0^{(\mathrm{het})}\right]^{-1}-1\right)\left(2\left[\phi_0^{(\mathrm{het})}\right]^{-1}+1\right)\right]}{\eta\left(2\eta\left[\phi_0^{(\mathrm{het})}\right]^{-1}-1\right)\left(2\left[\phi_0^{(\mathrm{het})}\right]^{-1}+1\right)^2}.$$

One can show that $s_0^{(\mathrm{het})} \to \infty$ if $\eta \to \bar{\eta}^{(\mathrm{het})} - 0$, and $s_0^{(\mathrm{het})} \to 0$ if $\eta \to \tilde{\eta}^{(\mathrm{het})} + 0$ (see also Fig. 21). If the environment is pure ($\mathcal{N}_{\mathrm{env}} = 0$), $s_0^{(\mathrm{het})}$ can be rewritten as

$$s_0^{(\mathrm{het})} = \ln\frac{(1-\eta)(\eta N+2)}{2-\eta(N+2)}$$

in second stage and as

$$s_0^{(\mathrm{het})} = \operatorname{arcosh}\frac{\eta^2(2N+1)^2-(1-\eta)^2-1}{2(1-\eta)}$$

in the third stage.

Analogously, if $\bar{\eta}^{(\mathrm{het})} < \eta \leqslant 1$ (the *third regime*), one can consider the quantity $s_\infty^{(\mathrm{het})}$, such that $R^{(\mathrm{het})}\left(s_\infty^{(\mathrm{het})}\right) = R^{(\mathrm{het})}(\infty)$. Due to the monotonicity of $R^{(\mathrm{het})}(s)$ in the second stage, the value $s_\infty^{(\mathrm{het})}$ can only correspond to the third stage, and it is equal to

$$s_\infty^{(\mathrm{het})} = \operatorname{arcosh}\left[F_\infty\phi_0 - \sqrt{1+4\eta F_\infty}\right]$$

where

$$F_\infty = N + \frac{1+\eta}{2} - \sqrt{\eta N + \left(\frac{1+\eta}{2}\right)^2}.$$

In particular, we have the limits

$$\lim_{\eta\to\bar{\eta}^{(\mathrm{het})}+0} s_\infty^{(\mathrm{het})} = 0$$

and

$$\lim_{\eta\to 1} s_{\infty}^{(\mathrm{het})} = \infty.$$

Also, if $\eta > \tilde{\eta}^{(\mathrm{het})}$, there is a minimum of $R^{(\mathrm{het})}$ in the third stage corresponding to the value

$$s_{\mathrm{R}}^{(\mathrm{het})} = \operatorname{arcosh}\left[\left\{N + \frac{1+\eta}{2} - \sqrt{\eta\,(1+N) - \mathcal{N}_{\mathrm{env}}(1+\mathcal{N}_{\mathrm{env}})(1-\eta)^2}\right\}\phi_0 - (2\mathcal{N}_{\mathrm{env}}+1)(1-\eta)\right]$$

which has its limits

$$\lim_{\eta\to\tilde{\eta}^{(\mathrm{het})}+0} s_{\mathrm{R}}^{(\mathrm{het})} = 0$$

and

$$\lim_{\eta\to 1} s_{\mathrm{R}}^{(\mathrm{het})} = \infty.$$

Taking into account the previous considerations, we have for optimal squeezing in environment $s_{\star}^{(\mathrm{het})}$ (providing the highest heterodyne rate for a given transmissivity) the equality

$$s_{\star}^{(\mathrm{het})} = \begin{cases} \infty, & \text{if } 0 < \eta \leqslant \bar{\eta}^{(\mathrm{het})} \\ 0, & \text{if } \bar{\eta}^{(\mathrm{het})} \leqslant \eta < 1 \end{cases}$$

which is similar to the analogous relation for capacity (131).

VI. Multiple Channel Uses

Let us now move to the case of multiple uses (multimode) of the lossy bosonic channel. We will consider those types of memory channel environments which give rise to spectral problems (in general, symplectic eigenvalues are not functions of matrix spectrum). One of the simplest models of this class is

$$V_{\mathrm{env}} = \bigoplus_{k=1}^{n} V_{\mathrm{env},k} \tag{160}$$

where each $V_{\mathrm{env},k} = V(\mathcal{N}_{\mathrm{env},k}, s_{\mathrm{env},k})$ [see (32)] is the single-mode environment corresponding to $k\mathrm{th}$ channel use. It follows from [18] that optimal matrices V_{in} and V_{mod} have the same form as (160), i.e., they are direct sums of some single-mode matrices. Then, the average amount of photons per mode in V_{in} is related with the amount taken for each mode [see (33)] as

$$N = \frac{1}{n}\sum_{k=1}^{n} N_k. \tag{161}$$

In the following, it will be useful to work with *total amount of input photons*

$$\mathcal{N} := nN$$

which will always be written in calligraphic font. Note that $\mathcal{N} = N$ for the single channel use. Similarly, we will search the maximum for *total capacity*

$$\mathcal{C} := n\,\underline{C}_n$$

where

$$\underline{C}_n = \frac{1}{n}\sum_{k=1}^{n} C_k \tag{162}$$

with C_k being the capacity of the single $(k\mathrm{th})$ channel use (mode) as studied in Section IV. In the following, we use the system of notations introduced in Section IV-A for the case of single channel use by adding extra index (usually, k) to all quantities in order to indicate which channel use the quantities are referred to.

Notice that apart from the model (160), also environment model of the form (28) (with commuting blocks $V_{\mathrm{env},qq}$ and $V_{\mathrm{env},pp}$) gives rise to spectral problem. It particular, in this case we conjecture that the maximum of χ-quantity (14) is achieved with matrices V_{in} and V_{mod} of the same form as (28), i.e., with null off-diagonal blocks. Furthermore, all diagonal blocks of all matrices will be mutually commuting. This conjecture is supported by numerical investigations relying on environment models of the form (28). Moreover, it was proved in [18] analytically for the case of all modes belonging to the third stage. Such form of covariance matrices makes symplectic eigenvalues functions of the usual eigenvalues, specifically

$$\nu_k = \sqrt{o_{qk}o_{pk}}, \quad \bar{\nu}_k = \sqrt{\bar{o}_{qk}\bar{o}_{pk}} \tag{163}$$

where

$$o_{uk} = \eta i_{uk} + (1-\eta)e_{uk}$$
$$\bar{o}_{uk} = \eta(i_{uk} + m_{uk}) + (1-\eta)e_{uk}.$$

Both energy constraint (25) and symplectic spectrum (163) are preserved under orthogonal transformations. Thus, without affecting the final result, in the following, we can consider all the involved matrices to be diagonal (see also the discussion in the appendix of [12]). Notice that if all matrices are diagonal, then the optimal input state is pure (it straightforwardly follows from Theorem 2 applied to each channel use).

More generally, according to the Williamson decomposition theorem, any covariance matrix can be put in a diagonal form by acting with a symplectic transformation [39]. However, such a symplectic transformation may not preserve the energy constraint. One can hence restrict the consideration to the class of models for which the symplectic transformation preserves the energy constraint (these are jointly symplectic and orthogonal). In particular, the models (28) belong to this class. The general form of such V_{env} matrices is presented in the appendix of [12] (see also [38]).

A. Convex Separable Programming

The optimization problem for multiple channel uses is formulated as follows. One needs to find the maximum over the variables i_{uk}, m_{uk}, and $m_{u_\star k}$ for the following functions[30]:

$$\underline{C}_n = \frac{1}{n}\sum_{k=1}^{n}\left[g\left(\bar{\nu}_k - \frac{1}{2}\right) - g\left(\nu_k - \frac{1}{2}\right)\right]$$

$$R_n^{(\mathrm{het})} = \frac{1}{n}\sum_{k=1}^{n}\left[\log_2 \bar{\nu}_k^{(\mathrm{het})} - \log_2 \nu_k^{(\mathrm{het})}\right]$$

$$R_n^{(\mathrm{hom})} = \frac{1}{2n}\sum_{k=1}^{n}\left[\log_2 \bar{o}_{u_\star k} - \log_2 o_{u_\star k}\right]$$

with the constraints

$$i_{uk} > 0$$
$$m_{uk}, m_{u_\star k} \geqslant 0$$
$$\frac{1}{n}\sum_{k=1}^{n}\left[i_{uk} + \frac{1}{4i_{uk}} + m_{uk} + m_{u_\star k}\right] = 2N + 1.$$

Then, the problem of finding the capacity[31] can be reformulated as finding the maximum for sum of concave[32] functions (each of them depending on one variable)

$$\mathcal{C}(N) = \sum_{k=1}^{n} C_k \tag{164}$$

over the distribution $P(N_k)$ of positive numbers N_k satisfying the constraint

$$\mathcal{N} = \sum_{k=1}^{n} N_k \tag{165}$$
$$N_k = \frac{1}{2}\left[i_{uk} + \frac{1}{4i_{uk}} + m_{uk} + m_{u_\star k} - 1\right] \geqslant 0$$

where N_k is the amount of energy granted for kth mode [see (161)], and $C_k = C_k(i_{uk}, m_{uk}, m_{u_\star k})$ [see the definition (162)] is parametrized by fixed parameters e_{uk}, $e_{u_\star k}$, and η, i.e., C_k only depends on the eigenvalues belonging to kth mode. Thus, the total optimization problem is split in two tasks: the first task is the "internal optimization" solved in Section IV, i.e., optimization inside each mode [see "box"(115)] and the second task is the "external optimization", i.e., finding the optimal distribution $P(N_k)$ of the total energy $\mathcal{N}$ over "boxes" to get maximal output sum $\sum_{k=1}^{n} C_k$:

$$N_1 \longrightarrow \boxed{C_1 = C_1(N_1)} \longrightarrow C_1$$
$$\cdots\cdots\cdots\cdots\cdots\cdots$$
$$N_n \longrightarrow \boxed{C_n = C_n(N_n)} \longrightarrow C_n.$$

This "external optimization" problem is known in mathematics as *convex separable programming* which was solved in [19] and [20]. In particular, the following theorem based on concavity of target function was proved [19].

Theorem 4: A feasible solution $\{N_k\}$ is an optimal solution to the problem (164), (165) if and only if there exists a $\lambda \in \mathbb{R}$ such that

$$N_k = 0, \qquad \text{if} \quad \lambda \geqslant \frac{\partial C_k}{\partial N_k}(N_k = 0) \tag{166}$$

$$N_k \,|\, \lambda = \frac{\partial C_k}{\partial N_k}(N_k), \qquad \text{if} \quad \lambda < \frac{\partial C_k}{\partial N_k}(N_k = 0). \tag{167}$$

Thus, the theorem states that any solution of "external optimization" problem satisfying its Lagrange equations is optimal because it is unique. Also, it follows from the theorem that the dependence $\lambda(N)$ is monotonic. Indeed, if λ is increasing, then some modes can change their "case" from (167) to (166), which results to zeroing their contribution to $N = \sum_{k=1}^{n} N_k$. Even if some modes remain in the case (167), their contribution N_k is decreasing because of the concavity and the monotonically increasing behavior of functions $C_k(N_k)$. Analogously, lower λ corresponds to higher N.

In the following, it will be convenient to use the *threshold functions* (see also [22])

$$\lambda_{1\to 2,k} \equiv \frac{dC_k}{dN_k}(N_k = 0) = \frac{\eta}{o_{u_\star k}} g_1(\nu_k)$$
$$\lambda_{2\to 3,k} \equiv \frac{dC_k}{dN_k}(N_{2\to 3,k}) = \frac{\eta}{\bar{\nu}_k} g_1(\bar{\nu}_k) \tag{168}$$

defined analogously to single-mode relations (122) and (123), where quantity $N_{2\to 3,k}$ is given by (81) applied to kth mode. Thus, the threshold functions are generalizations of the single-use threshold values written in λ-representation (see Section IV-L). Taking into account (113), one can see that $\lambda \in (0, \lambda_{\max})$ for $N > 0$, where

$$\lambda_{\max} = \max_k \frac{\partial C_k}{\partial N_k}(N_k = 0) = \max_k \lambda_{1\to 2,k}.$$

In the following, the notion of *stage* will be referred to each mode (in complete analogy with the single use case presented in Section IV). It allows the optimization problem to be interpreted as the search for the optimal *distribution of modes across stages*. In particular, the case $N_k = 0$ holds if and only if kth mode belongs to the first stage, and the case $\lambda = \lambda_{\max}$ corresponds to zero capacity, where all modes are in the first stage. Analogously, it follows from Theorem 4 that if it is

$$\lambda < \min_k \frac{\partial C_k}{\partial N_k}(N_k = 0) = \min_k \lambda_{1\to 2,k}$$

only the second and third stages exist (by comparing N_k granted for kth mode with its threshold value $N_{2\to 3,k}$ one can obtain its actual stage). The proposition 3 (see Section IV-L) applied to multiple uses threshold functions (168) shows the relationship between the level of noise in particular quadratures and their participation to information transmission. For example, for fixed value of total energy N, the kth mode can change its stage from first to second if the noise in quadrature e_{uk} or $e_{u_\star k}$ is sufficiently decreased. More generally, one can say that it is the most optimal case when less noisy modes get more input energy and

[30]Here, the homodyne rate corresponds to the measurement of (generally) different quadratures for different channel uses, where less noisy quadratures are used for information transmission. Such definition of homodyne rate is different from that given by the relation (31), where the same quadrature is measured in all modes.

[31]The case of rates is completely analogous to that of capacity; therefore, here it is omitted.

[32]The concavity of single-use capacity C_k over its energy constraint N_k was proved in Section IV-K.

thus transfer more information, which is similar to the case of classical channels.

The "external optimization" problem is reducible to single transcendental equation on λ

$$\mathcal{N} = \sum_{k=1}^{n} N_k(\lambda) \tag{169}$$

which has single root because of Theorem 4. It can be solved by using, e.g., method of bisection. Remember that $N_k(\lambda) = 0$ if $\lambda > \lambda_{1\to 2,k}$. Then, $N_k(\lambda)$ is given by (121) if $\lambda_{2\to 3,k} < \lambda < \lambda_{1\to 2,k}$. Finally, $N_k(\lambda)$ is given by (119) if $\lambda < \lambda_{2\to 3,k}$. Thus, (169) can be considered as giving feasible solution for *any* λ, the only difference is that such a solution corresponds to another value of $\mathcal{N}$.

As far as the solution is unique, it is sufficient to prove the convergence of the bisection method applied to (169), which can be done as follows. Notice that λ and $\mathcal{N}$ are related each other by one-to-one correspondence, and the dependence $\lambda(\mathcal{N})$ is monotonic. In particular, the limit $\lambda \to 0$ corresponds to the limit $\mathcal{N} \to \infty$, and the value $\lambda = \lambda_{\max}$ corresponds to $\mathcal{N} = 0$. Thus, as far as a unique λ corresponds to a given $\mathcal{N}$, the method of bisection applied to the transcendental equation (169) for the variable $\lambda \in (0, \lambda_{\max}]$ always converges to the solution.

Apart from the considered "blackbox" approach, the given optimization problem can be also interpreted in the following way. There are two effective unknown "variables" for the systems of Lagrange equations[33]: distribution of modes across stages and λ. In the simplest case, one of these variables can be set as internal and the another one as external during optimization process. The algorithm proposed in [19] uses λ as internal variable, while the aforementioned algorithm uses distribution of modes across stages for that. Since the latter algorithm is usually faster, below we will make use of it.

B. Classical Capacity and Rates

Remember that explicit analytical solution of the optimization problem is not possible and depends on the form of the threshold functions $\lambda_{1\to 2,k}$, $\lambda_{2\to 3,k}$ defined by environment matrix $V_{\rm env}$ and transmissivity η. However, if we are interested in finding approximate values of capacity, e.g., $\underline{C}_n^{(0)}$ or $\underline{C}_n^{(1)}$ relying on quantity $\lambda^{(0)}(N)$ [see (124)], a simplification of the general method is possible. In the following, we show this using $\underline{C}_n^{(0)}$ and $\underline{C}_n^{(1)}$ as examples, but the generalization to the case of rates is straightforward.

Notice that mode transcendental equation (88) can be formally written as the dependence $\bar{o}_{u_\star h} = f_h(i_{uh})$ for the hth channel use. Then, remember that $\lambda^{(0)}$ (which is the amount of input photons granted for each channel use in the λ-representation) is the same for all modes in the third and the second stages. As far as the variable $\bar{o}_{u_\star k}$ for any mode k can be used as an equivalent replacement of $\lambda^{(0)}$ [see (124)], we can introduce a new variable

$$\begin{aligned} x &:= \bar{o}_{qm} = \bar{o}_{pm} = \bar{o}_{ql} = \bar{o}_{pl} = \cdots \\ &= \bar{o}_{qh} = f_h(i_{ph}) = \bar{o}_{pt} = f_t(i_{qt}) \end{aligned} \tag{170}$$

[33]Note that each distribution of modes across stages results to its own system of Lagrange equations, where unknown variables are the eigenvalues of $V_{\rm in}$ and $V_{\rm mod}$. As far as the system of Lagrange equations itself does not provide an effective method to find distribution of modes across stages, some *a priori* properties are necessary to write a fast algorithm. In particular, concavity and monotonic behavior of capacity are such properties for the given problem.

getting a chain of equalities linking *all* modes of the second and third stages. Here, modes m and l belong to the third stage, while modes h and t to the second stage ($m_{ph} = m_{qt} = 0$). Modes of the first stage are not included in (170) and all give $V_{\rm in}$ eigenvalues equal to $\frac{1}{2}$. If some mode belongs to the third stage, its $V_{\rm in}$ eigenvalues can be found from the relations (74). If some mode belongs to the second stage, its input eigenvalues are given in Section IV-G [see (100) and (103)].

Taking into account stages discrimination, (24) can be rewritten as

$$\sum_{\{2,3|m_{uk}\neq 0\}} \left[\eta(i_{uk} + m_{uk}) + (1-\eta)\, e_{uk}\right] = \left[2n_3 + n_2\right] x \tag{171}$$

where n_j is the number of modes belonging to jth stage ($j = 1, 2, 3;\ n = n_1 + n_2 + n_3$) and $\sum_{\{2,3|m_{uk}\neq 0\}}$ stands for the summation over all eigenvalues of second and third stages, except for the ukth ones corresponding to $m_{uk} = 0$. Also, the energy constraint (25) can be rewritten as

$$\sum_{\{2,3|m_{uk}\neq 0\}} \left[i_{uk} + m_{uk}\right] = 2n\left[N + \frac{1}{2}\right] - n_1 - \sum_{k}{}'' i_{uk} \tag{172}$$

where $i_{uk} = f_k^{-1}(x)$ and the double prime sum extends over ukth eigenvalues of the second stage, such that $m_{uk} = 0$. Substituting (172) into (171), we get a transcendental equation for the single variable x. Since all unknown eigenvalues can be expressed through x [see (170)], we can formally arrive at $\underline{C}_n^{(0)}$ and $\underline{C}_n^{(1)}$.

Notice that as far as the relation $i_{uk} = f_k^{-1}(x)$ is explicit in the zeroth-order and the first-order approximations [see (100) and (103)], one can express the quantities $\underline{C}_n^{(0)}$ and $\underline{C}_n^{(1)}$ as functions of solution of only one algebraic equation [see (171) and (172)] for one variable x.

When all modes are in the third stage, we have the explicit analytical solution and the equalities $\underline{C}_n = \underline{C}_n^{(0)} = \underline{C}_n^{(1)}$. In particular, it is

$$\underline{C}_n = g\left[\eta N + (1-\eta)N_{\rm env}\right] - \frac{1}{n}\sum_{k=1}^{n} g\left[(1-\eta)\mathcal{N}_{\rm env,k}\right] \tag{173}$$

where

$$N_{\rm env} = \frac{1}{n}\sum_{k=1}^{n} N_{{\rm env},k} \tag{174}$$

is the average number of photons in the multiple uses environment. The analytical lower bound given by (173) generalizes the expression presented in [12]. Analogously, in the case of all modes belonging to the third stage, the heterodyne rate reads

$$\begin{aligned} R_n^{(\rm het)} = \log_2 &\left[\eta N + (1-\eta)N_{\rm env}^{(\rm het)} + \frac{1}{2}\right] \\ &- \frac{1}{n}\sum_{k=1}^{n} \log_2\left[(1-\eta)\mathcal{N}_{{\rm env},k}^{(\rm het)} + \frac{1}{2}\right] \end{aligned}$$

where $N_{\rm env}^{(\rm het)}$ is defined similarly to (174).

If all modes are in the second stage, the homodyne rate reads [see (101)]

$$R_n^{(\mathrm{hom})} = \frac{1}{n}\sum_{k=1}^{n} \log_2 \left[\sqrt{(\phi_k/4)^2 + \phi_k\, T_1^{(\mathrm{hom})}} - \phi_k/4\right]$$

where $T_1^{(\mathrm{hom})}$ [see (127)] is given by the root of equation [see the relations (128) and (129)]

$$\frac{1}{n}\sum_{k=1}^{n}\left[i_{uk} - \phi_k^{-1}\right] = 2N + 1 - T_1^{(\mathrm{hom})}$$

with

$$i_{uk} = \frac{1}{2}\left[\sqrt{(\phi_k/4)^2 + \phi_k\, T_1^{(\mathrm{hom})}} - \phi_k/4\right].$$

If the number of channel uses tends to infinity, the discussed procedure can be properly generalized by changing the transcendental equations [see, e.g., (171) and (172)] to equations on functions (spectral densities). However, if the considered model has some symmetry over stages, the general solution can be further simplified by considering some parameters which mark the boundaries between regions of modes belonging to different stages. In Section VI-C, we will show an example along this line.

C. Application to a Particular Memory Channel

In this section, we look for the capacity of channels whose environment is described by a covariance matrix of the form

$$V_{\mathrm{env}} = \left[\mathcal{N}_{\mathrm{env}} + \frac{1}{2}\right]\begin{pmatrix} e^{s\Omega} & 0 \\ 0 & e^{-s\Omega}\end{pmatrix} \qquad (175)$$

where Ω is a real symmetric $n \times n$ matrix and $s \in \mathbb{R}$ is a parameter describing the environment properties. In particular, we will consider the case of environment model (175) with

$$\Omega_{ij} = \delta_{i,j+1} + \delta_{i,j-1}, \quad i,j = 1,\ldots,n$$

describing a specific lossy bosonic channel with memory [11], which will be referred to as Ω-*model of the environment*. Notice that by taking $\Omega_{ij} = \delta_{ij}$, we recover the case of the memoryless channel.

The parameter s in (175) represents the degree of correlation among environment modes. We are interested in the asymptotic behavior of this channel. That implies to take the limit $n \to \infty$ in the equations of Section VI-B. It can be treated for some relations as the limit of Riemann sums resulting to the integral expressions. Thus, instead of a set of equations on eigenvalues, we get a set of equations on functions which are spectral densities for the involved (infinite-dimensional) matrices. In the following, we denote the spectral densities by the same symbols as proper eigenvalues, but written in calligraphic and replacing the mode number h by a continuous parameter ξ, i.e., $i_{uh} \to \mathcal{I}_{u\xi}$, $o_{qh} \to \mathcal{O}_{q\xi}$, etc.

It is convenient to use the parameter ξ as arising from the spectrum of V_{env} matrix [11]

$$\mathcal{E}_{u\xi} = \left(\mathcal{N}_{\mathrm{env}} + \frac{1}{2}\right) e^{\pm 2s\cos\xi} \qquad (176)$$

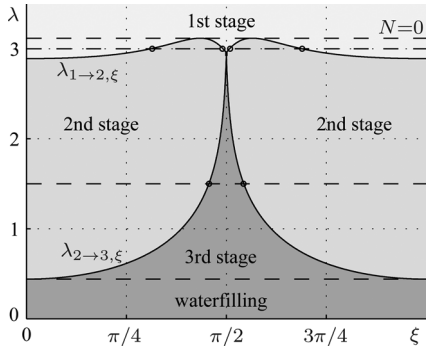

Fig. 22. Threshold functions $\lambda_{1\to 2,\xi}$ and $\lambda_{2\to 3,\xi}$ versus ξ for Ω-model. The value of other parameters are $\eta = 0.4$, $s = 0.5$, and $\mathcal{N}_{\mathrm{env}} = 0.01$. The horizontal dashed lines correspond to different values of N, where the top line is the case of $N = 0$ and the bottom line is the border case when all modes are in the third stage (below it, we have "waterfilling solution"). The points at which horizontal lines (corresponding to some values of λ or, equivalently, N) cross threshold functions $\lambda_{1\to 2,\xi}$ and $\lambda_{2\to 3,\xi}$ mark borders between modes with different stages. The regions corresponding to different stages are filled by different gray colors.

labeling both modes (if $\xi \in [0,\pi]$) and eigenvalues (if $\xi \in [0,2\pi]$). Plus and minus in (176) stand for $u = q$ and $u = p$, respectively. Due to the mirror symmetry of eigenvalues (176) over quadratures, the symplectic spectrum and the distribution of modes across stages have to be symmetric with respect to the point $\frac{\pi}{2}$; therefore, we restrict ourselves to consider spectral densities only defined in the interval $\left[0, \frac{\pi}{2}\right]$.

Threshold functions $\lambda_{1\to 2,\xi}$ and $\lambda_{2\to 3,\xi}$ (and also their analogs for rates) for Ω-model are shown in Figs. 22–25. In general, the equation $\lambda_{1\to 2,\xi} = \lambda$ (for the variable ξ) can have up to three different roots in the interval $\left[0, \frac{\pi}{2}\right]$. In the following, we will calculate the capacities $\underline{C}^{(0)}$ and $\underline{C}^{(1)}$ which are essentially simpler as the equation $\lambda^{(0)}_{1\to 2,\xi} = \lambda$ has at maximum a single root τ which marks the boundary between the modes belonging to the first and second stages (the equation $\lambda_{2\to 3,\xi} = \lambda$ has at most one root).

Suppose that all modes belong to the third stage, which holds true if (it can be obtained, e.g., from (75) or(81) by combining it with (176), see also Appendix in [11])

$$w := \frac{1}{2|s|}\ln\frac{\eta\,(2N+1) + (1-\eta)(2N_{\mathrm{env}}+1)\,I_0(2s)}{\eta + (1-\eta)(2N_{\mathrm{env}}+1)} \geqslant 1$$

where I_0 is the modified Bessel function of the first kind and zero order. The capacity $\underline{C}$ in this case is given by (76), where the amount of environment photons N_{env} is given by (34) after a formal replacement $\cosh s \to I_0(2s)$. This example explicitly shows the possibility of an enhancement of the capacity with increasing degree of memory s (however, at the cost of increasing the amount of environment photons N_{env}).

If $w < 1$, we can have one of the following distributions of modes across stages according to the properties of the threshold functions $\lambda^{(0)}_{1\to 2,\xi}$ and $\lambda^{(0)}_{2\to 3,\xi}$ (see Fig. 23):

1) a mixture of the second and the third stages (2,3,2);
2) a mixture of the second and the first stages (2,1,2);
3) all modes belonging to the second stage (2,2,2) which happens for a single value[34] N_2 of the parameter N, given s, η and $\mathcal{N}_{\mathrm{env}}$.

[34]Do not confuse this definition of N_2 with that used in Section VI-A.

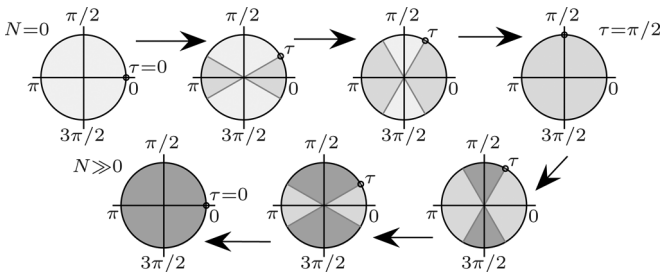

Fig. 23. Schematic representation of the "quantum water filling" for the capacities $\underline{C}^{(0)}$ and $\underline{C}^{(1)}$ and the environment model $\Omega_{ij} = \delta_{i,j+1} + \delta_{i,j-1}$ (it follows from the threshold functions $\lambda^{(0)}_{1\to 2,\xi}$ and $\lambda^{(0)}_{2\to 3,\xi}$ of variable ξ). The angle ξ parametrizing the spectral density corresponds to polar angle. White, gray, and black sectors correspond to the first, second, and third stages, respectively. Arrows show change of stages with increasing of N. The parameter τ marks the points of stage change.

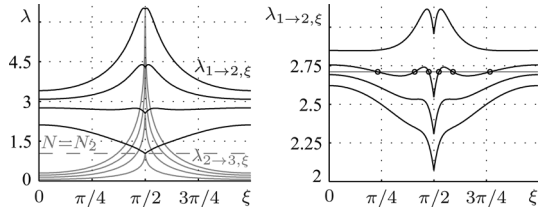

Fig. 24. Threshold functions $\lambda_{1\to 2,\xi}$ (black) and $\lambda_{2\to 3,\xi}$ (gray)are plotted versus ξ for capacity of the channel with the Ω-model of environment. The values of parameters at the left are $\mathcal{N}_{\rm env} = 0.01$, $s = 1$, and η (from bottom to top): 0.15, 0.35, 0.55, and 0.75. The values of parameters at the right are $\mathcal{N}_{\rm env} = 0.01$, $s = 1$, and η (from bottom to top): 0.29, 0.32, 0.35, and 0.4. Horizontal lines correspond to particular chosen values of input energy.

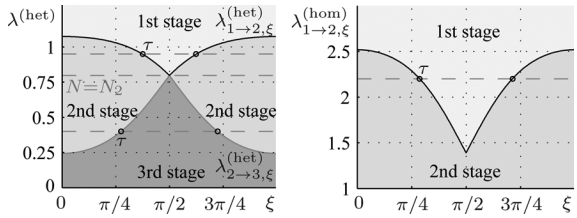

Fig. 25. Threshold functions for heterodyne (left) and homodyne (right) rates are plotted for the parameters $\mathcal{N}_{\rm env} = 0.5$, $s = 1$, and $\eta = 0.65$ (channel environment is given by Ω-model). Horizontal lines correspond to particular chosen values of input energy. These lines cross threshold functions at the points (marked by τ if $\xi \in [0, \frac{\pi}{2}]$) corresponding to stage change.

If $N > N_2$ or $N < N_2$, we have the (2,3,2) or (2,1,2) case with the center of the interval $[0, \pi]$ filled by the third or the first stage, respectively. We label by $\tau \in \left[0, \frac{\pi}{2}\right]$ the point corresponding to the boundary between the regions of modes corresponding to different stages. The possible distributions of modes across stages and the dependence of τ from N are sketched in Fig. 23. Notice that at the point τ, we must have $\bar{\mathcal{O}}_{u\tau} = \mathcal{O}_{u\tau}$ which can be rewritten as

$$x = x(\tau) = \eta\, \mathcal{I}_{u\tau} + (1-\eta)\, \mathcal{E}_{u\tau}. \tag{177}$$

Here, $u = q$ gives $\mathcal{I}_{q\tau} = e^{2s\cos\tau}/2$ [see (74)] for (2,3,2) case and $u = p$ gives $\mathcal{I}_{p\tau} = \frac{1}{2}$ for (2,1,2) case (we use different quadratures in these cases because of either q or p quadrature changes its stage in the interval which contains τ).

Then, the transcendental equation for x [see (171) and (172)] can be rewritten as an equation for τ

$$\eta\left[N + \frac{\tau_1}{\pi} - \frac{1}{\pi}\int_0^{\tau} \mathcal{I}_{q\xi}\, d\xi\right] + \frac{1-\eta}{\pi}\int_0^{\tau_2} \mathcal{E}_{p\xi} d\xi = \frac{\tau_2}{\pi} x \tag{178}$$

where (τ_1, τ_2) is equal to (τ, τ) for (2,1,2) and to $\left(\frac{\pi}{2}, \pi - \tau\right)$ for (2,3,2). Moreover, x is given by (177) and $\mathcal{I}_{q\xi}$ is the spectral density for the second stage which can be found as solution of functional equation obtained from (100) (or (103) in the case of $\underline{C}^{(1)}$) after the replacements discussed at the beginning of this section. By substituting $\tau = \frac{\pi}{2}$ in (178), we find N_2. Comparing it with the actual energy restriction N, we get the correct value of $\lambda^{(0)}$ and the distribution of modes across stages. Then, solving (178) with the found distribution of modes across stages we arrive at τ and x. Finally, $\underline{C}^{(0)}$ is expressed through these parameters as follows [see (8), (9), and (14)]:

$$\underline{C}^{(0)} = \left(1 - \frac{2}{\pi}\tau_3\right)\left[g\left(x - \frac{1}{2}\right) - g\left((1-\eta)\,\mathcal{N}_{\rm env}\right)\right] + \frac{2}{\pi}\int_0^{\tau}\left[g\left(\sqrt{x\mathcal{O}_{q\xi}} - \frac{1}{2}\right) - g\left(\sqrt{\mathcal{O}_{q\xi}\mathcal{O}_{p\xi}} - \frac{1}{2}\right)\right] d\xi$$

where

$$\mathcal{O}_{q\xi} = \eta\mathcal{I}_{q\xi} + (1-\eta)\,\mathcal{E}_{q\xi}$$
$$\mathcal{O}_{p\xi} = \frac{\eta}{4}\mathcal{I}^{-1}_{q\xi} + (1-\eta)\,\mathcal{E}_{p\xi}$$

τ_3 is equal to $\pi/2$ for (2,1,2) and to τ for (2,3,2).

The solution of the optimization problem for multiple channel uses can be interpreted as "quantum waterfilling" in analogy with usual (classical) "waterfilling" introduced for classical Gaussian channels with memory (see, e.g., [22], [30], and [35]). The dependence of the found spectral densities (also symplectic ones) from N is similar to filling a vessel with water. The form of the vessel is defined by the model $V_{\rm env}$ and transmissivity η. The symplectic spectral density $\bar{\nu}_\xi$ goes always up by increasing N [with respect to $\nu_\xi(N=0)$], while ν_ξ goes always down (or does not change). For environment models showing correlation (memory) among modes, the presence of the second stage gives rise to capillary effects on the edges of the vessel resulting to a "water level" with meniscus form. This "quantum water filling" effect for the considered model is shown in Fig. 26 for symplectic spectral densities $\bar{\nu}_\xi$, ν_ξ and spectral densities $\mathcal{M}_{q\xi}$, $\mathcal{I}_{q\xi}$. Graphs of $\mathcal{I}_{q\xi}$ calculated through exact mode transcendental equation, zeroth-order and first-order approximations are shown in Fig. 27. Despite some visible difference between exact and approximate spectral densities, the corresponding symplectic spectral densities are almost equal, thus resulting to a difference less than 0.05% between the capacities. The small value of this difference comes from the fact that the Holevo-χ has zero derivative with respect to the eigenvalues of $V_{\rm in}$ and $V_{\rm mod}$ in the neighborhood of the solutions of Lagrange equations (as they are equations for optimization problem).

In Fig. 30(left), the capacity $\underline{C}^{(1)}$ for Ω-model is plotted versus s for different values of η. The universal limit (110) for $s \to \infty$ is still valid.

D. Optimal Channel Memory and Superadditivity

Finally, let us discuss the role of squeezing and memory in lossy bosonic channel. Considering the capacity (76) as a function on the set of environment models with fixed $N_{\rm env}$, one can

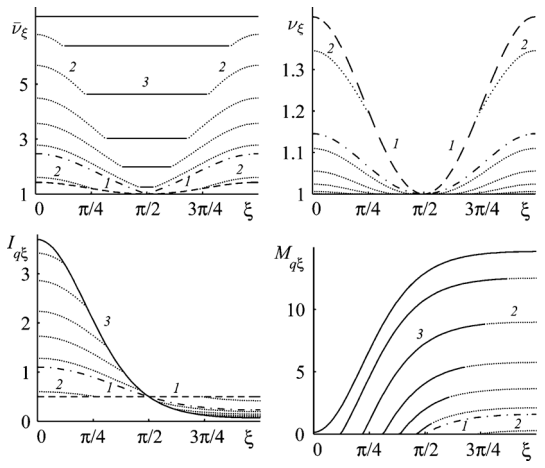

Fig. 26. Going from top-left clockwise, the spectral densities $\bar{\nu}_\xi$, ν_ξ, $\mathcal{M}_{q\xi}$, and $\mathcal{I}_{q\xi}$ (for $\Omega_{ij} = \delta_{i,j+1} + \delta_{i,j-1}$) are plotted versus the parameter ξ for $N = 0, 0.05, 0.67, 1, 2, 3.5, 6, 9, 11$ (from bottom to top curve for quantities $\bar{\nu}_\xi, \mathcal{M}_{q\xi}, \mathcal{I}_{q\xi}$, and from top to bottom curve for quantity ν_ξ). Solid, dotted, and dashed parts of curves correspond to third, second, and first stages, respectively. Dash-dotted curve corresponds to the case of all modes belonging to the second stage. The values of other parameters used are $\mathcal{N}_{\rm env} = s = 1$ and $\eta = 0.5$. Numbers 1, 2, and 3 are used to indicate the regions with corresponding stages.

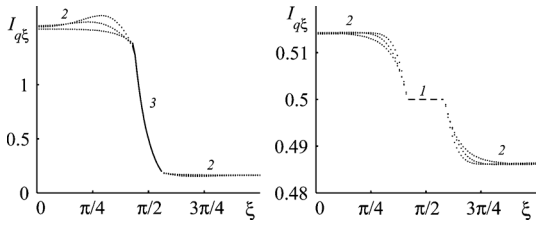

Fig. 27. Exact solution and first-order and zeroth-order approximations for spectral density $\mathcal{I}_{q\xi}$ versus ξ for $N = 1$ (left) and $N = 0.01$ (right). The values of other parameters are $\mathcal{N}_{\rm env} = 0.5$, $s = 2.5$, and $\eta = 0.95$. Solid, dotted, and dashed parts of curves correspond to third, second, and first stages, respectively. Functions with maximum and minimum variations correspond to exact solution and zeroth-order approximation, respectively.

see that it shows *violation of quadrature symmetry*. In fact, despite the symmetry of all equations over quadratures, the maximum of $\underline{C}$ is achieved when $e_q \neq e_p$ (see also [30]). This also follows from the environment purity theorem proved for the single channel use (see Appendix D). By applying this theorem to each channel use for the case of memory channel, one can see that optimal environment can always be chosen pure.

Now, let us analyze the symmetry of the capacity over modes. Suppose that the average (per mode) amount of photons in the environment $N_{\rm env}$ is fixed and the capacities for the single use of memoryless channel and multiple uses of memory channel (e.g., for Ω-model) are compared. As far as the Holevo-χ quantity (14) is symmetric over modes, one can expect that the capacity for the single channel use will always be higher. However, this is not true as results from the *violation of mode symmetry*. Indeed, this can be seen in Fig. 30(right) where the capacity $\underline{C}^{(1)}$ maximized over parameters s and $\mathcal{N}_{\rm env}$ (thus, we have always $\mathcal{N}_{\rm env} = 0$) for memory and for memoryless cases is plotted versus $N_{\rm env}$. We can see that the Ω-model for some parameters values provides higher capacity than memoryless model. Unfortunately, the form of the *optimal* (in terms of capacity) memory for the channel is still unknown. We consider the finding of the optimal channel memory to be an important and challenging problem.

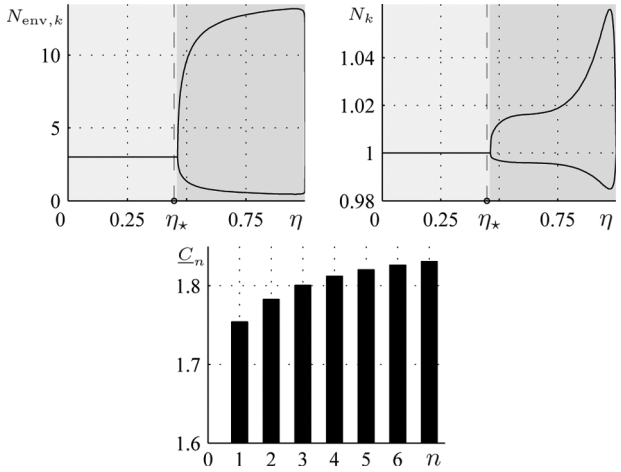

Fig. 28. Nontrivial behavior of optimal memory for capacity. Amounts of photons $N_{{\rm env},k}$ (top-left) and N_k (top-right) corresponding to optimal memory for capacity are plotted as functions of transmissivity η. The values of other parameters are $N_{\rm env} = 3$, $N = 1$, and $n = 5$. The lighter and the darker backgrounds indicate the additive and superadditive regions of transmissivity, correspondingly. Vertical dashed lines at $\eta = \eta_\star$ mark the analytically estimated boundary between additive and superadditive regions. Bottom: capacity for optimal memory model is plotted versus amount of channel uses n. The values of other parameters are $N_{\rm env} = 3$, $N = 1$, and $\eta = 0.8$.

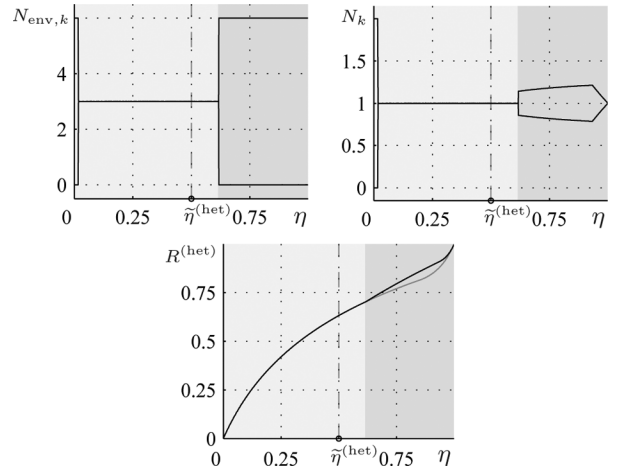

Fig. 29. Nontrivial behavior of optimal memory for heterodyne rate. Amounts of photons $N_{{\rm env},k}$ (top-left) and N_k (top-right) corresponding to optimal memory for heterodyne rate are plotted as functions of transmissivity η. Bottom: heterodyne rate for memoryless model (gray curve) and for optimal memory model (black curve). The values of other parameters for all three graphs are $N_{\rm env} = 3$, $N = 1$, and $n = 2$. The lighter and the darker backgrounds indicate the additive and superadditive regions of transmissivity, correspondingly. Vertical dashed lines at $\eta = \tilde{\eta}^{(\rm het)}$ mark the analytically estimated boundary between additive and superadditive regions.

Since the environment purity theorem always allows to choose the optimal environment in pure state, each its kth mode can be completely characterized by its squeezing s_k. Hence, the problem of finding optimal channel memory can be reformulated as finding the form of the function $s(k)$ (or $s(\xi)$ for the case of $n \to \infty$). This function is not a constant, but numerical study of this problem in simplest situations shows that only two different values of $s(k)$ are possible for all k and given values of η, N, and $N_{\rm env}$.

The aforementioned properties can be also treated from the superadditivity viewpoint. First, let us discuss the memoryless channel capacity. It was proved in Section IV-K that the one-shot capacity is monotonically increasing and concave function

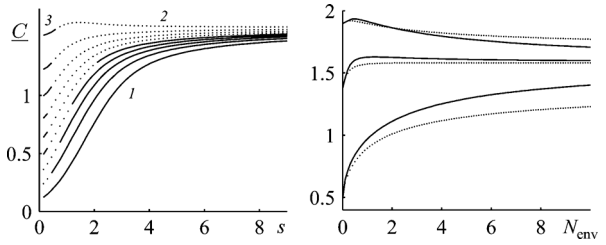

Fig. 30. (Left) Quantity $\underline{C}^{(1)}$ is plotted versus s for values of η going from 0.1 (bottom curve) to 0.9 (top curve) with step 0.1. The values of the other parameters are $N = \mathcal{N}_{\rm env} = 1$. Solid parts of curves correspond to the third and first stages, respectively. Dotted part of curves correspond to the second stage. Numbers 1, 2, and 3 are used to indicate the regions corresponding to the cases (2,1,2), (2,3,2), and (3,3,3), respectively. (Right) Maximum of $\underline{C}^{(1)}$ over $V_{\rm env}$ (i.e., over parameters s and $\mathcal{N}_{\rm env}$) is plotted versus $N_{\rm env}$ for values of $\eta = 0.1, 0.5, 0.9$ going from bottom to top curve. Solid and dotted curves corresponds to $\Omega = \delta_{ij}$ and $\Omega_{ij} = \delta_{i,j+1} + \delta_{i,j-1}$, respectively. The value of the other parameter is $N = 1$.

of N. In this case, the convex separable programming method (see Section VI-A) guarantees that optimal input state is the direct sum of identical single-use matrices. It automatically implies additivity of memoryless capacity. As far as concavity was also proved for rates, the conclusions valid for capacity are also applicable to rates. However, the problem of additivity can be posed in another way. Quite generally one can compare different multimode environments containing (in average) the same amount of photons and having the same purity. In particular, the optimal environment can be always realized by pure states as it is supported by environment purity theorem. In this case, it straightforwardly follows from the dependence $\underline{C}(s)$ studied in Section V that the dependence of $\underline{C}(N_{\rm env})$ [e.g., for pure environment state, see (34)] is in general nonmonotonic, which guarantees optimality of nonhomogenuous distribution of photons $N_{\rm env}$ over environment modes for some channel parameters.

In particular, one can expect that if $\eta < \eta_\infty$ and $N \geqslant \tilde{N}(0) \approx 0.3578$, then capacity is additive. In fact, in this case, the dependence $\underline{C}(N_{\rm env})$ corresponds to the concave and monotonically growing functions. Numerical calculations show that in this region of parameters, capacity is indeed additive. Similarly, if $\eta > \eta_\infty$, then $\underline{C}(N_{\rm env})$ has local maximum in the interval $0 < N_{\rm env} < \infty$ and numerical calculations shows that capacity is superadditive (nonhomogeneous distribution of environment energy of modes is optimal) for some values of input energy. This allows us to conjecture that the transitions between superadditive and additive cases happen at critical and supercritical parameters of single channel use. Notice that heterodyne rate is in general also nonmonotonic function of $N_{\rm env}$; therefore, it is also subjected to superadditivity property (see Fig. 29).

The value of transmissivity η [we consider $\eta > \eta_\infty$ and $N > \tilde{N}(0)$] corresponding to transition from additive to superadditive region for given parameters N, $N_{\rm env}$ can be qualitatively estimated in the following way. In the case of capacity, let us consider a family of curves $\underline{C}(N_{\rm env})$ (or, equivalently, $\underline{C}(s)$ because of purity) parametrized by the transmissivity η and plotted for fixed value of N (see Fig. 5(left) and Fig. 10). Each of these curves has maximum at the point of $N_{\rm env} = (\cosh(s_\star) - 1)/2$ [see the relation (34) and Definition 3]. Recall that $s_\star$ is a monotonically decreasing (over η) quantity which tends to infinity if η tends to η_∞ from the right (see Fig. 14). Hence, one can find a value of $\eta = \eta_\star$ corresponding to the curve $\underline{C}(N_{\rm env})$ which achieves a maximum at the given value of $N_{\rm env}$. The quantity $\eta_\star$ is shown in Fig. 28, where the optimal distribution of photons in environment as a function of transmissivity is plotted. Similarly, in the case of heterodyne rate, one can roughly use $\eta = \tilde{\eta}^{(\rm het)}$ [see (158)] to estimate the transition point (see Fig. 29).

VII. Conclusion

In this paper, we have developed powerful and versatile optimization methods for the estimation of Gaussian quantum channels' capacities and rates. We have applied them to the lossy bosonic channel in both memoryless and memory setting by restricting to Gaussian states.

First, we have thoroughly characterized the memoryless channel, thus generalizing the results of [3] and [7]. To do that we have exploited the single-mode channel whose environment's covariance matrix $V_{\rm env}$ can be described by two parameters: squeezing s and average amount of thermal photons $\mathcal{N}_{\rm env}$. Then, to completely specify the channel usage, we have fixed the values of transmissivity η and input energy N. It is the latter value that defines the kind of solution for the capacity C. For N increasing from 0 to $+\infty$ we have found three different *stages*, each characterized by a solution of a given form.

We have proved that the one-shot capacity is a concave and monotonically increasing function of N. Thus, as byproduct we have gotten the additivity of the memoryless capacity assuming covariance matrices for modulation, channel environment and input states to be mutually commuting. Moreover, due to this property, the derivative $dC(N)/dN$ can be used as the equivalent replacement for the amount N of photons granted for channel input, thus providing another channel's representation. Within this representation (called λ-representation) is easily visualizable the geometry of the stages transitions.

The one-shot capacity turns out to be a monotonic function of all parameters, except of environment squeezing. This makes the latter a special parameter. In particular, taking the limit $s \to +\infty$, we have defined different *regimes* depending on how the capacity tends this limit. This is determined by the value of transmissivity and amount of environment thermal photons. *Critical* values for these parameters can be defined at boundary of different regimes. Similarly, other regimes and critical parameters can be considered analyzing the other properties of $C(s)$ function. Totally, we have defined five different regimes and four triads of critical parameters, which characterize the existence and values of specific points of $C(s)$.

Already from that we can draw some general conclusions about the channel's properties. For instance, if

$$N \geqslant \left[\sqrt{3/2 + 5/(2\sqrt{3})} - 1\right]/2 \approx 0.3578 \tag{179}$$

then $C(s)$ is always monotonic over $0 < s < +\infty$ if

$$\eta \leqslant 1 - 1/\sqrt{3} \tag{180}$$

and has no more than one maximum in this interval otherwise. Also, $C(s)$ has no more than one maximum if

$$\mathcal{N}_{\rm env} \geqslant \left[\left(\sqrt{3}-2/\sqrt{5}\right)^{-1}-1\right]/2 \approx 0.0969. \qquad (181)$$

Another example is the case of $C(0) = C(\infty)$ for $N \to \infty$, which is possible only if

$$\eta \geqslant 2/e \qquad (182)$$

where inequality is saturated by pure environment state. As far as the critical parameters, in general, depend on N, $\mathcal{N}_{\rm env}$ [or N, η—depending on the parameter varied in analyzing the behavior of $C(s)$] and not all of them exist in all the regimes, we have defined three *domains*. Each domain is characterized by existence and/or relations among critical parameters. In turn, *supercritical* values for N and $\mathcal{N}_{\rm env}$ can then be defined at boundary of different domains. The nontrivial global maximal or minimal values of critical and supercritical parameters must be intended as fundamental constants characterizing the channel. Few of such constants which can be expressed in radicals are the above numbers (179), (181) for supercritical and (180), (182) for critical parameters.

Summarizing, in the space of parameters N, $\mathcal{N}_{\rm env}$, we have defined two functions and by equating them to zero, we have divided the space into three parts (domains). The boundaries of domains define the supercritical parameters. In turn, domains define the possible regimes (five at maximum). Critical parameters come out at the boundaries of regimes (this time in the space of parameters η, N, and $\mathcal{N}_{\rm env}$). Then, the towering achievement is the following route to determine the channel's "state":

1) find the channel *domain* by comparing the actual N, $\mathcal{N}_{\rm env}$ with their supercritical values (it gives the set of possible *regimes*);
2) find the channel *regime* by comparing the actual η, $\mathcal{N}_{\rm env}$ with their critical values;
3) find the relevant values of squeezing parameter for the given channel *regime* and compare them with the actual s;
4) find the channel *stage*.

The aforementioned steps tell us the type of the curve $C(s)$, how many extremal and specific points it has, in which interval we are in this curve and what is the type of solution (stage). This is particularly relevant to characterize channels and might be useful in practical situations to determine the optimal "work point" of a channel by having some freedom in its parameters values.

Then, we have presented the solution for the memory channel, thus generalizing the results of [10]–[12] and [24]. Here, the problem of finding the capacity has been reformulated in a multimode setting as a total optimization problem split in two tasks: the first task is the "internal optimization," i.e., optimization inside each mode and the second task is the "external optimization," i.e., finding the optimal distribution of the total input energy $\sum_{k=1}^{n} N_k$ over "boxes" (modes) to get maximal output sum $\sum_{k=1}^{n} C_k(N_k)$. Then, the first task has been addressed using the techniques developed for the single-mode channel, while the second one using convex separable programming techniques [19], [20]. For the latter, we have also given formal proofs of both the uniqueness of the solution and the convergence of the proposed algorithm.

The previous splitting has become possible because we were confined to the class of memory models which make the optimization problem spectral.

In the case of single-mode channel, we have derived theorems about the optimality of pure states showing that for any given $V_{\rm env}$, the optimal input channel state is pure, and for any fixed $\mathrm{Tr}(V_{\rm env})$, the optimal $V_{\rm env}$ is pure. In particular, purity of $V_{\rm env}$, once $\mathrm{Tr}(V_{\rm env})$, is fixed results in a violation of quadrature symmetry. When this result is extended to the memory channel (i.e., nonidentical multiple modes environment), with optimization over distribution of input energies, we have discovered violation of mode symmetry too. That is to say that optimization inside each box gives us "violation of quadrature symmetry" with "input and environment purity theorems"; then, maximization over our blackboxes gives us "violation of mode symmetry" and "optimal channel memory."

In this context, the enhancement (superadditivity) of classical capacity is possible (for only some values of the memory channel parameters), if energy is redistributed between environment modes to become (in general) different in different modes. This possible violation of mode symmetry points out the existence of nontrivial optimal channel's environment (memory). Such environment can always be chosen pure. One can also say that capacity is superadditive if mode symmetry is violated and additive otherwise, where transition between additive and superadditive cases is related with critical and supercritical parameters found for the single-use of the single-mode channel.

Notice that the main feature of the considered memory model is to be symbol independent, i.e., the action of the channel at a given use does not depend on the previous inputs, and without a causal structure. That made its characterization a daunting task, which nevertheless has been accomplished.

Transmission rates for heterodyne and homodyne measurements have been treated parallelly to the capacity because they can be considered as its logarithmic approximations. In the case of heterodyne, it has done by introducing heterodyne variables. Thus, most of the capacity properties can be also found analyzing the rates. In particular, it was shown that homodyne measurement for the single-use of the single-mode channel gives a rate which is always monotonically growing function of environment squeezing. However, this is not the case for heterodyne measurement which is monotonically growing function of squeezing only in neighborhood of $s \to \infty$; therefore, its critical parameters were also calculated and its regimes were studied to provide complete characterization.

Finally, besides a thorough characterization of the lossy channel, we have provided mathematical techniques for the solution of optimization problems in information transmission with Gaussian channels. The machinery developed herein seems applicable to other capacities and other Gaussian channels as witnessed by the similarities with a recent study on additive Gaussian noise channel [22], which can be characterized as well by critical parameters [34]. Above all, extension

to the amplification channel seems within reach and is planned as a future work.

APPENDIX A
PROOF OF THE INPUT PURITY THEOREM FOR CAPACITY

Let us prove Theorem 1. Since the dimension of matrices is 2×2, there is a symplectic transformation S which is orthogonal and diagonalizes $V_{\rm env}$. Let us apply S to matrices $V_{\rm out}$ and $\bar{V}_{\rm out}$ [see (23) and (24)]. The transformation S preserves energy constraint (25), symplectic eigenvalues[35] ν, $\bar{\nu}$ and does not change the Holevo function. If S is applied, then the matrices $V_{\rm in}$, $V_{\rm mod}$, and $V_{\rm env}$ can be represented in the form

$$V_{\rm in} = \begin{pmatrix} i_q & i_{qp} \\ i_{qp} & i_p \end{pmatrix}, \qquad V_{\rm mod} = \begin{pmatrix} m_q & m_{qp} \\ m_{qp} & m_p \end{pmatrix},$$
$$V_{\rm env} = \begin{pmatrix} e_q & 0 \\ 0 & e_p \end{pmatrix}.$$

Hence, we get for symplectic eigenvalues the relations

$$\bar{\nu}^2 = [\eta(i_q + m_q) + (1-\eta)\, e_q] \times [\eta(i_p + m_p) + (1-\eta)\, e_p] - \eta^2 (i_{qp} + m_{qp})^2$$
$$\nu^2 = [\eta i_q + (1-\eta)\, e_q]\, [\eta i_p + (1-\eta)\, e_p] - \eta^2 i_{qp}^2$$

where the latter can also be represented as

$$\nu^2 = \eta^2 \det V_{\rm in} + (1-\eta)^2 \det V_{\rm env} + \eta\,(1-\eta)\,(e_q i_p + i_q e_p).$$

Then, the energy constraint (25), can be equivalently written as

$$i_q + i_p + m_q + m_p = 2N + 1 \tag{183}$$

First, let us show that the case of mixed input ($i_q i_p - i_{qp}^2 > \frac{1}{4}$) is not optimal. Indeed, in this case there are values $i_q' < i_q$ and $m_q' > m_q$ such that the constraint (183) is preserved ($i_q + m_q = i_q' + m_q'$) and the input state is pure: $i_q' i_p - i_{qp}^2 = \frac{1}{4}$. New variables give the symplectic eigenvalues $\bar{\nu}' = \bar{\nu}$ and $\nu' < \nu$. Since new variables increase the Holevo function (14) we conclude that the optimality of input pure state is proved by contradiction.

Next, we notice that $i_{qp} m_{qp} > 0$ cannot be optimal. Indeed, if i_{qp} and m_{qp} have the same signs, then by changing m_{qp} to $-m_{qp}$ we do not violate the positivity of $V_{\rm mod}$, but preserve the value of ν and increase the value of $\bar{\nu}$. Since the Holevo function can be increased, we get the proof by contradiction. Thus, it is always true that $\mathrm{sign}(i_{qp}) = -\mathrm{sign}(m_{qp})$. In particular, without loss of generality for the optimal solution we can assume that

$$(i_{qp} + m_{qp}) = (|m_{qp}| - |i_{qp}|)^2$$

in the relation for $\bar{\nu}^2$.

Finally, let us prove that $i_{qp} = m_{qp} = 0$. If this is not true, only three following cases are possible:

1) $|m_{qp}| > |i_{qp}| \geq 0$
2) $|i_{qp}| > |m_{qp}| \geq 0$
3) $|m_{qp}| = |i_{qp}| > 0$

Below we always assume that $\det V_{\rm in} = \frac{1}{4}$ and $i_{qp} m_{qp} < 0$ because it is already proved.

In the first case one can always replace the value of m_{qp} by $m_{qp}' = -i_{qp}$. This replacement preserves positivity of $V_{\rm mod}$ and the value of the contraint (183). Also, it increases the value of $\bar{\nu}$ and does not change the value of ν. Hence, this replacement gives higher value for the Holevo function and the first case cannot be optimal.

In the second case one can choose the values $i_{qp}' = -m_{qp}$ and $i_q' < i_q$ which preserve the purity of input state: $i_q i_p - i_{qp}^2 = i_q' i_p - i_{qp}'^2 = \frac{1}{4}$. Since the input eigenvalue i_q is decreased, let us put the excess of energy in the modulation eigenvalue by taking $m_q' + i_q' = i_q + m_q$. As $\det V_{\rm in}$ is not changed and $i_q' < i_q$, the value of ν is decreased. Then, the value of $\bar{\nu}$ is increased because $(i_{qp} + m_{qp})^2$ becomes zero and the value of the first part of the expression for $\bar{\nu}^2$ is unchanged. Hence, such replacements increase the Holevo function and the second case cannot be optimal too.

In the third case one can consider new values $i_{qp}' = m_{qp}' = 0$ and apply the replacements used above (for the first and the second cases) together. If m_{qp} is set to zero, then neither positivity of $V_{\rm mod}$ nor energy constraint is changed. We also do not change the value $(i_{qp} + m_{qp})^2 = (i_{qp}' + m_{qp}')^2 = 0$. Since $i_{qp}' = 0$ we may also replace i_q by $i_q' < i_q$ such that the purity of input is preserved and excess of energy is moved to m_q. If all these transformations are applied, the value of $\bar{\nu}$ is unchanged, but the value of ν is decreased. Thus, the third case also cannot be optimal.

We have considered all three cases and provided methods to get higher values for the Holevo function. Hence, the case of diagonal matrices $V_{\rm in}$ and $V_{\rm mod}$ is the only possibility if $V_{\rm env}$ is diagonal.

Notice, that for scalar matrix $V_{\rm mod} = m_q$ corresponding to 1-D probability density, the quantity m_{qp} cannot be defined. In such a case the proof reduces to the consideration of only one (second) case, where it is sufficient to put $m_p = m_{qp} = 0$. The case $V_{\rm mod} = m_p$ can be proved analogously.

APPENDIX B
PROOF OF THE INPUT PURITY THEOREM FOR RATES

Let us prove Theorem 2. If quadrature p is measured for homodyne rate (31) (the case of q-quadrature is analogous), then one needs to maximize the quantity

$$R^{(\rm hom)} = \frac{1}{2} \log_2 \bar{o}_p - \frac{1}{2} \log_2 o_p \tag{186}$$

where $\bar{o}_p$ and o_p are diagonal elements of matrices $\bar{V}_{\rm out} = \mathrm{diag}(\bar{o}_q, \bar{o}_p)$ and $V_{\rm out} = \mathrm{diag}(o_q, o_p)$ [see (23) and (24)]. Similarly, we shall denote input and modulation matrices as $V_{\rm in} = \mathrm{diag}(i_q, i_p)$ and $V_{\rm mod} = \mathrm{diag}(m_q, m_p)$. Analogously, to find the heterodyne rate (30), one needs to maximize the quantity

$$R^{(\rm het)} = \log_2 \sqrt{(\bar{o}_q + 1/2)\,(\bar{o}_p + 1/2)} - \log_2 \sqrt{(o_q + 1/2)\,(o_p + 1/2)}. \tag{187}$$

[35] As far as only the single-mode case is discussed, index k [see (14)] is omitted for symplectic eigenvalues.

The maximum for both functions (186) and (187) is taken over the variables i_q, i_p, m_q, and m_p.

Suppose that the maximum is achieved with a nonpure state having $i_q i_p > \frac{1}{4}$. This means that some real number $\varepsilon > 0$ exist, such that $i_p = i'_p + \varepsilon$, where $i'_p = (4i_q)^{-1}$. New variables denoted with primes and defined by transformations

$$\begin{aligned} i'_p &= i_p - \varepsilon, \qquad & i'_q &= i_q, \\ m'_p &= m_p + \varepsilon, \qquad & m'_q &= m_q \end{aligned}$$

make V_{in} pure and preserve the energy constraint (25). They also preserve the values of the first terms and decrease the values of the second terms in (186) and (187), thus providing higher maximum than initial variables. Hence, the theorem is proved by contradiction.

Appendix C
Proof of the Proposition

Let us prove Proposition 2. Suppose that $m_u > 0$ and $m_{u_\star} = 0$ are optimal for $e_u > e_{u_\star}$ in the second stage. We will consider three possible cases $\bar{o}_u > \bar{o}_{u_\star}$, $\bar{o}_u < \bar{o}_{u_\star}$ and $\bar{o}_u = \bar{o}_{u_\star}$ separately. If $\bar{o}_u > \bar{o}_{u_\star}$, then our assumption leads to contradiction due to proposition 1. In what follows, we will use the equivalence between $\bar{o}_u \leqslant \bar{o}_{u_\star}$ and $i_{u_\star} \geqslant i_{u_\star \min}$, where

$$i_{u_\star \min} = N + \frac{1}{2} + \frac{1-\eta}{2\eta}\left(e_u - e_{u_\star}\right).$$

Notice that our condition $e_u > e_{u_\star}$ leads to $i_u < i_{u_\star}$, where the latter is equivalent to $i_u < \frac{1}{2}$ due to optimality of pure input state (see Theorem 1). For the interval $i_u < \frac{1}{2}$, one can show that ν^2 is a decreasing function of i_u. In addition, for $i_{u_\star} > i_{u_\star \min}$, one can see that $\bar{\nu}^2$ is a decreasing function of $i_{u_\star}$. Indeed, for these intervals, the derivatives of ν^2 and $\bar{\nu}^2$ are negative:

$$\begin{aligned} \frac{d\nu^2}{di_{u_\star}} &= \eta(1-\eta)\left(e_{u_\star} - \frac{e_u}{4i_u^2}\right) < 0 \\ \frac{d\bar{\nu}^2}{di_{u_\star}} &= 2\eta^2\left(i_{u_\star \min} - i_{u_\star}\right) < 0. \end{aligned} \tag{188}$$

First, let us consider the strict inequality $\bar{o}_u < \bar{o}_{u_\star}$. If the variables i_u, $i_{u_\star}$, and m_u are changed according to transformations

$$i'_u = \frac{1}{4\left(i_{u_\star} - \varepsilon\right)} \tag{189}$$

$$i'_{u_\star} = i_{u_\star} - \varepsilon \tag{190}$$

$$m'_u = 2N + 1 - i_{u_\star} + \varepsilon - \frac{1}{4\left(i_{u_\star} - \varepsilon\right)}$$

where $0 < \varepsilon < i_{u_\star} - i_{u_\star \min}$, then the energy constraint (65) is preserved (the variable $m_{u_\star} = 0$ remains unchanged). Since $i'_u > i_u$ and $i'_{u_\star} < i_{u_\star}$ the new symplectic eigenvalues satisfy $\nu'^2 < \nu^2$ and $\bar{\nu}'^2 > \bar{\nu}^2$ [see (188)]. As far as g is an increasing function, the new variables increase the first term in (60) and decrease the second term, thus providing higher capacity.

Next, we consider the case $\bar{o}_u = \bar{o}_{u_\star}$. Now, we change the variables i_u, $i_{u_\star}$ according to transformations (189), (190) and variables m_u, $m_{u_\star}$ as follows:

$$\begin{aligned} m'_u &= 2N + 1 - i_{u_\star} - \frac{1}{4\left(i_{u_\star} - \varepsilon\right)} \\ m'_{u_\star} &= \varepsilon \end{aligned}$$

where we choose ε [also for (189) and (190)] from the interval $0 < \varepsilon < \frac{1}{2}\left(\bar{o}_{u_\star} - \bar{o}_u\right)$. Since $i'_u > i_u$ and $i'_{u_\star} < i_{u_\star}$ we have $\nu'^2 < \nu^2$. In addition, the equalities $\bar{o}_u = \bar{o}_{u_\star} = \bar{o}'_u = \bar{o}'_{u_\star}$ lead to $\bar{\nu}'^2 = \bar{\nu}^2$. Thus, the new variables preserve the first term and decrease the second term in (60), thus providing higher capacity.

Finally, we have shown that for all possible cases ($\bar{o}_u > \bar{o}_{u_\star}$, $\bar{o}_u < \bar{o}_{u_\star}$ and $\bar{o}_u = \bar{o}_{u_\star}$), the capacity can be increased by a suitable change of variables. Hence, the proposition is proved by contradiction.

Appendix D
Proof of the Environment Purity Theorem

Let us prove Theorem 3. At first, notice that the following Lemma holds.

Lemma 1: Suppose one has real positive numbers a, b, c, d, where $c > a$, $b - a > d - c$ and $f(x)$ is a monotonically growing concave function in the interval $x \in (0, \infty)$, then

$$f(b) - f(a) > f(d) - f(c).$$

In the case of the first stage $\underline{C} \equiv 0$. In the case of the third stage

$$\max_{\mathcal{N}_{\text{env}}} \underline{C} = \underline{C}(\mathcal{N}_{\text{env}} = 0)$$

i.e., it is optimal to make the environment pure. Then, suppose that we have the case of second stage and environment in mixed state is optimal. Remember that it was proved for $e_q > e_p$ that $m_q = 0$ and $o_q > \bar{o}_p > o_p$ [see Proposition 2 and (68)]. Let us now change the environment variables by preserving N_{env} and making the new environment state pure ($\mathcal{N}'_{\text{env}} = 0$). It corresponds to the change of variables $e_q \to e'_q$, $e_p \to e'_p$ (the eigenvalues i_u and m_u remain the same), where the new value of squeezing s' is given by the relation

$$\cosh s' = (2\mathcal{N}_{\text{env}} + 1)\cosh s.$$

This results to $o'_q > o_q$ and $o'_p < o_p$, i.e., $o'_q - o'_p > o_q - o_p$, while $o'_q + o'_p = o_q + o_p$. It means that $\nu' < \nu$ (see analogous proofs in Section IV-E). One can then write down:

$$o'_q\left(o'_p + \eta\, m_p\right) - o'_q o'_p > o_q\left(o_p + \eta\, m_p\right) - o_q o_p,$$

which is equivalent to $o'_q > o_q$. Taking into account the above inequality and applying the Lemma for $f(x) = \sqrt{x}$, one gets

$$\sqrt{o'_q\left(o'_p + \eta m_p\right)} - \sqrt{o'_q o'_p} > \sqrt{o_q\left(o_p + \eta m_p\right)} - \sqrt{o_q o_p}$$

i.e., $\bar{\nu}' - \nu' > \bar{\nu} - \nu$. Finally, applying again the Lemma for the function $f(x) = g\left(x - \frac{1}{2}\right)$, one gets $\underline{C}' > \underline{C}$. Hence, the theorem is proved by contradiction.

Appendix E
Second Derivative of Solution Over Input Energy

Let us show that $d^2\underline{C}/dN^2 < 0$. In the second stage, it is

$$\frac{d^2\underline{C}}{dN^2} = \frac{\partial^2\underline{C}}{\partial N^2} + 2\frac{\partial^2\underline{C}}{\partial N \partial i_u}\frac{\partial i_u}{\partial N} + \frac{\partial^2\underline{C}}{\partial i_u^2}\left(\frac{\partial i_u}{\partial N}\right)^2 + \frac{\partial\underline{C}}{\partial i_u}\frac{\partial^2 i_u}{\partial N^2}. \tag{191}$$

Taking into account that $\partial\underline{C}/\partial i_u = 0$ for any values of N, we get an equality

$$\frac{d}{dN}\left(\frac{\partial\underline{C}}{\partial i_u}\right) = \frac{\partial^2\underline{C}}{\partial N \partial i_u} + \frac{\partial^2\underline{C}}{\partial i_u^2}\frac{\partial i_u}{\partial N} = 0$$

which allows us to rewrite the derivative (191) as

$$\frac{d^2\underline{C}}{dN^2} = \frac{\partial^2\underline{C}}{\partial N^2} + \frac{\partial^2\underline{C}}{\partial N \partial i_u}\frac{\partial i_u}{\partial N} = \frac{\partial^2\underline{C}}{\partial N^2} - \frac{\partial^2\underline{C}}{\partial i_u^2}\left(\frac{\partial i_u}{\partial N}\right)^2 \tag{192}$$

where

$$\frac{\partial i_u}{\partial N} = -\frac{\partial\mathcal{F}}{\partial N}\left(\frac{\partial\mathcal{F}}{\partial i_u}\right)^{-1}$$

and

$$\frac{\partial^2\underline{C}}{\partial N^2} = [g_2(\bar{\nu}) - g_1(\bar{\nu})]\left(\frac{\eta}{\bar{o}_{u_*}}\right)^2.$$

One can show that

$$\frac{\partial^2\underline{C}}{\partial N \partial i_u} = \frac{\eta^2}{2}\mathcal{L}, \quad \frac{\partial\mathcal{F}}{\partial N} = \eta\mathcal{L} \tag{193}$$

where

$$\mathcal{L} = g_1(\bar{\nu})\left(\frac{1}{\bar{\nu}^2} + \frac{1}{\bar{o}_{u_*}^2}\right) + g_2(\bar{\nu})\left(\frac{1}{\bar{\nu}^2} - \frac{1}{\bar{o}_{u_*}^2}\right).$$

Since it always is $\bar{\nu}^2 > \bar{o}_{u_*}^2$, $g_1 > 0$ and $g_2 < 0$ [see (19)], the quantity $\mathcal{L}$ and the derivatives (193) are positive. Also it can be found that

$$\frac{\partial\mathcal{F}}{\partial i_u} = -\frac{\eta}{2}\left[g_1(\bar{\nu})\left(\frac{1}{o_u} + \frac{1}{\bar{o}_{u_*}}\right)^2 - g_1(\nu)\left(\frac{1}{o_u} + \frac{1}{4i_u^2 o_{u_*}}\right)^2 - g_2(\bar{\nu})\left(\frac{1}{o_u} - \frac{1}{\bar{o}_{u_*}}\right)^2 + g_2(\nu)\left(\frac{1}{o_u} - \frac{1}{4i_u^2 o_{u_*}}\right)^2 + \frac{g_1(\nu)}{\eta o_{u_*} i_u^3}\right].$$

It was shown in [22] for additive noise channel that

$$\frac{\partial i_u}{\partial N} > 0, \qquad \frac{d^2\underline{C}}{dN^2} < 0$$

in the second stage, which can be similarly proved also for lossy channel. In addition, it is evident from (92) that $\partial i_u/\partial N > 0$ in the zeroth-order approximation. Then, in the third stage, we have

$$\frac{d^2\underline{C}}{dN^2} = \frac{\partial^2\underline{C}}{\partial N^2} = \frac{\eta^2}{\bar{\nu}^2}g_2(\bar{\nu}) < 0. \tag{194}$$

Thus, we have shown that the second derivative of capacity is negative in the case of both the second and third stages.

Derivative (194) also holds for rates if the replacement (56) is applied. Besides it, for the heterodyne rate, the replacement (55) must be applied.

Acknowledgment

O. V. Pilyavets thanks Zborovskii V. G., Karpov E. A., and Schäfer J. for fruitful discussions.

References

[1] A. S. Holevo, "On the mathematical theory of quantum communication channels," *Probl. Inf. Transm.*, vol. 8, pp. 62–71, 1972.
[2] C. H. Bennett and P. W. Shor, "Quantum information theory," *IEEE Trans. Inf. Theory*, vol. 44, no. 6, pp. 2724–2742, Oct. 1998.
[3] A. S. Holevo and R. F. Werner, "Evaluating capacities of bosonic Gaussian channels," *Phys. Rev. A*, vol. 63, pp. 032312-1–032312-14, 2001.
[4] S. L. Braunstein and A. K. Pati, *Quantum Information Theory With Continuous Variables*. Dordrecht, The Netherlands: Kluwer, 2003.
[5] M. Navascues, F. Grosshans, and A. Acin, "Optimality of Gaussian attacks in continuous-variable quantum cryptography," *Phys. Rev. Lett.*, vol. 97, pp. 190502-1–190502-4, 2006.
[6] J. Eisert and M. M. Wolf, *Gaussian Quantum Channels Quantum Information with Continuous Variables of Atoms and Light*. London, U.K.: Imperial College Press, 2007, pp. 23–42.
[7] V. Giovannetti, S. Guha, S. Lloyd, L. Maccone, J. H. Shapiro, and H. P. Yuen, "Classical capacity of the lossy bosonic channel: The exact solution," *Phys. Rev. Lett.*, vol. 92, pp. 027902-1–027902-4, 2004.
[8] V. Giovannetti, S. Lloyd, L. Maccone, and P. W. Shor, "Entanglement assisted capacity of the broadband lossy channel," *Phys. Rev. Lett.*, vol. 91, pp. 047901-1–047901-4, 2003.
[9] M. M. Wolf, D. Perez-Garcia, and G. Giedke, "Quantum capacities of bosonic channels," *Phys. Rev. Lett.*, vol. 98, pp. 130501-1–130501-4, 2007.
[10] V. Giovannetti and S. Mancini, "Bosonic memory channels," *Phys. Rev. A*, vol. 71, pp. 062304-1–062304-6, 2005.
[11] O. V. Pilyavets, V. G. Zborovskii, and S. Mancini, "A lossy bosonic quantum channel with non-Markovian memory," *Phys. Rev. A*, vol. 77, pp. 052324-1–052324-8, 2008.
[12] C. Lupo, O. V. Pilyavets, and S. Mancini, "Capacities of lossy bosonic channel with correlated noise," *New J. Phys.*, vol. 11, pp. 063023-1–063023-18, 2009.
[13] C. Lupo, V. Giovannetti, and S. Mancini, "Capacities of lossy bosonic memory channels," *Phys. Rev. Lett.*, vol. 104, pp. 030501-1–030501-4, 2010.
[14] P. Hausladen, R. Jozsa, B. Schumacher, M. Westmoreland, and W. K. Wootters, "Classical information capacity of a quantum channel," *Phys. Rev. A*, vol. 54, pp. 1869–1876, 1996.
[15] B. Schumacher and M. D. Westmoreland, "Sending classical information via noisy quantum channels," *Phys. Rev. A*, vol. 56, pp. 131–138, 1997.
[16] A. S. Holevo, "Quantum coding theorems," *Russ. Math. Surveys*, vol. 53, pp. 1295–1331, 1998.
[17] V. Giovannetti, S. Guha, S. Lloyd, L. Maccone, and J. H. Shapiro, "Minimum output entropy of bosonic channels: a conjecture," *Phys. Rev. A*, vol. 70, pp. 032315-1–032315-14, 2004.
[18] T. Hiroshima, "Additivity and multiplicativity properties of some Gaussian channels for Gaussian inputs," *Phys. Rev. A*, vol. 73, pp. 012330-1–012330-9, 2006.
[19] S. M. Stefanov, "Convex separable minimization subject to bounded variables," *Comput. Opt. Appl.*, vol. 18, pp. 27–48, 2001.

[20] S. M. Stefanov, *Separable Programming. Theory and Methods*. Dordrecht, The Netherlands: Kluwer, 2001.
[21] N. J. Cerf, J. Clavareau, J. Roland, and P. Macchiavello, "Information transmission via entangled quantum states in Gaussian channels with memory," *Int. J. Quantum Inf.*, vol. 4, pp. 439–452, 2006.
[22] J. Schäfer, E. Karpov, and N. J. Cerf, "Gaussian capacity of the quantum bosonic memory channel with additive correlated Gaussian noise," *Phys. Rev. A*, vol. 84, pp. 032318-1–032318-16, 2011.
[23] H. P. Yuen and J. H. Shapiro, "Optical communication with two-photon coherent states—Part III: Quantum measurements realizable with photoemissive detectors," *IEEE Trans. Inf. Theory*, vol. IT-26, no. 1, pp. 78–92, Jan. 1980.
[24] C. Lupo and S. Mancini, "Entanglement enhanced bit rate over multiple uses of a lossy bosonic channel with memory," *Opt. Spectrosc.*, vol. 108, pp. 319–325, 2010.
[25] M. De Gosson, *Symplectic Geometry and Quantum Mechanics: Operator Theory, Advances and Applications*. Cambridge, MA: Birkhäuser, 2006, vol. 166.
[26] R. Simon, N. Mukunda, and B. Dutta, "Quantum-noise matrix for multimode systems $U(n)$ invariance, squeezing, and normal forms," *Phys. Rev. A*, vol. 49, pp. 1567–1583, 1994.
[27] M. B. Hastings, "Superadditivity of communication capacity using entangled inputs," *Nature Phys.*, vol. 5, pp. 255–257, 2009.
[28] G. Bowen and S. Mancini, "Quantum channels with a finite memory," *Phys. Rev. A*, vol. 69, pp. 012306-1–012306-6, 2004.
[29] D. Kretschmann and R. F. Werner, "Quantum channels with memory," *Phys. Rev. A*, vol. 72, pp. 062323-1–062323-19, 2005.
[30] A. S. Holevo, M. Sohma, and O. Hirota, "Capacity of quantum Gaussian channels," *Phys. Rev. A*, vol. 59, pp. 1820–1828, 1999.
[31] C. Lupo, S. Pirandola, P. Aniello, and S. Mancini, "On the classical capacity of quantum Gaussian channels," *Phys. Scr.*, vol. T143, pp. 014016-1–014016-6, 2011.
[32] C. M. Caves and P. D. Drummond, "Quantum limits on bosonic communication rates," *Rev. Mod. Phys.*, vol. 66, pp. 481–537, 1994.
[33] J. H. Shapiro, "Optical waveguide tap with infinitesimal insertion loss," *Opt. Lett.*, vol. 5, pp. 351–353, 1980.
[34] J. Schäfer, E. Karpov, and N. J. Cerf, "Quantum water-filling solution for the capacity of Gaussian information channels," in *Proc. SPIE*, Bellingham, WA, 2010, vol. 7727, pp. 77270J-1–77270J-12.
[35] T. M. Cover and J. A. Thomas, *Elements of Information Theory*. New York: Wiley-Interscience, 1991.
[36] J. Schäfer, D. Daems, and E. Karpov, "Capacity of a bosonic memory channel with Gauss-Markov noise," *Phys. Rev. A*, vol. 80, pp. 062313-1–062313-11, 2009.
[37] R. M. Corless, G. H. Gonnet, D. E. G. Hare, D. J. Jeffrey, and D. E. Knuth, "On the Lambert W function," *Adv. Comput. Math.*, vol. 5, pp. 329–359, 1996.
[38] C. Lupo and S. Mancini, "Transitional behavior of quantum Gaussian memory channels," *Phys. Rev. A*, vol. 81, pp. 052314-1–052314-8, 2010.
[39] J. Williamson, "On the algebraic problem concerning the normal forms of linear dynamical systems," *Amer. J. Math.*, vol. 58, pp. 141–163, 1936.
[40] A. S. Holevo, "Single-mode quantum Gaussian channels: Structure and quantum capacity," *Probl. Inf. Transmiss.*, vol. 43, pp. 3–14, 2007.
[41] R. Garcia-Patron and N. J. Cerf, "Unconditional optimality of Gaussian attacks against continuous-variable quantum key distribution," *Phys. Rev. Lett.*, vol. 97, pp. 190503-1–190503-4, 2006.
[42] V. Giovannetti, S. Lloyd, L. Maccone, J. H. Shapiro, and B. J. Yen, "Minimum Rényi and Wehrl entropies at the output of bosonic channels," *Phys. Rev. A*, vol. 70, pp. 022328-1–022328-8, 2004.
[43] V. Giovannetti and S. Lloyd, "Additivity properties of a Gaussian channel," *Phys. Rev. A*, vol. 69, pp. 062307-1–062307-9, 2004.
[44] S. Lloyd, V. Giovannetti, L. Maccone, N. J. Cerf, S. Guha, R. Garcia-Patron, S. Mitter, S. Pirandola, M. B. Ruskai, J. H. Shapiro, and H. Yuan, The bosonic minimum output entropy conjecture and Lagrangian minimization arXiv:0906.2758v3, 2010.
[45] B. J. Yen and J. H. Shapiro, "Multiple-access bosonic communications," *Phys. Rev. A*, vol. 72, pp. 062312-1–062312-10, 2005.
[46] G. S. Agarwal, "Entropy, the Wigner distribution function, and the approach to equilibrium of a system of coupled harmonic oscillators," *Phys. Rev. A*, vol. 3, pp. 828–831, 1971.
[47] H. P. Yuen and M. Ozawa, "Ultimate information carrying limit of quantum systems," *Phys. Rev. Lett.*, vol. 70, pp. 363–366, 1993.
[48] H. P. Yuen, "States that give the maximum signal-to-quantum noise ratio for a fixed energy," *Phys. Lett.*, vol. 56A, pp. 105–106, 1976.

Oleg V. Pilyavets was born in Frunze, USSR in 1983. He received his B.Sc. and M.Sc. degree in Applied Physics and Mathematics from Moscow Institute of Physics and Technology, the department of Problems of Physics and Power Engineering. In 2009 he earned the Ph.D. in Physics from the P. N. Lebedev Physical Institute, Moscow. In 2010 he received the Ph.D. in Physics also from the University of Camerino, Italy. Then he spent one year at University of Camerino as a PostDoctoral fellow.

Now he has a postdoctoral position at Centre for Quantum Information and Communication of the Université Libre de Bruxelles, Belgium. During the last years his research interest was mainly on information transmission through Gaussian quantum channels.

Cosmo Lupo received the Ph.D. degree in Fundamental and Applied Physics from the University of Napoli "Federico II", Italy, in 2007. He was Marie Curie Fellow at the Research Center for Quantum Information (RCQI) in 2008. From 2008 he is a PostDoctoral fellow at the School of Science and Technology, University of Camerino, Italy. He has been engaged in geometric quantum computation, then in entanglement characterization and more recently in quantum channels capacities.

Stefano Mancini received the Ph.D. degree in physics from the University of Perugia, Italy, in 1998. He was Postdoctoral Fellow at the University of Milan for three years. Subsequently, with temporary lecturer positions held at University of Milan and at University of Camerino, Italy, he have contributed to establish the first Italian academic courses on quantum information and computation.

From 2004 to 2010 he has been researcher of theoretical physics and mathematical methods at Faculty of Science, University of Camerino. Since September 2010 he is professor of theoretical physics and mathematical methods at School of Science and Technology, University of Camerino. He has been involved in the fields of theoretical quantum optics, quantum control theory and quantum information theory. He has given significant contributions to the characterization of entanglement, to the formalism of quantum feedback, to the models of quantum memory channels and to the development of quantum cryptographic protocols.

He has authored or coauthored more than 150 papers published in leading international journals. He has been Editor of four journals for special issues devoted to quantum information topics. He is currently a member of the Editorial Board of the International Journal of Quantum Information.